2. DESCRIPTION OF A HYPOTHETICAL SITE

2.1 Introduction

The purpose of this chapter is to describe the characteristics of a hypothetical sedimentary rock site that could be encountered during geoscientific site characterization activities on the margin of the Michigan Basin in southern Ontario. The description is provided in-lieu of geoscientific information that would be derived through site-specific surface and sub-surface investigations. The intent is to provide information necessary to support an illustrative safety assessment, the focus of which is to demonstrate the methodology to assess the postclosure safety of a deep geological repository for Canada's used nuclear fuel in a sedimentary rock geosphere at an approximate depth of 500 metres below ground surface (mBGS).

Although the data represent a hypothetical sedimentary basin site, the information is consistent with reported values obtained from both regional and site-specific investigations for Ontario Power Generation's Deep Geological Repository for Low & Intermediate Level Waste (INTERA 2011, Sykes et al. 2011). The following sections describe typical site features through the presentation of descriptive geologic (Section 2.2.1), hydrogeologic (Section 2.2.2) and geochemical (Section 2.2.3) site models. The site models are supported by numerical groundwater simulations, presented in Section 2.3.

2.1.1 Site Attributes

There are several key site attributes that relate to demonstrating the geoscientific suitability of the hypothetical sedimentary site and these attributes are described below:

- Site Predictability – near-horizontally layered, undeformed sedimentary shale and limestone formations of large lateral extent;
- Multiple Natural Barriers – multiple low permeability bedrock formations enclose and overlie the repository site;
- Low rates of Contaminant Transport – the deep groundwater flow system is stagnant, with long travel times and no indication of perturbations from glaciation;
- Shallow Groundwater Resources are Isolated – near-surface groundwater aquifers are isolated from the deep saline groundwater system;
- Rock Strength – the host rock should be capable of withstanding mechanical and thermal stresses induced by the repository without significant structural deformation or fracturing that could compromise the containment and isolation functions of the repository;
- Rock Volume – the volume of available competent rock at repository depth should be sufficient to host the repository and to provide sufficient distance from active geological features such as zones of deformation or faults and unfavourable heterogeneities; and
- Seismically quiet - comparable to a Canadian Shield setting.

These attributes would be tested and confirmed through a site characterization and Geosynthesis program at a real candidate site.

2.1.2 Modelling Strategy

The behaviour and stability of the geosphere at repository depth are illustrated through the use of a reference case contrasted with comparative sensitivity cases, based upon the conceptual

model described in Section 2.2. In the sensitivity cases, key geosphere parameters are varied to illustrate the role they play in influencing groundwater flow and transport. The reference case and the geosphere parameters varied in the sensitivity cases are described in Section 2.3.

The reference case simulates current site conditions at the regional scale and includes groundwater salinity distributions to allow simulation of density-dependent flow.

Sensitivity cases, in which the distribution of total dissolved solids are varied, are conducted to examine the role of spatially variable groundwater density (salinity) distributions in governing hydraulic gradients, groundwater velocities, groundwater system stability and dominant mass transport processes. The permeability of the rock mass is also varied within an expected range of uncertainty to illustrate the sensitivity of estimated groundwater performance measures and, in particular, designation of mass transport regimes.

The purpose of the paleohydrogeologic scenarios is to assess the influence of a glacial event on groundwater system stability. In particular, the simulations explore transient hydraulic gradients, groundwater velocities and the depth of penetration by glacial recharge, which are relevant to illustrating long-term DGR safety. The paleohydrogeologic boundary conditions are varied to include cold and warm based glaciers in order to illustrate groundwater system response to external perturbations. The effect of hydromechanical coupling during paleohydrogeologic scenarios is investigated.

2.2 Conceptual Model for Hypothetical Site

The following section describes the geosphere model for the hypothetical sedimentary site, including information on the site and regional scale geology, surface features (topography and hydrology), hydrogeological and geochemical conditions, and natural resource potential.

2.2.1 Descriptive Geological Model

The geologic site model describes the geologic composition and structural features of the geosphere, and provides the basis for geoscientific understanding of the current conditions as well as its past evolution.

2.2.1.1 Geologic Description

The geology of the site is comprised of a layer of Quaternary-aged glacial drift, overlying thick sequences of Paleozoic-aged sedimentary rock, which sits upon basement bedrock of Precambrian-aged granitic gneiss. Fractures within the regional study area are expected to be sparse and infrequent, and will not penetrate Paleozoic sedimentary rocks younger than Ordovician in age (NWMO, 2011). The stratigraphic column for the sedimentary rock found at the centre of the hypothetical repository site is shown in Table 2-1. Table 2-1 also includes geologic formations that are not present at the repository site, but are found within the regional modelling area (described in Section 2.3). Formation thicknesses will vary across the regional modelling area, and a total of 15 formations pinch-out within 10 km of the repository site.

Table 2-1: Formation Thicknesses at the Hypothetical Site

Period	Geological Unit	Unit Top Depth (mBGS)	Thickness (m)
Quaternary	Drift	0.0	29.4
Devonian	Hamilton Group	-	-
	Dundee	-	-
	Detroit River Group	-	-
	Bois Blanc	-	-
Silurian	Bass Islands	-	-
	Unit G	-	-
	Unit F	-	-
	Unit F Salt	-	-
	Unit E	-	-
	Unit D	-	-
	Unit B and C	29.4	52.3
	Unit B Anhydrite	-	-
	Unit A-2 Carbonate	81.7	27.0
	Unit A-1 Upper Carbonate	108.7	3.0
	Unit A-1 Carbonate	111.7	22.1
	Unit A-1 Evaporite	133.8	2.0
	Unit A0	135.8	2.3
	Guelph	138.1	71.4
	Goat Island	-	-
	Gasport	-	-
	Lions Head	-	-
	Reynales/Fossil Hill	209.5	6.8
	Cabot Head	216.3	15.8
	Manitoulin	232.1	15.6
Ordovician	Queenston	247.7	77.6
	Georgian Bay/Blue Mountain	325.3	154.3
	Cobourg	479.6	46.4
	Sherman Fall	526.0	47.3
	Kirkfield	573.3	39.5
	Coboconk	612.8	8.0
	Gull River	620.8	53.4
	Shadow Lake	674.2	7.6
Cambrian	Cambrian	-	-
Precambrian	Upper Precambrian	681.8	20.0
	Precambrian	701.8	-

Note: Repository location at the hypothetical site is in the Cobourg Formation.

2.2.1.1.1 Basement Geology

The basement geology at the repository site is found at a depth of 682 mBGS. The Precambrian bedrock beneath the repository site is composed of metamorphic rock types ranging from felsic gneiss to mafic metavolcanics to marble.

2.2.1.1.2 Sedimentary Bedrock Geology

The sedimentary rock overlying the Precambrian basement at the repository site has a thickness of 682 m and comprises a thick sequence of limestones and dolostones, as well as shales and evaporites.

Cambrian

The Cambrian lithologies include fine- to medium-grained crystalline dolostones, sandy dolostone, argillaceous dolostone, as well as fine and coarse sandstone. The Cambrian pinches-out against the Precambrian surface and is assumed not to be present at the repository site.

Ordovician

The Ordovician rocks beneath the repository site are composed of a thick sequence of shales overlying carbonates. The Ordovician shales include the Queenston and the Georgian Bay/Blue Mountain Formations, and have a total thickness 232 m. The Ordovician carbonates include the argillaceous limestone of the Cobourg Formation, as well as the limestones of the Sherman Fall and Kirkfield formations. At the base of the Ordovician sequence is the Black River Group, which is comprised of the Shadow Lake, Gull River and Coboconk formations. The Shadow Lake Formation is made up of poorly sorted shales, sandstones and argillaceous dolostones, with rare conglomerates (Armstrong and Carter 2006). The overlying Gull River Formation is composed of limestone. At the top of the Black River Group, the Coboconk is composed of bioclastic limestone.

Overlying the Black River Group is the Trenton Group, which is comprised of the Kirkfield, Sherman Fall and Cobourg formations. The Kirkfield Formation is composed of limestone with thin shale interbeds. The overlying Sherman Fall Formation ranges from argillaceous limestone at its base to fossiliferous limestone in its upper section.

The Cobourg Formation is composed of fine-grained to argillaceous limestone. The Cobourg Formation is the proposed host rock for the repository discussed herein.

The upper part of the Ordovician sequence at the repository site is made up of a thick sequence of shale, and is comprised of the Blue Mountain, Georgian Bay and Queenston formations. The Blue Mountain Formation is composed of non-calcareous shale. The Georgian Bay Formation is composed of shale with intermittent siltstone and limestone interbeds. The Queenston Formation is composed of shale and minor amounts of siltstone, sandstone and limestone (Armstrong and Carter 2010).

Silurian

The Silurian lithologies can be grouped into three sets of formations, the Lower, Middle and Upper Silurian. The Lower Silurian rocks unconformably overlie the Queenston Formation and

are comprised of the Manitoulin and Cabot Head formations. The Manitoulin Formation is composed of argillaceous dolostone with minor shale. The overlying Cabot Head Formation is composed of noncalcareous shale with minor sandstone and carbonate interbeds (Armstrong and Carter 2010).

The Middle Silurian rocks are composed of the Fossil Hill, Lions Head, Gasport, Goat Island and Guelph formations. The Fossil Hill Formation is composed of a fossiliferous dolostone. Lying overtop of the Fossil Hill, the Lions Head, Gasport, Goat Island and Guelph formations form the Niagaran Group, which is included within the regional geologic framework model (Section 2.3.3.2). The Lions Head is a sparsely fossiliferous dolostone with minor chert nodules (Armstrong and Carter 2010). The Gasport Formation is composed of dolostone. The Goat Island is lithologically similar to the Gasport, but is more argillaceous. The Guelph Formation is composed of reefal to inter-reefal dolostones (Armstrong and Goodman 1990). Reefal facies represent pinnacle, patch and barrier reefs.

The Upper Silurian rocks are composed of the Salina Group, which include a thick sequence of carbonates and evaporites. The Salina Group at the repository site includes the following units: Unit A0 (carbonate), Unit A1-Evaporite, Unit A1-Carbonate, Unit A1-Upper Carbonate, Unit A2 Carbonate and Unit B and C (carbonate).

In addition to the Salina units described above, the following units are found regionally: Unit D (carbonate and evaporite), Unit E (carbonate and shale), Unit F (carbonate, shale and evaporite), and Unit G (carbonite, shale, evaporite).

Lying on top of the Salina Group, and at the top of the Silurian lithologies, the Bass Island Formation is composed of microcrystalline dolostone.

Devonian

Overlying the Silurian strata are the Devonian formations and groups, which include the Bois Blanc Formation, the Detroit River Group, the Dundee Formation and the Hamilton Group. These strata are found regionally, but are not present at the hypothetical repository site. The Bois Blanc Formation is composed of cherty dolostone. The Amherstburg and the Lucas formations comprise the Detroit River Group, which is made up of mixed limestones and dolostones. Overlying the Detroit River Group is the Dundee Formation, which is composed of fossiliferous limestones with minor dolostones (Armstrong and Dodge 2007).

Quaternary

The Quaternary cover found at the repository site is composed of a thick sequence of glacial till, glaciofluvial sands and gravels, and glaciolacustrine clays and silts.

2.2.1.2 Surface Features

2.2.1.2.1 Topography

A representative regional area encompassing a watershed was selected for this case study, and is shown in Figure 2-1 with an area of 18,000 km^2. The lateral boundaries for the regional domain were selected to correspond with surface and groundwater divides, which represent planes across which groundwater flow is not expected.

The top surface of the domain was defined by a Digital Elevation Model (DEM) from the Shuttle Radar Topography Mission (SRTM) and a river network in ArcGIS. Based on the assumption that the water table is a subdued reflection of surface topography, the topographic divides representing no-flow boundaries are a reasonable choice for the upper flow regime. The higher permeability Niagaran Group, within the intermediate flow regime, subcrops within the modelling domain, while the western boundary occurs at a groundwater divide beneath Lake Huron. The modelling domain includes the local topographic high in southern Ontario and the domain extends to the deepest portions of both Lake Huron and Georgian Bay. The bathymetric data of both water bodies, provided by National Oceanic and Atmospheric Administration (NOAA), was combined with the DEM to provide a continuous surface for the top of the Earth's solid surface.

The regional watershed and hydrogeologic conditions are described in Section 2.3.

2.2.1.2.2 Surface Hydrology

The regional domain contains two major lakes and is located in the western and northern portions of the regional area, as shown in Figure 2-1. Smaller rivers flowing into the two major lakes can also be found in Figure 2-1.

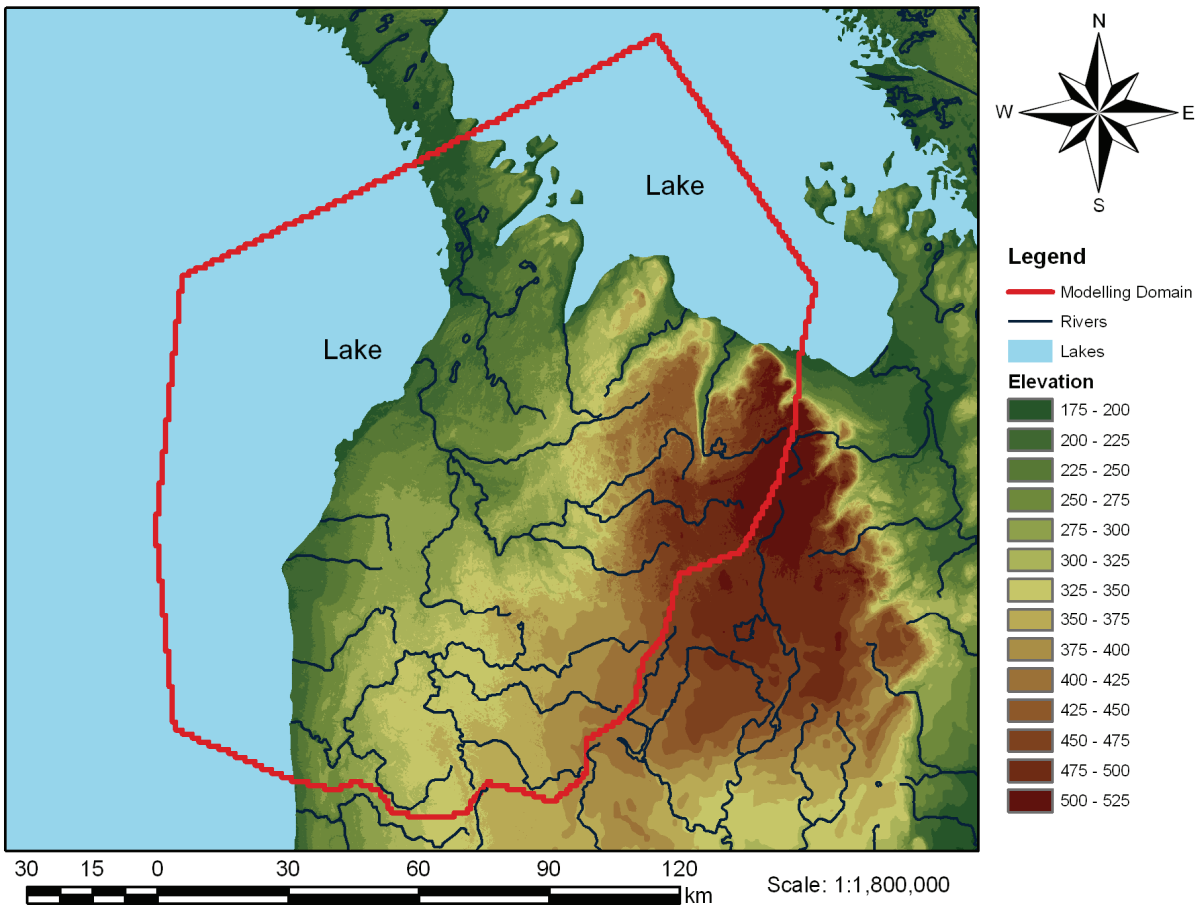

Note: Elevation is measured in metres above sea level (mASL). The elevation for the lakes shown is 176 mASL.

Figure 2-1: Regional Scale Topography

2.2.2 Descriptive Hydrogeologic Model

2.2.2.1 Groundwater Systems

Three groundwater systems are considered for the site. The groundwater systems are identified, in part, by the regional distribution of hydraulic conductivities, as well as groundwater total dissolved solids (TDS) concentrations and redox conditions (a detailed geochemical conceptual model is presented in Section 2.2.3). The primary characteristics of the three groundwater systems are described below.

Shallow Groundwater System (0 - 215 mBGS)

The shallow groundwater system, located near surface, is predominately driven by local- and sub-regional scale topographic changes. Meteoric water, in the form of rain or snowmelt, initially recharges the groundwater system by infiltration in near surface weathered zones, and flows from topographic highs near the surface before discharging into streams, rivers, lakes or swamps and bogs associated with local topographic lows. The average travel time for groundwater to recharge, and then subsequently discharge, in the shallow groundwater zone is typical less than 1,000 years. The groundwater in the shallow groundwater zone is fresh and oxygen-rich, with low TDS concentrations (further discussion can be found in Section 2.2.3).

Intermediate Groundwater System (215 - 250 mBGS)

The groundwater in the intermediate groundwater system transitions from fresh and oxygen-rich, to more mineralized and chemically reducing with depth. At the hypothetical site, the shift from oxidizing to reducing conditions occurs within this system. In the intermediate groundwater system, larger domains of low permeability rock tend to decrease mass transport rates.

Deep Groundwater System (> 250 mBGS)

In contrast to the shallow and intermediate groundwater zones, groundwaters in the deep system have higher total dissolved solids concentrations and, hence, higher fluid densities. The geochemical redox potential is reducing. The increased fluid density will influence both energy gradients within the groundwater regime and vertical upward movement of groundwater between the shallow/intermediate and deep groundwater zones (Park et al. 2009).

2.2.2.2 Hydraulic Parameters

The key hydraulic parameters, including the horizontal and vertical hydraulic conductivities (K_H, and K_V respectively), anisotropy ratio for the hydraulic conductivity ($K_H : K_V$), porosity, specific storage (S_s), tortuosity (τ), fluid density, and loading efficiencies (ζ) for the hypothetical site are shown in Table 2-2.

Table 2-2: Regional Hydrogeologic Parameters

Formation	Unit Top Depth (mBGS)	Thickness (m)	K_H (m/s)	K_V (m/s)	$K_H : K_V$	Porosity	Fluid Density (kg/m^3)	Initial TDS (g/L)	S_s [1] (m^{-1})	ζ [1]	τ [2]
Drift	0	29.4	$1x10^{-7}$	$5x10^{-8}$	2:1	0.2	1,000	0	$1x10^{-4}$	0.99	$4.00x10^{-1}$
Hamilton Group	-	-	$2x10^{-11}$	$2x10^{-12}$	10:1	0.1	1,008	12	$2x10^{-6}$	0.8	$1.19x10^{-1}$
Dundee	-	-	$8x10^{-8}$	$8x10^{-9}$	10:1	0.1	1,005	8	$2x10^{-6}$	0.8	$1.19x10^{-1}$
Detroit River Group	-	-	$6x10^{-7}$	$2x10^{-8}$	30:1	0.077	1,001	1.4	$1x10^{-6}$	0.84	$1.56x10^{-1}$
Bois Blanc	-	-	$1x10^{-7}$	$1x10^{-8}$	10:1	0.077	1,002	3.2	$1x10^{-6}$	0.84	$1.56x10^{-1}$
Bass Islands	-	-	$5x10^{-5}$	$2x10^{-6}$	25:1	0.056	1,004	6	$2x10^{-6}$	0.92	$1.07x10^{-1}$
Unit G	-	-	$1x10^{-11}$	$1x10^{-12}$	10:1	0.172	1,010	14.8	$1x10^{-6}$	0.55	$3.01x10^{-3}$
Unit F	-	-	$5x10^{-14}$	$5x10^{-15}$	10:1	0.1	1,040	59.6	$1x10^{-6}$	0.68	$4.93x10^{-2}$
Unit F Salt	-	-	$5x10^{-14}$	$5x10^{-15}$	10:1	0.1	1,040	59.6	$1x10^{-6}$	0.68	$4.93x10^{-2}$
Unit E	-	-	$2x10^{-13}$	$2x10^{-14}$	10:1	0.1	1,083	124	$7x10^{-7}$	0.51	$5.66x10^{-2}$
Unit D	-	-	$2x10^{-13}$	$2x10^{-14}$	10:1	0.089	1,133	200	$6x10^{-7}$	0.53	$6.35x10^{-2}$
Unit B and C	29.4	52.3	$4x10^{-13}$	$4x10^{-14}$	10:1	0.165	1,198	296.7	$1x10^{-6}$	0.38	$8.75x10^{-2}$
Unit B Anhydrite	-	-	$3x10^{-13}$	$3x10^{-14}$	10:1	0.089	1,214	321	$7x10^{-7}$	0.53	$1.04x10^{-3}$
Unit A-2 Carbonate	81.7	27	$3x10^{-10}$	$3x10^{-11}$	10:1	0.12	1,091	136	$7x10^{-7}$	0.46	$1.20x10^{-2}$

Table 2-2: Regional Hydrogeologic Parameters (Continued)

Formation	Unit Top Depth (mBGS)	Thickness (m)	K_H (m/s)	K_V (m/s)	$K_H : K_V$	Porosity	Fluid Density (kg/m^3)	Initial TDS (g/L)	S_s [1] (m^{-1})	ζ [1]	τ [2]
Unit A-2 Evaporite	-	-	$3x10^{-13}$	$3x10^{-14}$	10:1	0.089	1,030	45.6	$6x10^{-7}$	0.53	$1.04x10^{-3}$
Unit A-1 Upper Carbonate	108.7	3	$2x10^{-7}$	$2x10^{-7}$	1:1	0.07	1,019	28.6	$5x10^{-7}$	0.59	$1.17x10^{-1}$
Unit A-1 Carbonate	111.7	22.1	$9x10^{-12}$	$9x10^{-13}$	10:1	0.019	1,128	192	$4x10^{-7}$	0.84	$1.14x10^{-2}$
Unit A-1 Evaporite	133.8	2	$3x10^{-13}$	$3x10^{-14}$	10:1	0.007	1,217	325	$4x10^{-7}$	0.94	$5.16x10^{-3}$
Unit A0	135.8	2.3	$3x10^{-13}$	$3x10^{-14}$	10:1	0.032	1,240	360	$5x10^{-7}$	0.76	$1.13x10^{-3}$
Guelph	138.1	71.4	$3x10^{-8}$	$3x10^{-8}$	1:1	0.057	1,247	370	$4x10^{-7}$	0.47	$6.12x10^{-1}$
Goat Island	-	-	$2x10^{-12}$	$2x10^{-13}$	10:1	0.02	1,200	300	$3x10^{-7}$	0.72	$9.03x10^{-3}$
Gasport	-	-	$2x10^{-12}$	$2x10^{-13}$	10:1	0.02	1,200	300	$3x10^{-7}$	0.72	$9.03x10^{-3}$
Lions Head	-	-	$5x10^{-12}$	$5x10^{-13}$	10:1	0.031	1,200	300	$3x10^{-7}$	0.62	$4.66x10^{-1}$
Rochester	-	-	$5x10^{-12}$	$5x10^{-13}$	10:1	0.031	1,200	300	$3x10^{-7}$	0.62	$4.66x10^{-1}$
Reynales/Fossil Hill	209.5	6.8	$5x10^{-12}$	$5x10^{-13}$	10:1	0.031	1,200	300	$3x10^{-7}$	0.62	$1.67x10^{-3}$
Cabot Head	216.3	15.8	$9x10^{-14}$	$9x10^{-15}$	10:1	0.116	1,204	306	$1x10^{-6}$	0.6	$3.22x10^{-2}$

Formation	Unit Top Depth (mBGS)	Thickness (m)	K_H (m/s)	K_V (m/s)	$K_H : K_V$	Porosity	Fluid Density (kg/m^3)	Initial TDS (g/L)	S_s [1] (m^{-1})	ζ [1]	τ [2]
Manitoulin	232.1	15.6	$9x10^{-14}$	$9x10^{-15}$	10:1	0.028	1,233	350	$8x10^{-7}$	0.86	$6.45x10^{-3}$
Queenston	247.7	77.6	$2x10^{-14}$	$2x10^{-15}$	10:1	0.073	1,207	310	$9x10^{-7}$	0.71	$1.65x10^{-2}$
Georgian Bay/Blue Mountain	325.3	154.3	$4x10^{-14}$	$3x10^{-15}$	13:1	0.07	1,200	299.4	$1x10^{-6}$	0.79	$1.41x10^{-2}$
Cobourg	479.6	46.4	$2x10^{-14}$	$2x10^{-15}$	10:1	0.015	1,181	272	$3x10^{-7}$	0.8	$2.97x10^{-2}$
Sherman Fall	526	47.3	$1x10^{-14}$	$1x10^{-15}$	10:1	0.016	1,180	270	$5x10^{-7}$	0.88	$1.65x10^{-2}$
Kirkfield	573.3	39.5	$8x10^{-15}$	$8x10^{-16}$	10:1	0.021	1,156	234	$5x10^{-7}$	0.85	$2.41x10^{-2}$
Coboconk	612.8	8	$4x10^{-12}$	$4x10^{-15}$	1,000:1	0.009	1,170	255	$5x10^{-7}$	0.93	$3.61x10^{-2}$
Gull River	620.8	53.4	$7x10^{-13}$	$7x10^{-16}$	1,000:1	0.022	1,135	203	$5x10^{-7}$	0.85	$1.42x10^{-2}$
Shadow Lake	674.2	7.6	$1x10^{-9}$	$1x10^{-12}$	1,000:1	0.097	1,133	200	$7x10^{-7}$	0.56	$1.61x10^{-2}$
Cambrian	-	-	$3x10^{-6}$	$3x10^{-6}$	1:1	0.071	1,157	235	$4x10^{-7}$	0.34	$2.88x10^{-1}$
Upper Precambrian	681.8	20	$1x10^{-10}$	$1x10^{-10}$	1:1	0.038	1,200	300	$3x10^{-7}$	0.49	$9.50x10^{-3}$
Precambrian	701.8	-	$1x10^{-12}$	$1x10^{-12}$	1:1	0.005	1,200	300	$2x10^{-7}$	0.88	$7.22x10^{-2}$

Notes: For this study, the permeability of the upper 50 m of the domain is set to $1.0x10^{-7}$ m/s in order to reflect weathering of the geologic units near surface.
[1] S_s represents specific storage and ζ represents loading efficiencies.
[2] The estimated tortuosities for formations below the drift are based upon a free solution diffusion coefficient for NaI of 1.662E-9 m^2/s (Weast 1983), porosity values specified above, the effective diffusion coefficients ($D_{e,v}$) for NaI in Table 1 of APM-REF-01900-29841, assuming a diffusion accessible porosity factor of 0.5 for NaI (INTERA 2011). The tortuosity for the drift was adopted from Sykes et al. (2011).

2.2.2.3 Paleohydrogeology Boundary Conditions

Paleohydrogeological simulations are used to illustrate the long-term evolution and stability of the geosphere to external perturbations. Glaciation is expected to be the largest external perturbation to which the repository would be subjected.

Over the last one million years, the sedimentary rocks chosen for the host rock at the repository site have been subjected to nine glacial cycles, each lasting for a period of approximately 100,000 years (Peltier 2002). During the last glacial advance and retreat, up to three kilometres of ice overrode the hypothetical repository site. In assessing the long-term stability and evolution of groundwater systems at depth in sedimentary rock, the loading and unloading of the geosphere by the glacier will represent one of the most significant perturbations from the current conditions.

The University of Toronto (UofT) Glacial Systems Model (GSM) provides the hydraulic and mechanical paleoclimate boundary conditions and permafrost depths for the paleohydrogeologic simulations (Peltier 2011). Peltier (2011) describes eight models that "span the apparent range of model characteristics that provide acceptable fits to the totality of the observational constraints." Of these eight models, nn9921 and nn9930 are two of the best models based on aggregate misfit, and both include high-resolution permafrost development. Paleoclimate simulation nn9930 represents a single realization of a glacial cycle, as predicted by the GSM. A plot of various nn9930 GSM outputs for the grid cell containing the sub-regional modelling domain is shown in Figure 2-2. These outputs include ice thickness, meltwater production rate, lake depth, permafrost depth, and ice-sheet basal temperature relative to the pressure melting point of ice. Only the ice thickness, lake depth, and permafrost depth outputs are applied to the paleohydrogeologic groundwater simulations. The isostatic movement of the ground surface due to ice loading is not considered; applied hydraulic boundary conditions are stated in terms of elevation, assuming the grid does not move vertically. The application of lake depth is also a relative term independent of isostatic movement, although isostatic depression is required for a proglacial lake to form. Although lake depth could be interpolated across the TIN (Triangulated Irregular Network) in a similar manner to permafrost depth and vertical stress due to ice, large gradients could be created across the domain which would not exist in the presence of a large proglacial body of water because isostatic movement is not considered. Due to this, lake depth is added to the existing lake elevation and the hydraulic boundary conditions are adjusted accordingly.

The alternate paleoclimate simulation, nn9921, GSM model outputs for the grid cell containing the sub-regional modelling domain are shown in Figure 2-3. The paleoclimate simulation nn9921 represents a cold-based ice sheet, whereas paleoclimate simulation nn9930 represents a warm-based ice sheet. The main difference between the two glaciation scenarios is the duration of permafrost during the 121,000 years GSM simulation; the length of time nn9930 is subject to permafrost and glaciated conditions is less than that of nn9921. In addition, more frequent glacial advances and retreats occur in paleoclimate simulation nn9921. The paleoclimate boundary conditions presented in Figure 2-2 and Figure 2-3 are applied to the paleoclimate simulations described in Section 2.3.4.3. Permafrost hydraulic conductivity is discussed in Section 2.3.3.2.1.

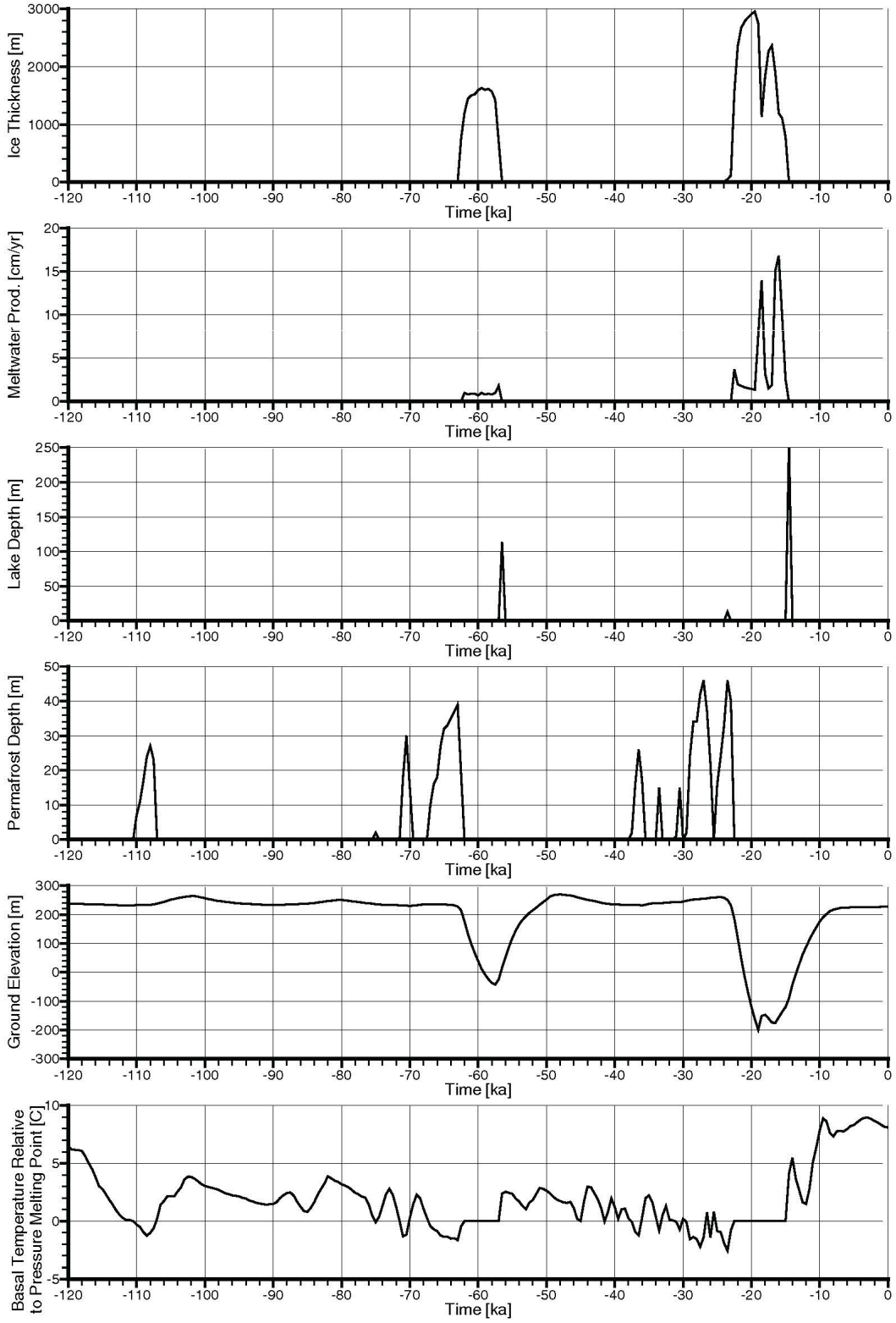

Figure 2-2: nn9930 GSM Model Outputs for the Grid Block Containing the Repository Footprint for this Study

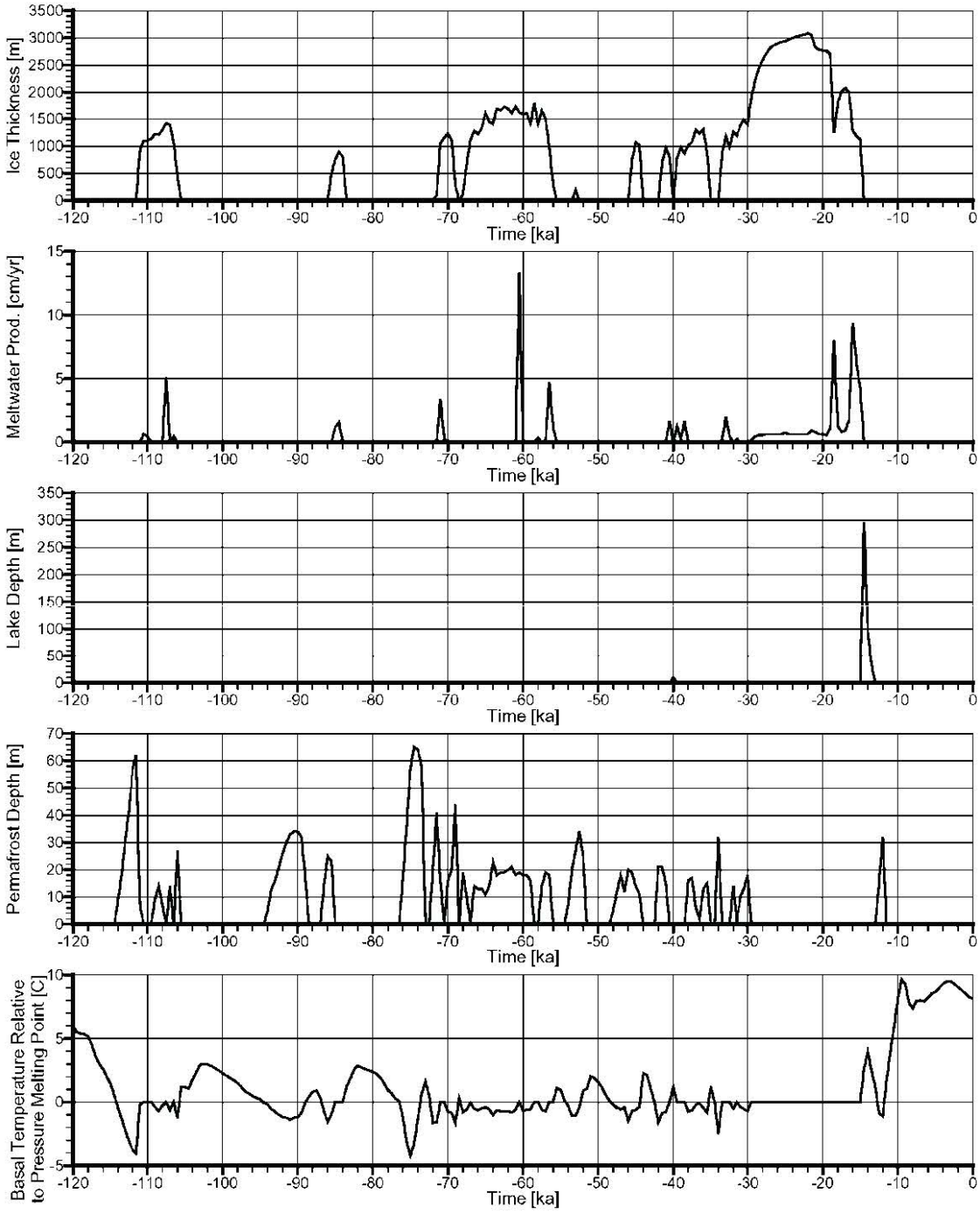

Figure 2-3: nn9921 GSM Model Outputs for the Grid Block Containing the Repository Footprint for this Study

2.2.2.4 Abnormal Pressure Distributions

Within the Michigan Basin, abnormal pressure distributions have been observed. Where the Cambrian Formation is present within the regional area, overpressures with respect to ground elevation have been observed in the formation (NWMO 2011). However, the Cambrian Formation is not present at the hypothetical site. For the purpose of this study, hydrostatic pressure with depth is assumed at the repository site.

2.2.2.5 Unsaturated Groundwater Flow

Although there is evidence of residual gas phases in some formations in the Michigan Basin, the geoscience scenarios investigated for this study only consider fully-saturated groundwater flow.

2.2.3 Descriptive Geochemical Model

Groundwaters and porewaters in sedimentary basin environments can often be typified by the following characteristics.

- $\delta^{18}O$ and $\delta^{2}H$ signatures are enriched relative to the Global Meteoric Water Line (GMWL), typically plotting to the right and below the GMWL on a plot of $\delta^{18}O$ versus $\delta^{2}H$.
- Formation waters are attributed to an ancient seawater or evaporated seawater origin, with relatively high concentrations of sodium (Na), calcium (Ca) and chloride (Cl).
- Variations in formation water chemistry from a seawater or evaporated seawater signature are often attributed to a variety of natural processes, such as water-rock interaction, mixing with other waters, dilution, and microbially-mediated reactions. Groundwater and porewater geochemistry is modified over both time and space by such processes.
- High total dissolved solids (TDS) concentrations which are typical of sedimentary formations as a result of the aforementioned processes.

The regional hydrogeochemical data (presented in Hobbs et al. 2011) generally indicates increasing salinity with depth below ground surface in southwestern Ontario. A vertical salinity profile, between ground surface and a depth of 865 m, collected at the Bruce site (presented in NWMO 2011; Figure 4.6), located near Tiverton, Ontario, is consistent with the regional trend.

Numerous geochemical processes have been proposed to account for the high salinity of sedimentary brines. In the context of southern Ontario, processes that are considered possible include:

1. The evaporation of seawater (e.g., Carpenter 1978, Kharaka et al. 1987);
2. The dissolution of halite or other evaporites (e.g., Rittenhouse 1967, Land and Prezbindowski 1981);
3. Membrane filtration (Bredehoeft et al. 1963, Berry 1969, Kharaka and Berry 1973, Graf 1982); and/or
4. Ingress of concentrated brines from crystalline shield-type rocks (e.g., Land 1997).

It is generally agreed that most chloride in sedimentary basin brines has been derived from some combination of entrapped and/or infiltrated evaporated seawater and dissolved, subsurface evaporites (e.g., Kharaka and Hanor 2005, Hanor 2001).

Sedimentary formation waters typically have chemistries that vary considerably from what would be expected of evaporated meteoric water or seawater. During the diagenetic evolution of the brines, calcium and strontium concentrations can increase by up to an order of magnitude compared to evaporated seawater, whereas magnesium and potassium concentrations may decrease by as much as an order of magnitude (Kharaka and Hanor 2005). Variations in the chemistry of brines from that expected for evaporated seawater are often explained using water-rock reaction processes, including:

1. Dissolution or precipitation of evaporite minerals, including halite and gypsum and/or anhydrite;
2. Calcite precipitation or dissolution;
3. Dolomitization;
4. Dissolution or precipitation of aluminosilicates; and
5. Ion exchange reactions with clays (e.g., McIntosh and Walter 2006).

Dolomitization is the most extensive diagenetic process to have influenced the sedimentary sequence underlying southern Ontario (Hobbs et al. 2011).

Information on the geochemical conditions collected as part of detailed site characterization activities would be combined with available regional information to define site-specific conditions. The geochemical conditions in the shallow, intermediate and deep groundwater systems assumed for the hypothetical site are described below. Microbiology, sorption, and the anticipated gas species in groundwaters within the sedimentary setting at the proposed repository horizon are also described in Sections 2.2.3.1 to 2.2.3.3, respectively.

For the site, a hypothetical TDS profile (presented in Section 2.3.4.1), suggests the presence of three distinct groundwater systems within the sedimentary package: a shallow system (0-215 m), consisting of relatively fresh water, with TDS of ≤ 5 g/L; an intermediate system (215-250 m); and, a deep system (>250 m) with significantly elevated groundwater and porewater salinities (200-300 g/L TDS). The transition zone between the shallow and deep systems is loosely termed the intermediate system, which is marked by a change in salinity from ~5 g/L TDS to ~275 g/L over a vertical distance of approximately 35 m.

Table 2-3 shows the average TDS (g/L) values, which are based on the modelled salinity profile presented in Section 2.3.4.1. The groundwaters and porewaters in the sedimentary formations at the site show the following general salinity distribution trends with depth. The TDS values are indicative of relatively fresh water (<5 g/L) in the shallow system between ground surface and 215 m depth. The TDS values begin to increase at the base of the Fossil Hill Formation (215 m). Between the base of the Fossil Hill Formation and the top of the Manitoulin Formation, TDS values increase from ~5 g/L to ~260 g/L. Maximum salinity (~290 g/L) is projected to occur near the contact between the Queenston Formation and the Georgian Bay/Blue Mountain Formation at a depth of approximately 330 m. Salinity values are relatively consistent with depth through the remainder of the shales until just above the Georgian Bay/Blue

Mountain-Cobourg Formation contact, where TDS values begin to decrease steadily with depth to a value of 200 g/L in the Shadow Lake Formation (680 m).

The geochemical conditions described below pertain to the overall properties of both the groundwaters and porewaters present within the shallow, intermediate and deep groundwater systems at the hypothetical site.

Shallow Groundwater System (0 - 215 mBGS)

The shallow groundwater system extends from ground surface to approximately 215 m depth. The shallow groundwater system is characterized by relatively fresh waters (<5 g/L TDS) and includes the Quaternary, Late Silurian and Middle Silurian groundwaters and porewaters. Based on regional observations, as well as data collected at the Bruce site, the shallow groundwater system is expected to be oxidizing.

Intermediate Groundwater System (215 - 250 mBGS)

The intermediate groundwater system is characterized by a transition in salinity from approximately 5 g/L TDS at the top of the Cabot Head Formation to a salinity of approximately 275 g/L TDS at the base of the Manitoulin Formation, over a vertical distance of ~35 m. The intermediate groundwater system represents a transition zone from oxidizing to reducing conditions as well (NWMO 2011). Although no site-specific data exists, similar conditions are anticipated for the hypothetical site. Such conditions would be verified during site characterization activities.

Deep Groundwater System (>250 mBGS)

The deep groundwater system is characterized by high salinity, ranging between 200 and 300 g/L TDS. Based on regional data, as well as data collected at the Bruce site, reducing conditions are expected at all depths below 250 m.

Table 2-3: Average TDS Values for Sedimentary Formation Groundwaters and Porewaters

Formation	Average TDS (g/L)
Drift	0.1
Unit B and C	0.3
Unit A-2 Carbonate	0.6
Unit A-1 Upper Carbonate	0.8
Unit A-1 Carbonate	2
Unit A-1 Evaporite	3
Unit A-0	3
Guelph	3
Reynales/Fossil Hill	4
Cabot Head	12
Manitoulin	142
Queenston	294
Georgian Bay/Blue Mountain	298
Cobourg	279
Sherman Fall	260
Kirkfield	244
Coboconk	235
Gull River	219
Shadow Lake	204
Upper Precambrian	203
Precambrian	250

Saline groundwater conditions are expected at the depth of the hypothetical repository (500 mBGS). Groundwater chemistry at this depth in sedimentary formations of southern Ontario is typically Na-Ca-Cl or Ca-Na-Cl water under reducing conditions (Hobbs et al. 2011). A reference composition has been defined for the porewaters anticipated to be found within the proposed repository horizon. The composition is presented in Table 2-4.

Table 2-4: Reference SR-270-PW Composition

Composition	SR-270-PW
Water Type	Na-Ca-Cl
pH	5.8
Environment Type	Reducing
Eh	-200 mV
Density	1,181
Solutes (mg/L)	
Na	50,100
K	12,500
Ca	32,000
Mg	8,200
HCO_3	110
SO_4	440
Cl	168,500
Br	1,700
Sr	1,200
Li	5
F	1
I	3
B	80
Si	4
Fe	30
NO_3	<5
PO_4	-
TDS	275,000

Based on diffusion experiments performed on core collected during site investigations at the Bruce site, effective diffusion coefficients (D_e) for iodide and tritiated water (HTO) were estimated for the proposed host rock, and for the surrounding Silurian and Ordovician shale and carbonate rocks. The D_e values obtained with HTO are on average 1.9 times greater than the D_e values obtained with an iodide tracer. The D_e values at the hypothetical site are anticipated to be similar to those measured for the Bruce site (see below), but would have to be verified during site characterization activities:

Silurian carbonate: 10^{-13} to 10^{-10} m^2/s, and

Ordovician shale and carbonate: 10^{-13} to 10^{-11} m^2/s (INTERA 2011).

2.2.3.1 Microbial Conditions in Sedimentary Environments

A number of studies have been performed on sedimentary rock in attempts to characterize microbial populations and activities. Microbial metabolism requires a carbon source, a terminal electron donor and terminal electron acceptor. Additional nutrients are required for growth and maintenance, including nitrogen (N), phosphorous (P), sulfur (S), potassium (K), magnesium (Mg), sodium (Na), calcium (Ca) and iron (Fe), as well as a suite of other trace elements. Subsurface microbial communities are capable of using an array of terminal electron accepting processes. The dominant species in a given environment tend to be those bacteria that generate the most energy from the available nutrient sources.

Some of the most extensive work on microbial activity in low permeability sedimentary systems has been performed on the Opalinus Clay Formation at the Mont Terri Rock Laboratory in Switzerland. Clay-rich formations, such as the Opalinus Clay, have been the focus of significant attention as possible host formations for nuclear waste repositories due to their low permeability, diffusion-dominated transport regimes, geochemical stability and capacity for self-sealing (Wersin et al. 2011, Stroes-Gascoyne et al. 2011). Due to the low salinity of the waters at Mont Terri, application of the results of such studies to the hypothetical site is somewhat limited. However, aspects of the Mont Terri work are relevant to the hypothetical site in the context of repository safety. A key result of the work indicated that contamination during drilling could promote anaerobic microbial activity (in particular, NO_3-, Fe- and SO_4- reducers and methanogens; Wersin et al. 2011, Stroes-Gascoyne et al. 2011) and that the effects of drilling and excavation disturbances are both temporary and spatially limited. In a state-of-science review documenting the role of microorganisms in relation to the design and performance of a DGR, Sherwood Lollar (2011) concluded that hydrology, geochemistry, and resident microbial populations may be sensitive to changes (i.e., perturbations) in any given system, but that many systems possess a geochemical buffering capacity to counter the effects of perturbations. In the context of the hypothetical site, properties of the deep system, such as low porosity and very high salinity, are anticipated to provide a natural buffering capacity to the proposed host and surrounding rock.

Microbial analyses were performed on samples of Queenston Formation shale and Cobourg Formation limestone from drill core collected during site characterization activities at the Bruce nuclear site (Stroes-Gascoyne and Hamon 2008). Samples of crushed and powdered Cobourg limestone, and samples of crushed Queenston shale, were analyzed for microbial activity. Crushed or powdered rock samples were suspended in a buffering solution or a synthetic porewater solution and plated on regular agar. The synthetic porewater solutions were intended to simulate geochemical conditions (e.g., high salinity, low water activity) at depth and the results used to assess the likelihood of a sustainable microbial community under such conditions. The results of the analyses indicate only the presence of common near-surface aerobic and anaerobic microorganisms, which were attributed to contamination of the rock samples after core recovery. Samples were analyzed for the presence of phospho-lipid fatty acid (PLFA), neutral-lipid fatty acid (NLFA) and glycol-lipid fatty acid (GLFA) as a means to measure microbial activity. The presence of PLFA is used to indicate viable (live) microbial cells, while NLFA and GLFA are indicators of dead cells. In the Cobourg Formation powdered limestone sample, no viable biomass was identified and only NLFA and GLFA were identified, indicating a lack of on-going microbial activity. Based on the existing microbiological data for deep sedimentary formations, it is anticipated that similar conditions – i.e., low water activity,

low microbial activity – would occur at the hypothetical site at the proposed repository depth of 500 m.

2.2.3.2 Sorption

The sorption of radionuclides onto mineral surfaces within the geosphere is a potential mechanism for slowing the transport of radionuclides from the repository to the surface environment. There are many factors that impact radionuclide sorption processes in the geosphere, such as rock type, mineral surface area, groundwater salinity, pH, redox conditions, temperature, the presence or absence of complexing ligands and radionuclide concentration.

Sorption of radionuclides is generally reduced in groundwaters with high salinity (Vilks 2009). Experiments to develop a further understanding of sorption processes in Na-Ca-Cl brine solutions within Canadian sedimentary rocks were initiated in 2009 (Vilks et al. 2011). Sorption of several elements on shale and limestone was tested in Na-Ca-Cl brine solutions with TDS values as high as 300 g/L. The results demonstrated that some elements will not sorb, notably elements such as Sr(II) that sorb by ion exchange. The results showed that sorption of other elements, including Eu(III) (an analogue to trivalent actinides), and U(VI) to shale and limestone is measurable in brine solutions (Vilks et al. 2011). The formation of complexes with carbonate was observed to reduce the sorption of Eu(III) and U(VI).

2.2.3.3 Gas Characterization

Natural gases commonly encountered in deep sedimentary formations include methane, helium and carbon dioxide. Both concentrations and isotopes of methane, helium and carbon dioxide can be helpful in assessing fluid origin and solute transport.

Sherwood Lollar et al. (1994) examined natural gases from within Ordovician and Cambrian reservoirs in southwestern Ontario, and characterized the gases using isotopic and compositional indicators. Consistent with the findings of Barker and Pollock (1984), gases from the Cambrian and Ordovician reservoirs are composed predominantly of CH_4. The Cambrian and Ordovician gases were found to be thermogenic in origin, with no evidence of bacterial CH_4 contributions. Where the sedimentary rocks were in direct contact with the Precambrian basement, the gases sampled had elevated helium concentrations (Sherwood Lollar et al. 1994). The elevated helium concentrations, and associated high $^3He/^4He$ ratios, may reflect mixing between gases generated in-situ (in the Cambrian and Ordovician strata) and an end-member enriched in helium. Possible sources for the helium-rich end-member include gas deep within the Precambrian basement rock or an external helium-enriched fluid that migrated from deeper within the sedimentary system along pathways controlled by basement-structures (Sherwood Lollar et al. 1994).

Data collected at the Bruce site is generally consistent with regional scale findings. Thermogenic methane has been identified in the Ordovician Trenton and Black River Groups, while the overlying shales and Cobourg Formation are characterized by the presence of biogenic methane (NWMO 2011; Section 4.4.3.1). There is little evidence of mixing between the biogenic and thermogenic gas, and it is hypothesized that the thermogenic methane may have been generated in-situ in association with peak burial and/or has been transported from a deeper basinal or Precambrian source. $^3He/^4He$ ratios in the Trenton and Black River groups are observed to be elevated relative to the overlying Ordovician shales, and also relative to

values estimated for in-situ formation due to natural decay processes in the rock, which suggests an enriched end-member for mixing, possibly of deep basin or Precambrian origin. Carbon dioxide was also analyzed for both concentration and isotopic composition, but only the isotopic data is considered to be reliable for interpretation purposes. The isotopic composition ($\delta^{13}C$ and $\delta^{18}O$ of CO_2) of the carbon dioxide is consistent with the assessment of biogenic gas formation in the Ordovician shales and thermogenic (non-biotic) gas formation in the Trenton and Black River groups.

At the hypothetical site, which, like the Bruce site, is located along the eastern margin of the Michigan Basin, it is anticipated that similar gas distributions and signatures would be observed. This would require verification during site characterization activities.

2.3 Regional Scale Hydrogeologic Modelling

The primary objective of the analyses of this section is to investigate the role of key geosphere parameters and processes, such as sedimentary rock permeabilities and groundwater salinity, on geosphere stability at repository depth. The following sections describe the suite of regional scale numerical groundwater models that were developed.

2.3.1 Computational Models

The numerical groundwater modelling was performed using FRAC3DVS-OPG v1.3.0 (Therrien et al., 2010). This computational model is designed to solve the equation for three-dimensional variably-saturated groundwater flow and solute transport in discretely-fractured media. The numerical solution to the governing equations is based on implementations of both the control volume finite element method and the Galerkin finite-element method. The FRAC3DVS-OPG model couples fluid flow with salinity transport through fluid density, which is dependent on the total dissolved solids concentration. Details of the model that are pertinent to the study are described in Therrien et al. (2010) and in Normani et al. (2007). FRAC3DVS-OPG was developed and is maintained as nuclear grade software in a Quality Assurance framework. Details on the validation of FRAC3DVS-OPG are found in Therrien et al. (2010).

Important attributes of FRAC3DVS-OPG include:

1. Its ability to describe arbitrary combinations of porous, discretely fractured and dual porosity media;
2. Its flexible pre- and post-processing capabilities;
3. The accurate handling of fluid and mass exchanges between fracture zones and matrix, including matrix diffusion effects and solute advection in the matrix;
4. Fluid and solute mass balance tracking; and
5. Adaptive time-stepping schemes with automatic generation and control of time steps.

Additional attributes added in previous work supported by the NWMO and OPG includes sub-gridding and sub-timing capabilities (Park et al. 2008). Additionally, algorithms to estimate performance measures of groundwater age and life expectancy for the domain groundwater are available also (Cornaton and Perrochet 2006a, 2006b).

2.3.2 System Performance Measures

The safety case for a potential deep geologic repository relies, in part, on the ability of the geosphere to provide a long-term barrier to solute transport. The behaviour and stability of the groundwater flow and transport regimes found at repository depth can be illustrated by determining and quantifying what impact, if any, the variability of model parameters will have upon the model results. By demonstrating and determining the sensitivity of the model to perturbations in model parameters, a more rigorous understanding of the groundwater system at depth can be achieved.

Common measures of the performance of a groundwater system include the flow state variables of equivalent freshwater head or environmental head and the derived porewater velocity, the solute concentration for a conservative tracer, the Péclet number of molecular diffusion (Bear 1988, Huysmans and Dassargues 2005) and, as shown in Normani et al. (2007), mean lifetime expectancy (MLE) and groundwater age. Lifetime expectancy can be estimated by determining the Probability Density Function (PDF) for the time required for water particles at a spatial position in a groundwater system to reach potential outflow points. Particles can migrate to the boundary by both advection and hydrodynamic dispersion; particles at a given point in the system will not follow the same path to the boundary due to hydrodynamic dispersion. In this case study, the first moment of the PDF for lifetime expectancy is estimated with the value being expressed as the MLE. MLE correctly replicates the transport processes, but is subject to the classical problems of numerical instability. For a model with large grid blocks and, hence, a large numerical dispersivity that meets grid or cell Péclet number criteria, MLE tends to underestimate the average time for particles to reach discharge points.

2.3.3 Regional Scale Conceptual Model

2.3.3.1 Model Domain and Spatial Discretization

The regional scale modelling domain boundary was chosen by Sykes (2007). The southeastern portion of the boundary follows the regional surface water divides. These divides were determined using a Digital Elevation Model (DEM) from the Shuttle Radar Topography Mission (SRTM) and a river network in ArcGIS. Based on the assumption that the water table is a subdued reflection of surface topography, topographic divides are chosen as no-flow boundaries for the upper flow regime, as well as for the higher permeability Niagaran Group within the intermediate flow regime. The eastern boundary of the modelling domain is at a topographic high (west of the Algonquin Arch) and the domain extends to the deepest portions of both the lakes to the north and west. The bathymetric data of both water bodies, provided by National Oceanic and Atmospheric Administration (NOAA), was combined with the DEM to provide a continuous surface for the top of the Earth's solid surface.

The reference case data set for the conceptual model consists of 32 stratigraphic units, as defined by the 3DGF geologic framework model (Table 2-2 from ITASCA CANADA and AECOM 2011). In this case study, the Niagaran Group in the 3DGF model was divided into the Guelph, Goat Island, Gasport, and Lions Head (Rochester) formations; the A-1 Carbonate unit in the 3DGF was divided into the A1-Upper Carbonate and the A1-Carbonate. Some stratigraphic units are sub-divided into multiple model layers, as shown in Table 2-5. In total, 102 model layers were developed for the regional scale domain.

Table 2-5: Sub-divisions of Geologic Formations

Period	Formation	Model Layers
Quaternary	Drift	1
Devonian	Hamilton Group	1
	Dundee	2
	Detroit River Group	6
	Bois Blanc	1
Silurian	Bass Islands	2
	Unit G	1
	Unit F	1
	Unit F Salt	1
	Unit E	1
	Unit D	1
	Units B and C	4
	Unit B Anhydrite	2
	Unit A-2 Carbonate	6
	Unit A-2 Evaporite	6
	Unit A-1 Upper Carbonate	6
	Unit A-1 Carbonate	6
	Unit A-1 Evaporite	4
	Unit A0	4
	Guelph	6
	Goat Island	2
	Gasport	2
	Lions Head/Rochester	2
	Reynales/Fossil Hill	1
	Cabot Head	1
	Manitoulin	1
Ordovician	Queenston	2
	Georgian Bay/Blue Mtn.	3
	Cobourg	1
	Sherman Fall	1
	Kirkfield	1
	Coboconk	1
	Gull River	1
	Shadow Lake	4
Cambrian	Cambrian	6
Precambrian	Upper Precambrian	4
	Precambrian	6

A two-dimensional square grid (1 km × 1 km) was developed to fit within the conceptual model boundary. The grid has an east-west extent of 152 km, a north-south extent of 179 km, and covers an area of 18,887 km^2. The two-dimensional grid forms a horizontal template to develop the three-dimensional grid by interpolating the vertical position of each node from the 32 interfaces provided by ITASCA CANADA and AECOM (2011). Four additional interfaces are generated by the refinement of both the Niagaran Group and the A-1 Carbonate.

A block-cut view of the assigned FRAC3DVS-OPG geologic layer zone identifiers within the model domain are shown in Figure 2-4. Each zone identifier is associated with a specific geologic layer or geologic grouping. Note that the vertical exaggeration is 40:1 in this and other figures showing the regional scale spatial domain (152 km × 179 km). A view of all geologic units and the spatial variation in their thickness is shown in Figure 2-5. The inset block in the Cobourg represents a 20 km x 20 km area around the hypothetical site.

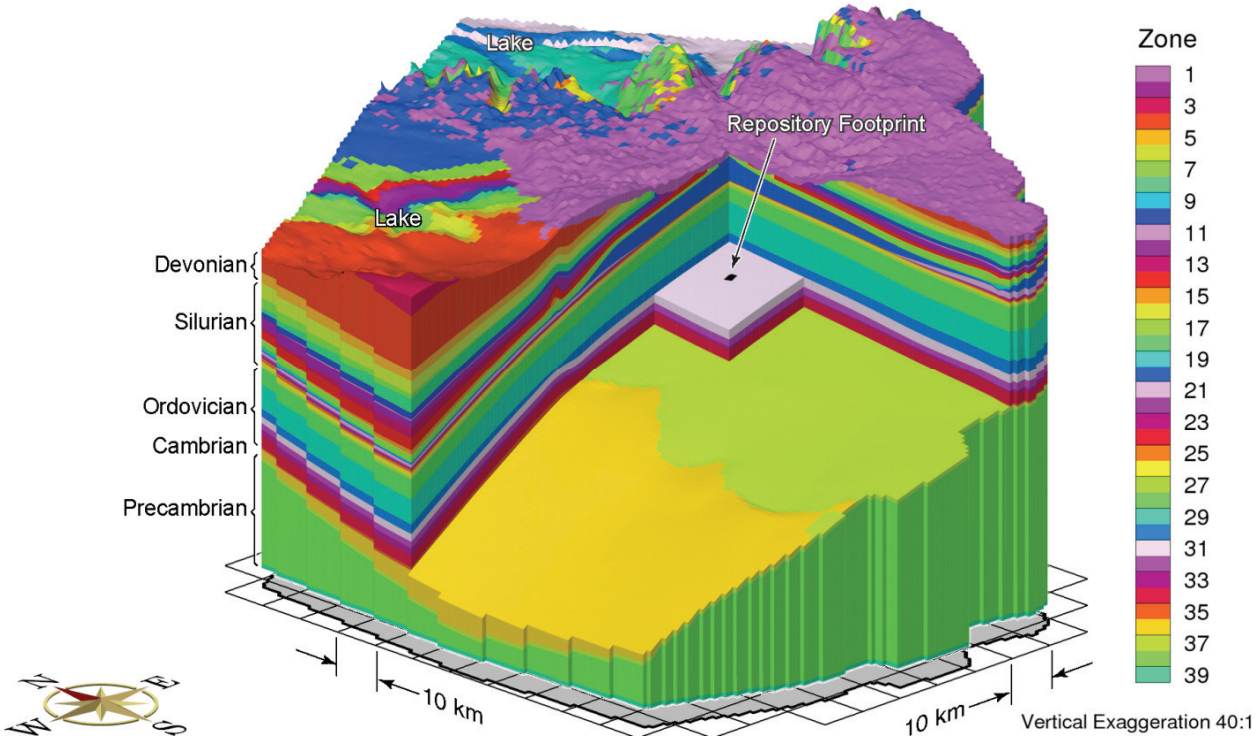

Figure 2-4: Block Cut View of FRAC3DVS-OPG Zone Identifiers for Regional Scale Domain

2.3.3.2 Model Parameters

The physical hydrogeological parameters defined in this section are applied to the regional scale numerical models. All groundwater flow parameters summarized in Table 2-2 are consistent with parameters used for regional modelling for the OPG Low & Intermediate Level Waste Deep Geologic Repository (Sykes et al. 2011). For the scenario with a Biot coefficient of 0.5, alternate computed loading efficiency and specific storage values for each geologic unit are listed in Table 2-6.

2.3.3.2.1 Hydraulic Conductivity of Permafrost

For paleohydrogeologic simulations, the interpolated permafrost depths from the Glacial Systems Model (GSM) simulations (Peltier 2011) were used to select any FRAC3DVS-OPG grid block whose top face was within the permafrost zone for each time step. A detailed description of selected paleoclimate simulations is discussed in Section 2.3.4.3. A permafrost hydraulic conductivity of 5×10^{-11} m/s is applied (McCauley et al. 2002). Permafrost within a grid block would limit vertical flow in and out of the groundwater system due to its very low effective hydraulic conductivity.

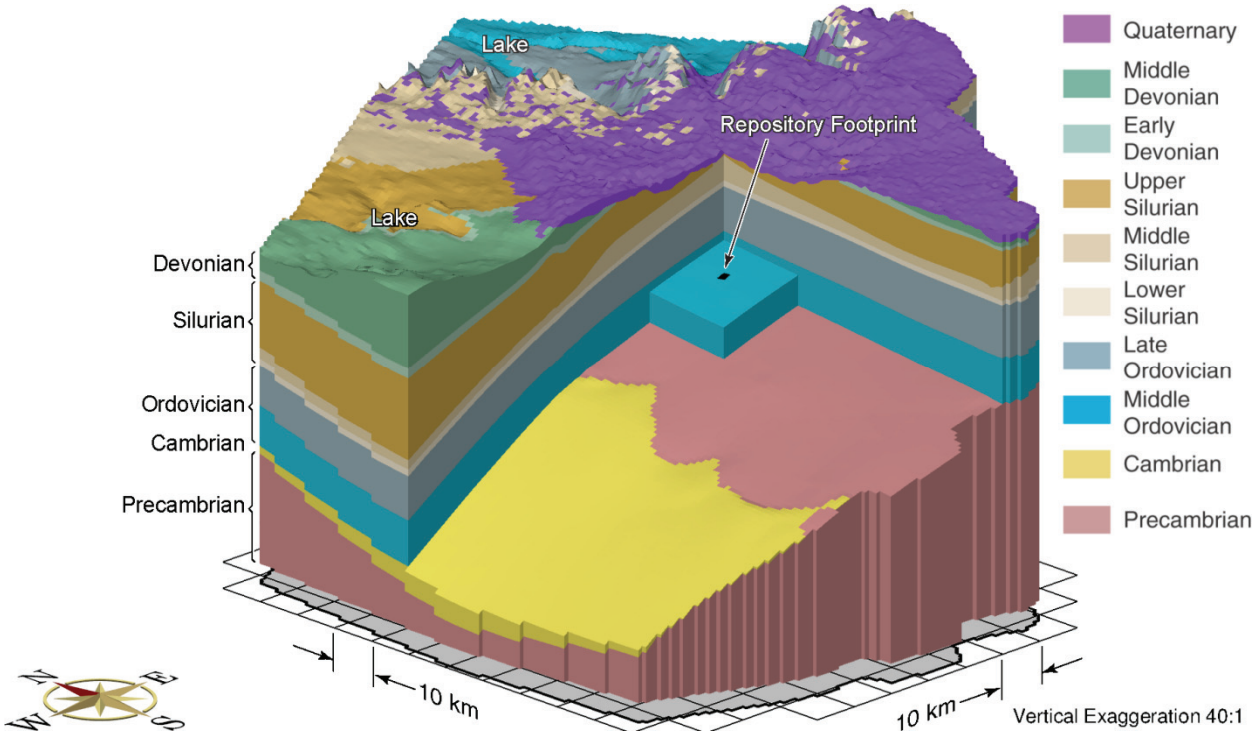

Figure 2-5: Block Cut View Showing Spatial Extent of the Bedrock Units

2.3.3.2.2 Precambrian Hydraulic Conductivity

Horizontal and vertical permeabilities for the Precambrian units, as a function of depth, are expressed following Normani (2009), as determined for data from various Canadian field studies at the Whiteshell Research Area (WRA):

$$\mathbf{k_H} = \mathbf{10^{-14.5-4.5\left(1-e^{-0.002469d}\right)}} \tag{2-1}$$

$$k_V = \begin{cases} 10k_H, & \text{for } d \leq 300 \text{ m;} \\ [0.09(400-d)+1]k_H, & \text{for } 300 < d \leq 400 \text{ m;} \\ k_H, & \text{for } d > 400 \text{ m.} \end{cases} \tag{2-2}$$

where k_H is the horizontal permeability [L^2];

k_V is the vertical permeability [L^2]; and

d is the depth relative to a constant reference elevation of 176 m for the top of the Precambrian [L].

As shown in Figure 2-6, the matrix permeabilities decrease exponentially with increasing depth.

2.3.3.2.3 Groundwater Transport Parameters

Table 2-2 lists various transport parameters that are used in this study to simulate the movement of variably dense pore fluids, for tracer movement to determine the depth of recharge water penetration, and for mean life expectancy calculations. The large grid spacing used for the regional scale domain necessitates relatively large dispersivity values employed in the modelling phase of this case study, in order to maintain numerically stable results. The dispersivity values used for MLE calculations are triple the values listed in Table 2-7.

Table 2-6: Loading Efficiency (ζ) and Specific Storage (S_s) for Scenario (fr-base-paleo-biot05) with a Biot Coefficient of 0.5

Formation	S_s (m^{-1})	ζ
Drift	9.9×10^{-5}	0.99
Hamilton Group	1.1×10^{-6}	0.54
Dundee	1.1×10^{-6}	0.54
Detroit River Group	1.0×10^{-6}	0.56
Bois Blanc	1.0×10^{-6}	0.56
Bass Islands	1.3×10^{-6}	0.71
Unit G	8.7×10^{-7}	0.36
Unit F	7.2×10^{-7}	0.45
Unit F Salt	7.2×10^{-7}	0.45
Unit E	5.1×10^{-7}	0.32
Unit D	4.9×10^{-7}	0.35
Unit B and C	7.7×10^{-7}	0.24
Unit B Anhydrite	5.3×10^{-7}	0.35
Unit A-2 Carbonate	5.7×10^{-7}	0.29
Unit A-2 Evaporite	4.5×10^{-7}	0.35
Unit A-1 Upper Carbonate	3.9×10^{-7}	0.39
Unit A-1 Carbonate	2.8×10^{-7}	0.62
Unit A-1 Evaporite	2.6×10^{-7}	0.71
Unit A0	3.5×10^{-7}	0.54
Guelph	3.1×10^{-7}	0.30
Goat Island	1.8×10^{-7}	0.51
Gasport	1.8×10^{-7}	0.51
Lions Head	2.1×10^{-7}	0.42
Rochester	2.1×10^{-7}	0.42
Reynales/Fossil Hill	2.1×10^{-7}	0.42
Cabot Head	7.7×10^{-7}	0.41
Manitoulin	5.1×10^{-7}	0.63
Queenston	6.4×10^{-7}	0.50
Georgian Bay/Blue Mountain	8.0×10^{-7}	0.58
Cobourg	1.8×10^{-7}	0.58
Sherman Fall	3.7×10^{-7}	0.59
Kirkfield	3.8×10^{-7}	0.56
Coboconk	3.4×10^{-7}	0.62
Gull River	3.7×10^{-7}	0.56
Shadow Lake	5.9×10^{-7}	0.35
Cambrian	3.2×10^{-7}	0.19
Upper Precambrian	2.2×10^{-7}	0.29
Precambrian	1.1×10^{-7}	0.60

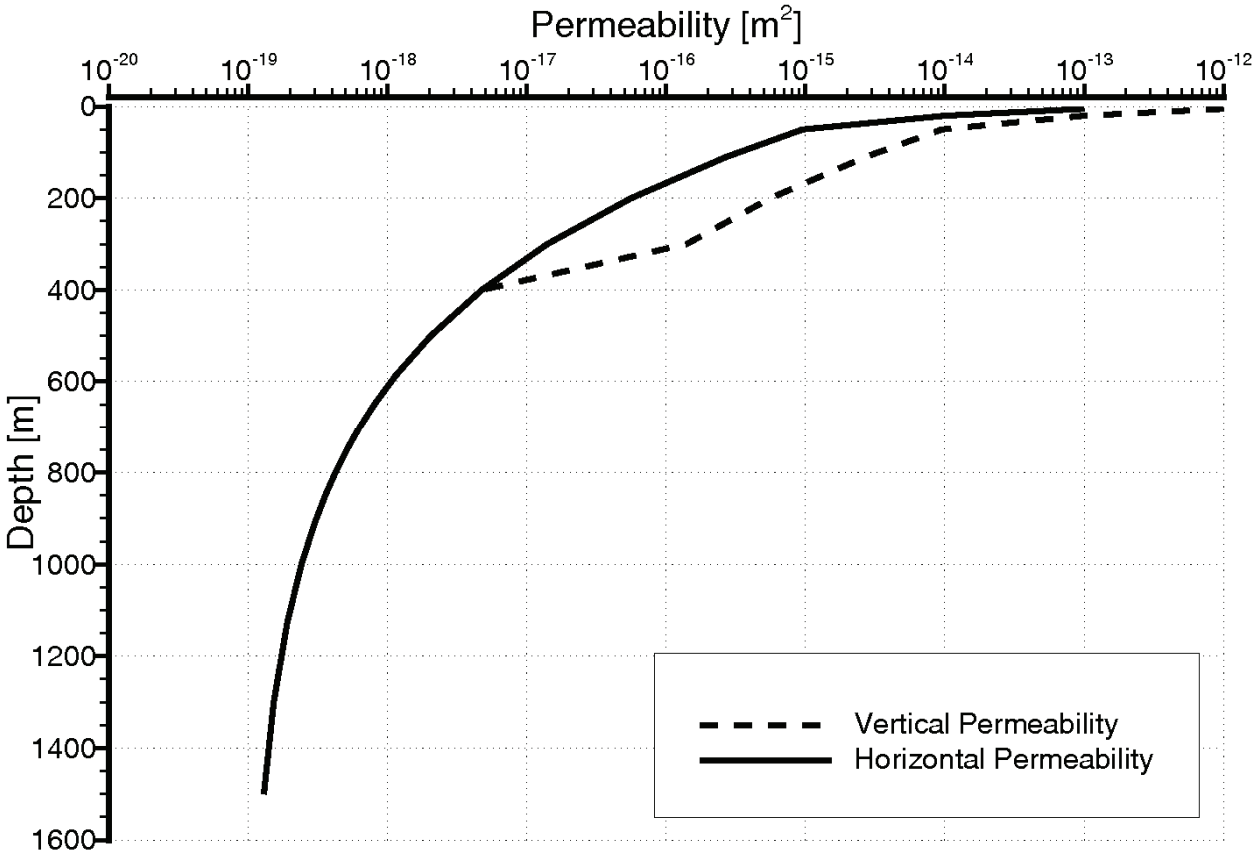

Note: Figure from Normani (2009).

Figure 2-6: Precambrian Horizontal and Vertical Matrix Permeabilities as a Function of Depth

Table 2-7: Groundwater Transport Parameters

Parameter	Value	Reference
Brine diffusion coefficient	1.484×10^{-9} m^2/s	Weast (1983, p. F-46)
Tracer diffusion coefficient	2.66×10^{-9} m^2/s	Singh and Kumar (2005, p. 37)
Longitudinal dispersivity	500 m	
Horizontal transverse dispersivity	50 m	
Vertical transverse dispersivity	5 m	

2.3.3.3 Flow Boundary Conditions

For the solution of the groundwater flow equation, a specified head (Dirichlet) boundary condition is applied to all surface nodes to set the water table 3 m below ground surface, regardless of streams or other inland water bodies such as lakes or wetlands, but not less than the elevation of the larger lakes which were set to a mean water elevation of 176 m. Zero flux boundary conditions are applied to both the lateral and bottom boundaries of the modelling domain. Based on results of sensitivity analyses conducted by Sykes et al. (2011) for a regional modelling domain of similar lateral extent, the assigned lateral and bottom boundary conditions are not expected to impact rates of mass transport at the location of the proposed repository. For simulations involving coupled density-dependent flow and transport of brine, a Dirichlet boundary condition equal to the TDS value at the bottom of the modelling domain is applied to all bottom nodes and a mixed (Cauchy) boundary condition with zero concentration for recharging waters is applied to all surface nodes.

A tracer representing recharge waters is used in the paleohydrogeologic simulations and its boundary conditions are set to zero concentration for all bottom nodes and a concentration of unity using a Cauchy boundary condition for all surface nodes. Lateral boundary conditions for both brine and tracer transport are zero-gradient.

2.3.3.4 Initial Conditions and Solution of Density-Dependent Flow

Salinity plays an important role with regard to fluid flow at depth. An increase in the concentration of TDS will result in an increase in the fluid density, which will then act as an inhibiter of active flow at depth (Park et al. 2009). The method for developing a solution for density-dependent flow is described in the following paragraphs.

In the absence of a source term for salinity, a transient analysis is required to determine an equilibrium solution at a time, *t,* for density-dependent flow. The analysis requires the specification of an initial distribution throughout the spatial domain for both freshwater heads and total dissolved solids concentrations. In a transient analysis, the initial prescribed salinity distribution is allowed to equilibrate to a new state that reflects the boundary conditions, hydraulic properties and transport properties of the regional scale domain. For the coupled density-dependent flow and transport system, fresh water can recharge at the surface, reducing the TDS concentration in the shallow groundwater system. The time to flush TDS from a unit is a function of the permeability of the unit and the energy potential of the displacing fluid as compared to the energy potential of the fluid being displaced. Fluids with lower total dissolved solids, such as recharging water, will have a lower energy potential when compared to water with higher total dissolved solids at the same elevation and pressure. Therefore, for low-permeability regions with a relatively high total dissolved solids concentration, the time to flush the region or displace the fluids can be very long (i.e., millions of years). Complete flushing may only occur as a result of diffusion because energy gradients and/or low permeabilities may yield low fluid fluxes that may not be sufficient for advective displacement to occur. In using this method to synthesize a spatial salinity distribution, the total mass of dissolved solids, and its distribution in the model domain, is assumed to be known and will be a maximum initially because there are no internal sources to generate dissolved solids resulting from rock-water interaction. With this approach, as time progresses, the dissolved solids will gradually decrease as the groundwater discharges from the system.

The initial condition for total dissolved solids must specify concentrations for all lithologies at all locations in the regional scale domain. Field data are not available for the spatial distribution of TDS in the shallow low permeability units, such as the Queenston shale where it outcrops, or for the spatial distribution in the deeper units. The values from Table 2-2 for a given lithology were assigned to all areas of the spatial domain assigned to that zone. For the model zones representing the Precambrian, a depth-dependent initial TDS distribution was determined using the data described by the dashed line in Figure 2-7, and represented by Equation 2-3, where *TDS* is in units of g/L.

$$TDS = \begin{cases} 10^{0.001981697d}, & \text{for } d \leq 1250 \text{ m}; \\ 300, & \text{for } d > 1250 \text{ m}. \end{cases} \quad (2\text{-}3)$$

The depth, *d,* is the depth relative to a constant reference elevation of 176 m for the top of the Precambrian; there is no Precambrian above this elevation in the regional scale domain. If the concentration from the dashed line in Figure 2-7 at a given depth was lower than that assigned to the lowest sedimentary rock at the location (Shadow Lake or Cambrian sandstone, where present), the higher zone TDS concentration was assigned. The initial TDS distribution developed for this study is shown in block-cut view in Figure 2-8. A linear relationship is assumed between fluid density and TDS such that a fluid density of 1200 kg/m^3 is equal to 300 g/L. Further discussion of the linear relationship between fluid density and TDS can be found in Normani et al. (2007).

For this study, the final freshwater head distribution for the reference case analysis was calculated using the following three-step process:

1. The steady-state solution was calculated for a density-independent groundwater flow system;
2. The total dissolved solids concentration distribution in Figure 2-8 was assigned throughout the domain as an initial condition using the procedure described in the preceding paragraph. The density-independent freshwater heads were allowed to equilibrate to the assigned TDS distribution in a transient analysis, while fixing the TDS distribution;
3. A further transient analysis was performed to allow evolution of the TDS distribution over a one million year time interval.

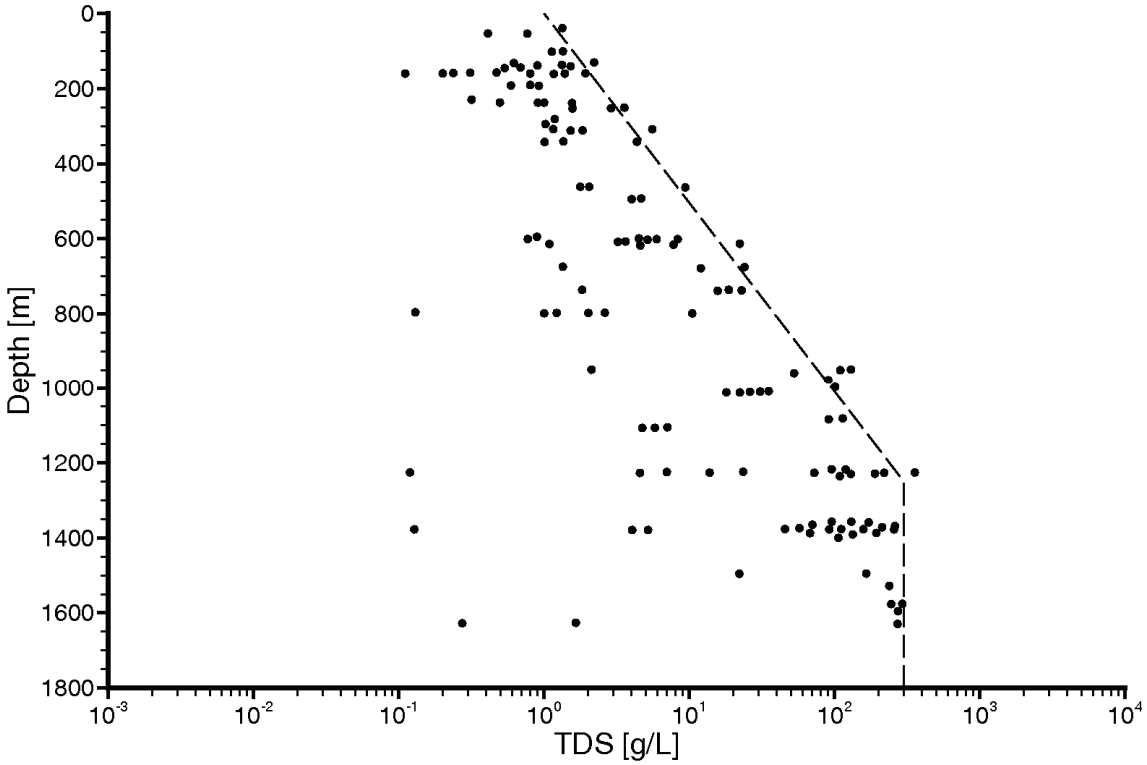

Note: Figure adapted from Figure 2b in Frape and Fritz (1987).

Figure 2-7: Plot of TDS versus Depth for Groundwater from the Canadian Shield

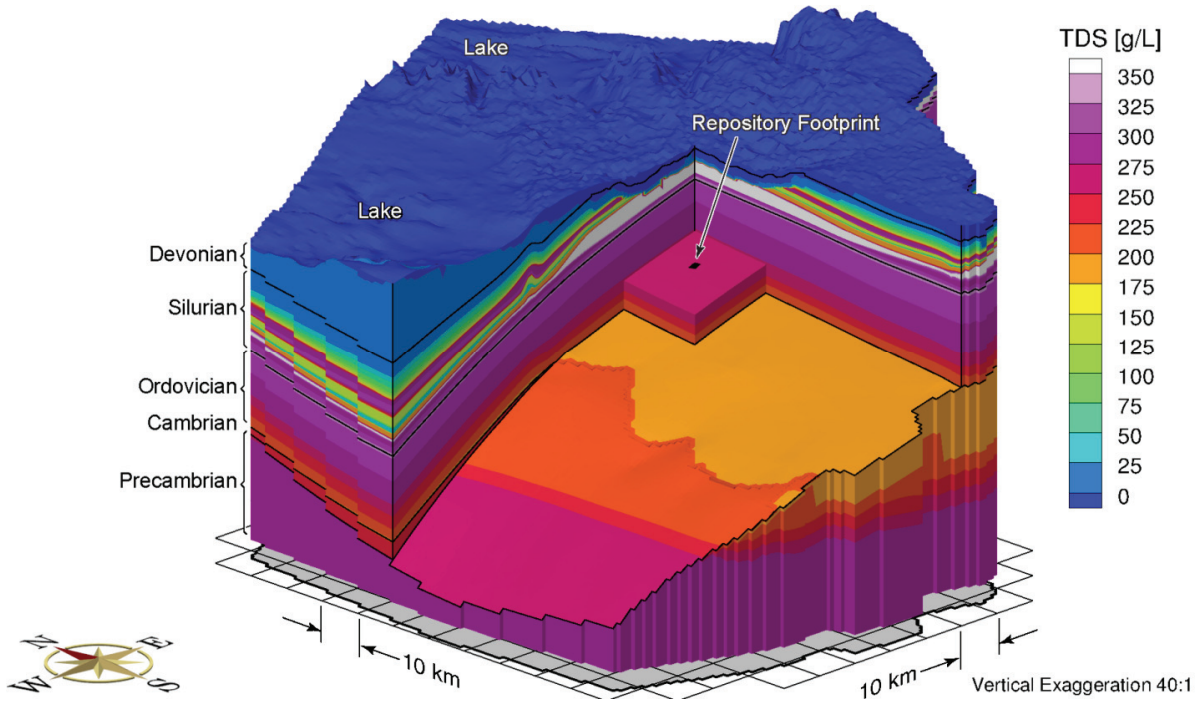

Figure 2-8: Block Cut View of Initial Total Dissolved Solids Concentration Distribution

After one million years, the model, having been allowed to reach pseudo-equilibrium between freshwater heads and TDS distribution, produces a salinity distribution that is compatible with the boundary conditions, geochemical framework and, hence, the flow domain. Generally, pseudo-equilibrium is reached when the model TDS reasonably matches field measurements (for detailed discussion, see Normani 2009). Note that in this study, no field data were available for comparison. In recharge areas, brine will be flushed because of a combination of the absence of a source term for brine and the effect of meteoric recharge. This is contrasted with discharge locations, which tend to transport higher concentration brines from deeper in the groundwater system. Both the freshwater heads and brine concentrations at one million years are used as the initial conditions for the paleohydrogeologic simulations.

2.3.3.5 Model Uncertainties and Sensitivities

Uncertainty is unavoidable and inherent to groundwater models, due to uncertain estimates of model parameter values. System performance measures, such as mean life expectancies, porewater velocities, Péclet number, and recharge water tracer migration, are monotonically related to model parameters through the governing equations describing groundwater flow and solute transport. As such, model parameter bounding scenarios are used in this study to investigate groundwater system behaviour.

In addition to the regional scale reference case analysis, two temperate sensitivity cases were developed. An increase in fluid density by salinity tends to retard groundwater flow at depth (Park et al. 2009). The regional scale reference scenario accounts for pore fluid density effects by assuming a linear relationship between fluid density and salinity, expressed as TDS. A conservative bounding case regarding pore fluid density is represented by a steady-state freshwater groundwater flow simulation. The second sensitivity case included enhanced hydraulic conductivities of one order of magnitude to evaluate the impact of enhanced advection on the system performance measures. Additionally, a conservative bounding case was simulated by increasing hydraulic conductivities by three orders of magnitude (see Section 2.3.5).

In terms of paleohydrogeologic simulations, additional uncertain model parameters include alternate paleoclimate simulations, paleohydrogeologic surface boundary conditions, one-dimensional loading efficiencies and Biot coefficients. In addition to the warm-based paleoclimate simulation used for the paleohydrogeologic reference case, an alternate cold-based paleoclimate simulation includes greater permafrost extent and more frequent glacial episodes. The bounding scenarios for paleohydrogeologic surface hydraulic boundary conditions include 100% of ice-sheet thickness expressed as equivalent freshwater heads and a free draining surface boundary condition. The impacts of no hydro-mechanical coupling and full hydro-mechanical coupling were investigated by setting the one-dimensional loading efficiencies to zero and unity, respectively. Incompressible mineral grains are assumed for the reference paleohydrogeologic scenario, resulting in a Biot coefficient of 1.0. To investigate the effects of compressible mineral grains, as suggested by ITASCA (2011), an alternate Biot coefficient of 0.5 is assumed for all lithologic layers. The resulting changes to both specific storage and loading efficiency are listed in Table 2-6.

2.3.4 Regional Scale Analyses

2.3.4.1 Reference Case Simulation

As described in Section 2.3.3.4, the reference case is comprised of a three-step simulation procedure: steady-state groundwater flow, transient groundwater flow equilibrated to a static TDS distribution, and a transient groundwater simulation with temporally varying TDS distribution for one million years. The steady-state freshwater head distribution, as a block-cut view, is shown in Figure 2-9. The freshwater steady-state heads shown are calculated without the influence of density. The freshwater heads for the shallow groundwater regime above the Salina Formation (within the Silurian) are dominated by the prescribed Dirichlet boundary condition representing local topography. Beneath the shallow groundwater zone, the heads are not controlled to the same extent by local topography.

The pseudo-equilibrium at one million years is taken to represent the present day state of the density-dependent groundwater flow system. The equivalent freshwater heads at a pseudo-equilibrium time of one million years are shown in Figure 2-10. For a density-dependent flow system, freshwater heads increase with an increase in fluid density and include the effects of both topographic and density gradients. However, the plot of freshwater heads can only be used to interpret horizontal head gradients, not vertical gradients. The main control for the horizontal head gradients at depth is the elevation difference between the lakes and the topographic high at the escarpment.

The distribution of total dissolved solids concentrations at a pseudo-equilibrium time of one million years is shown in Figure 2-11. Meteoric water recharging into the shallow groundwater zone above the Salina will dilute any salinity that diffuses upward through the Silurian or Ordovician formations, resulting in relatively fresh groundwater within the shallow groundwater regime. High TDS concentrations for the deep groundwater zone, including the Ordovician formations and below, are attributed to the initial high TDS concentration and the low permeability layers. The TDS transitional zone occurs in the Silurian, specifically where most of the Salina units pinch out. A TDS distribution plot shown as an east-west cross-section through the hypothetical repository in Figure 2-12 clearly displays the sharp transition of TDS concentrations in the vicinity of the hypothetical repository footprint due to significantly varying lithology. Within 10 km of the hypothetical repository footprint, a total of 15 units pinch out, based on the three-dimensional regional geologic framework model (see Section 2.3.3.2). In addition, a total of 7 units pinch out west of the 20 km by 20 km inset block shown in Figure 2-5.

The reference case porewater velocity magnitudes at a pseudo-equilibrium time of one million years are presented in Figure 2-13. Relatively high velocities occur in the shallow groundwater zone and permeable geologic units, including the Guelph and Cambrian formations. The reduction of velocities beneath the lake in the northeastern part of the domain are the result of the absence of a horizontal gradient. The low velocities in the Salina units and the Ordovician result from the low permeability of each unit. Within the Ordovician in the vicinity of the hypothetical repository footprint, the majority of porewater velocity magnitudes are less than 1×10^{-6} m/a. For a brine diffusion coefficient of 1.484×10^{-9} m^2/s and a characteristic length of 1 m, the Péclet number of molecular diffusion (Bear 1988) is less than 2.13×10^{-5}, indicating solute transport in the Ordovician is diffusion dominated.

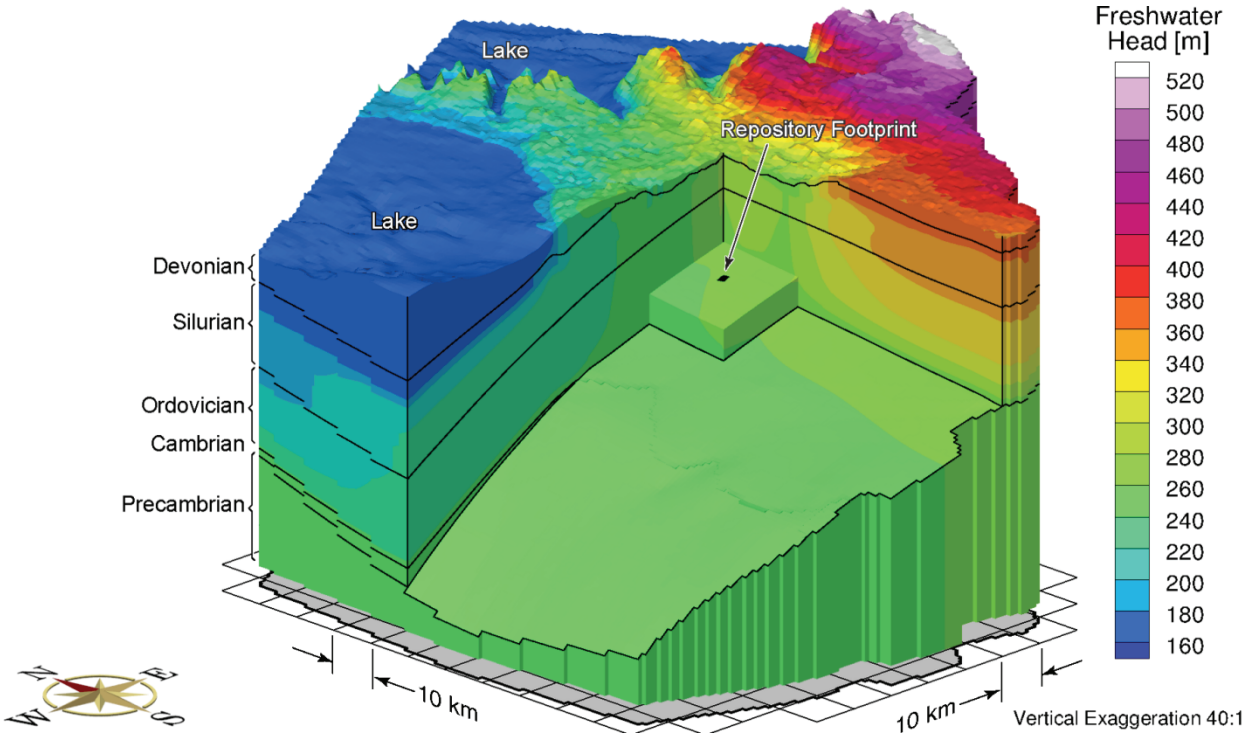

Figure 2-9: Block Cut View of Steady-State Density-Independent Freshwater Heads

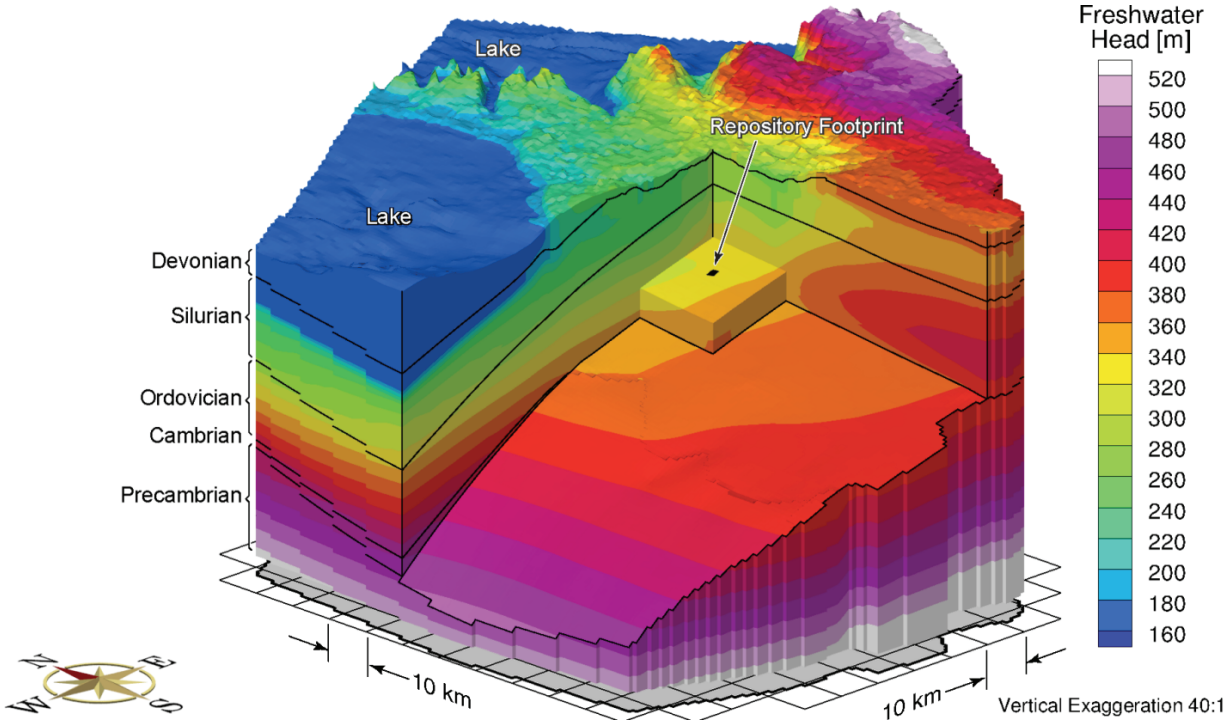

Figure 2-10: Block Cut View of Freshwater Heads at Pseudo Equilibrium Time of One Million Years with Temporally Varying TDS Distribution

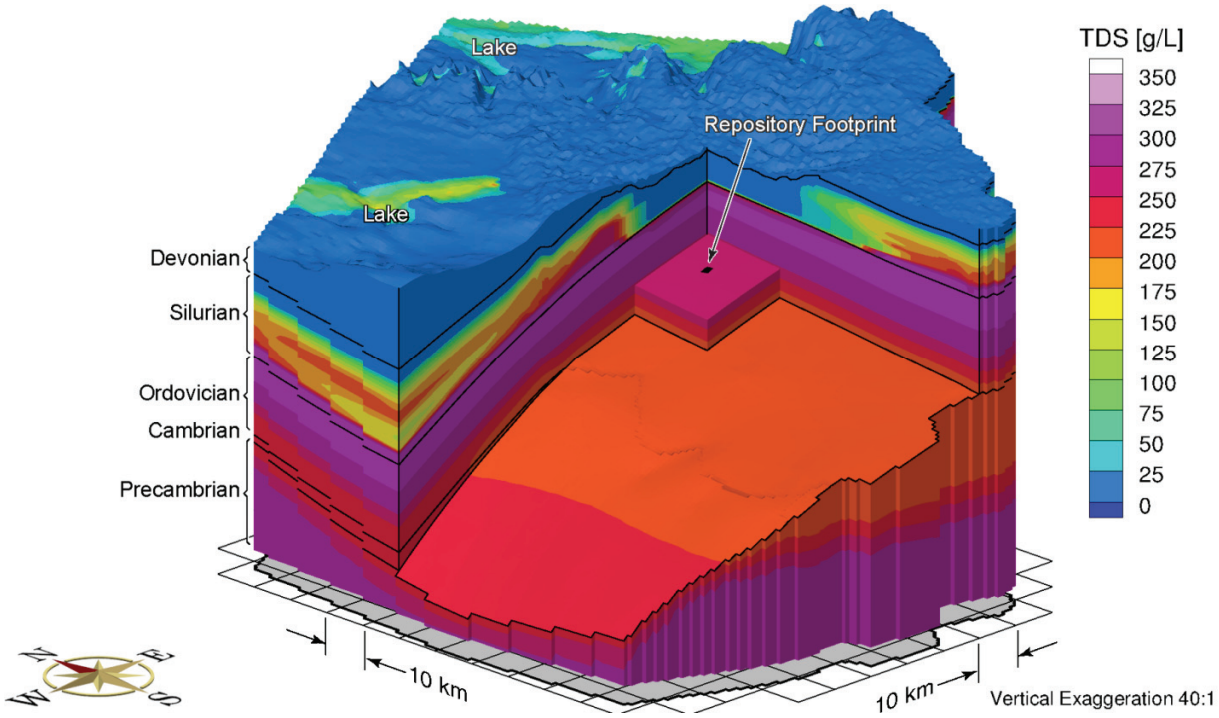

Figure 2-11: Block Cut View of Total Dissolved Solids Concentration at Pseudo Equilibrium Time of One Million Years with Temporally Varying TDS Distribution

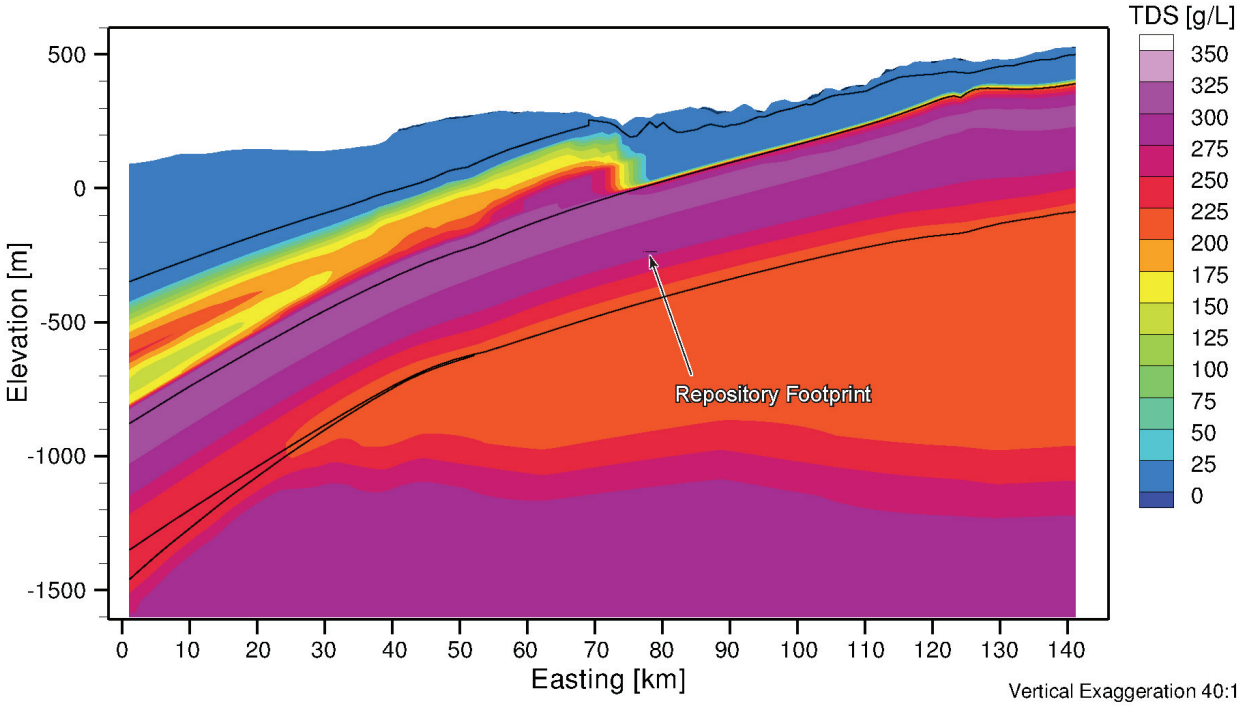

Figure 2-12: Base Case Total Dissolved Solids Concentration at Pseudo Equilibrium Time of One Million Years at East-West Cross-Section through the Hypothetical Repository Footprint

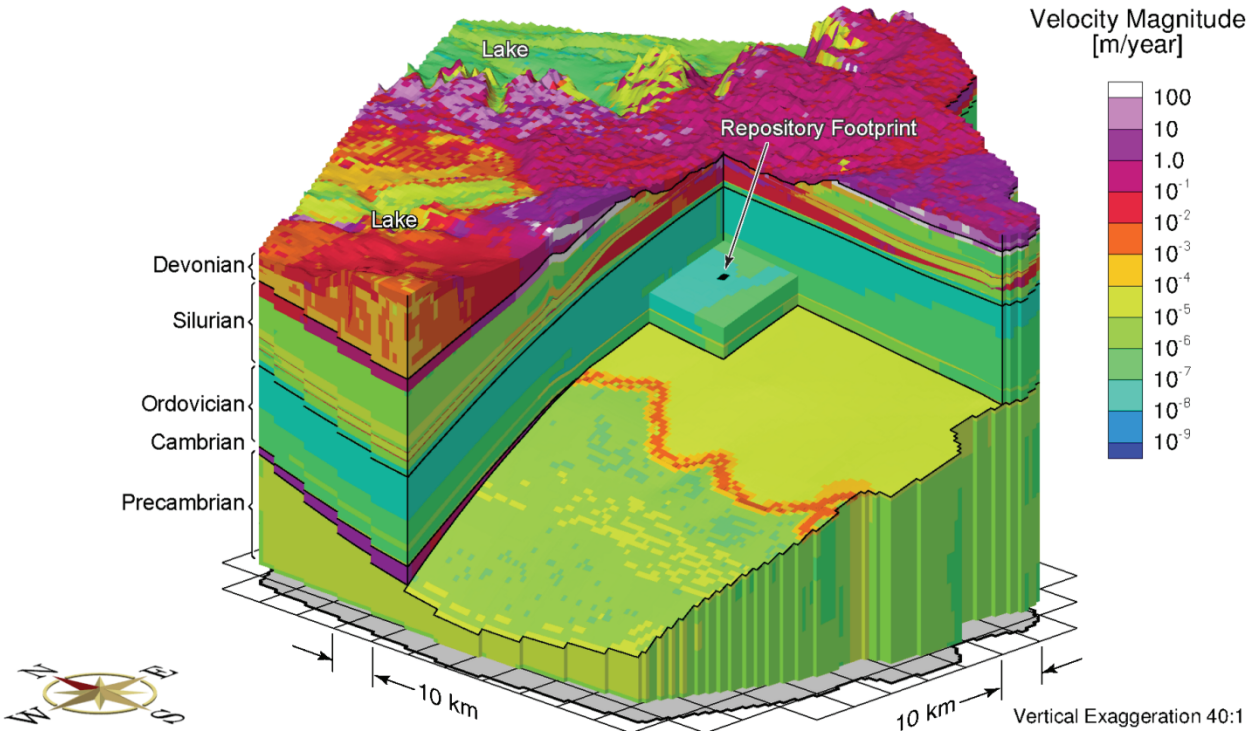

Figure 2-13: Block Cut View of Reference Case Porewater Velocity Magnitude at Pseudo Equilibrium Time of One Million Years

The ratio of the vertical component of velocity to velocity magnitude for the regional scale domain is shown in Figure 2-14. The figure can be used to determine the predominant direction of the calculated velocity vectors in the hydrostratigraphic units of the regional scale model. The vertical component of the velocity vector will equal the velocity magnitude only when there are no horizontal components to the velocity vector; the ratio of the vertical component of the velocity vector to the velocity magnitude will be positive 1.0 for solely upward velocity and negative 1.0 for solely downward velocity. In the figure, blue corresponds to zones where the vertically downward velocity component dominates, white to zones where horizontal velocity components dominate the velocity vector, and red to zones where the velocity vectors are dominated by the vertically upward component. Transition zones are evident in the figure. It is important to note that the figures cannot be used to interpret velocity magnitude; they can only be used to interpret the direction of the calculated velocity vectors at a given location. This figure should be referred to in conjunction with Figure 2-13, which shows the porewater velocity magnitudes. In the upper Precambrian, sharp transitions in flow direction over relatively short distances, in combination with low velocity magnitude, indicate stagnant flow where subtle changes in topography and total dissolved solids concentration impact the direction of the velocity vectors.

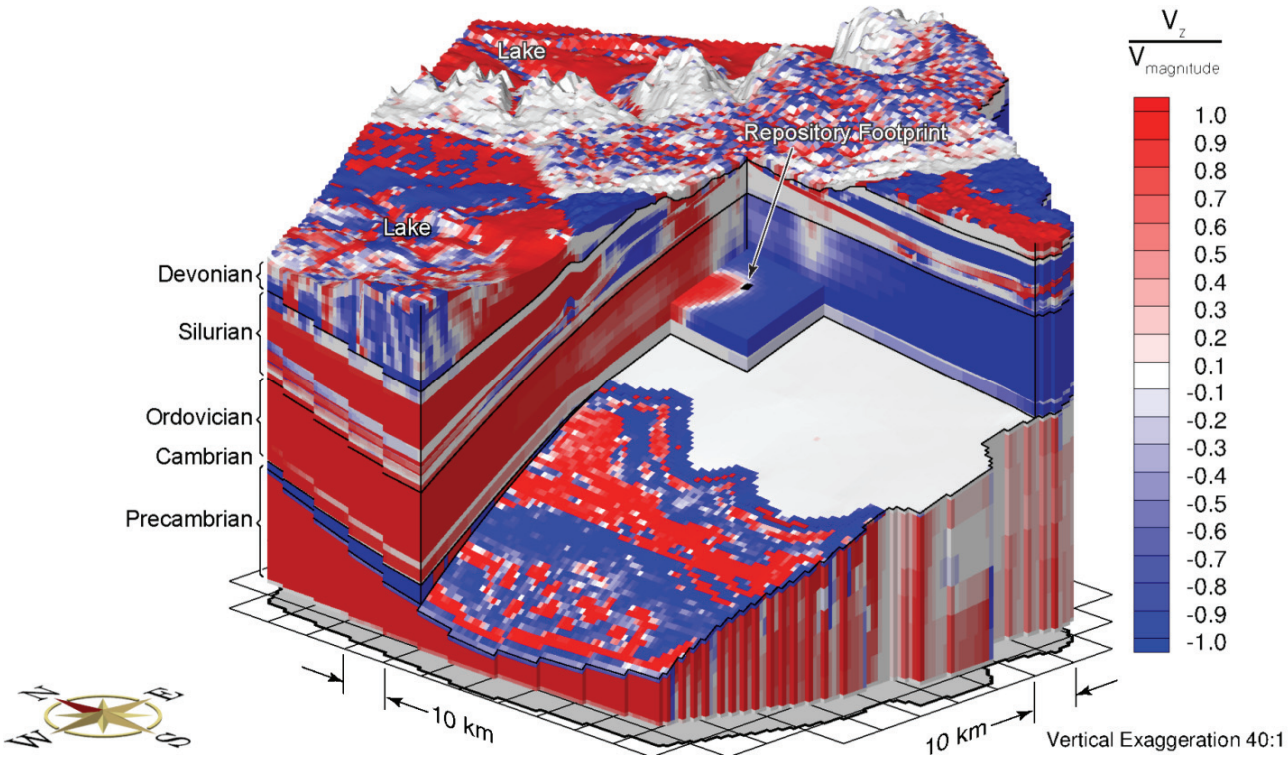

Figure 2-14: **Block Cut View of Reference Case Ratio of Vertical Velocity to Velocity Magnitude at Pseudo Equilibrium Time of One Million Years**

The performance measure selected for the evaluation of the groundwater system is mean life expectancy (MLE), as shown in Figure 2-15. The shallow groundwater zone has significantly shorter mean life expectancies compared to the deep groundwater system. The areas of recharge versus discharge can be noted in the figure as the recharge areas have high MLEs while the discharge areas have low MLEs. As a result of many geologic units pinching out, the sharp MLE transition zones in the Silurian, as shown in Figure 2-16, correspond with the behavior of the TDS distribution shown in Figure 2-12. The MLEs in the vicinity of the hypothetical repository footprint are greater than 100,000,000 years for the reference case simulation.

2.3.4.2 Temperate Transient Sensitivity Cases

The attributes of the sensitivity cases investigated in this study are summarized in Table 2-8. This section provides a comparison of two temperate sensitivity cases to the reference case. The first comparison investigates the role of fluid density between a steady-state freshwater simulation and the density-dependent reference case. The second comparison investigates the effects relative to the reference case of enhanced hydraulic conductivity on porewater velocities, TDS and MLE for all geologic units, excluding the upper 50 m of bedrock.

The impact of assuming groundwater flow is independent of density is shown by comparing porewater velocity magnitudes and mean life expectancies between a steady-state groundwater flow simulation (fr-base-nobrine) and the reference transient density-dependent flow simulation (fr-base). Figure 2-17 shows the ratio or quotient of porewater velocity magnitudes between scenarios fr-base-nobrine and fr-base on a logarithmic scale. In the figure, blue corresponds to zones where the density-independent groundwater flow from the steady-state simulation has lower velocity magnitudes than those of the reference case. Red zones indicate porewater velocities in the steady-state model are greater than in the density-dependent reference case model.

Porewater velocities are generally about the same or less without brine present; in some portions of the domain, the velocities can be slightly greater, for instance, in the close vicinity of the hypothetical repository footprint. The reduced velocities in the density-independent case are caused by the attainment of an equilibrium state, while the groundwater flow system of the reference case with salinity is experiencing slow evolution even after one million years of simulated time. A slight change in TDS distribution will have an impact on the magnitude and direction of porewater velocities, especially in the high permeability units.

Within the Ordovician formation containing the hypothetical repository footprint, the velocity magnitude ratio is close to unity due to the dominance of diffusive solute transport. Calculating the ratio of MLE between a steady-state freshwater system without brine and the pseudo-equilibrium transient brine simulation, as shown in Figure 2-18, shows order-of-magnitude changes across the domain. The mean life expectancies are generally similar or greater in the freshwater simulation, except for the portion beneath the lake, where the MLEs are reduced by one order of magnitude. At the location of the hypothetical repository footprint, a MLE of 183 Ma was estimated for the case of density-independent flow when compared to a MLE of 177 Ma for the reference case including salinity. It is non-intuitive that MLE is less in the density-independent system, as density usually retards active groundwater flow at depth and results in a smaller value of MLE. The reason lies in the fact that the groundwater movement attained in the freshwater simulation is steady-state and purely driven by topography.

Table 2-8: Table of Regional Scale Simulations for this Study

Attribute	Sensitivity Case	fr-base	fr-sens	fr-base-nobrine		fr-base-paleo	fr-base-paleo-sens	fr-base-paleo-nobrine	fr-base-paleo-cold	fr-base-paleo-80	fr-base-paleo-30	fr-base-paleo-0	fr-base-paleo-lbiot05	fr-base-paleo-le1	fr-base-paleo-le0	fr-base-paleo-0-le1
Conductivity	Reference	•		•		•		•	•	•	•	•	•	•	•	•
	Sensitivity		•				•									
Surface BC	Dirichlet at surface	•	•	•												
Density	Brine	•	•			•	•		•	•	•	•	•	•	•	•
	no brine			•				•								
Paleo Simulation	nn9930					•	•	•		•	•	•	•	•	•	•
	nn9921								•							
Paleo Surface BC	Dirichlet 100%					•	•	•	•				•	•	•	
	Dirichlet 80%									•						
	Dirichlet 30%										•					
	Dirichlet 0%											•				•
Hydro-mechanical Coupling	Biot 1.0					•	•	•	•	•	•	•		•	•	•
	Biot 0.5												•			
Loading Efficiency	Actual					•	•	•	•	•	•	•	•			
	1.0													•		•
	0.0														•	

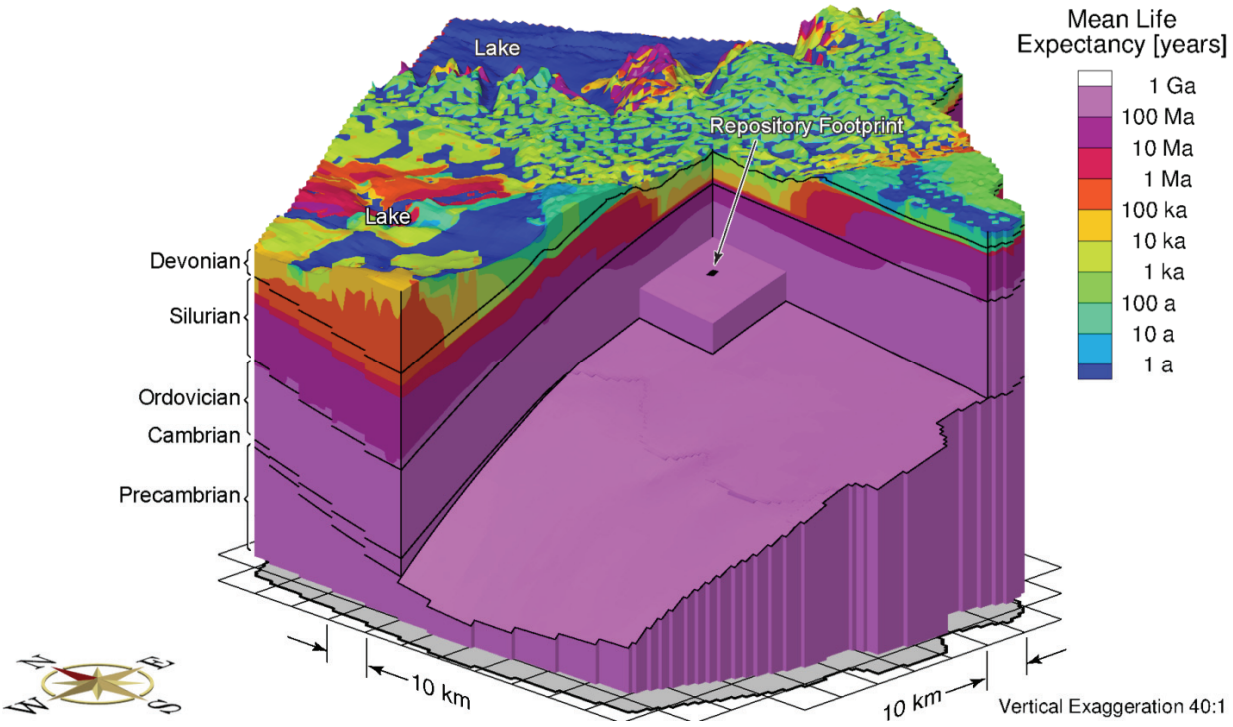

Figure 2-15: Block Cut View of Base Case Mean Life Expectancy at Pseudo Equilibrium Time of One Million Years

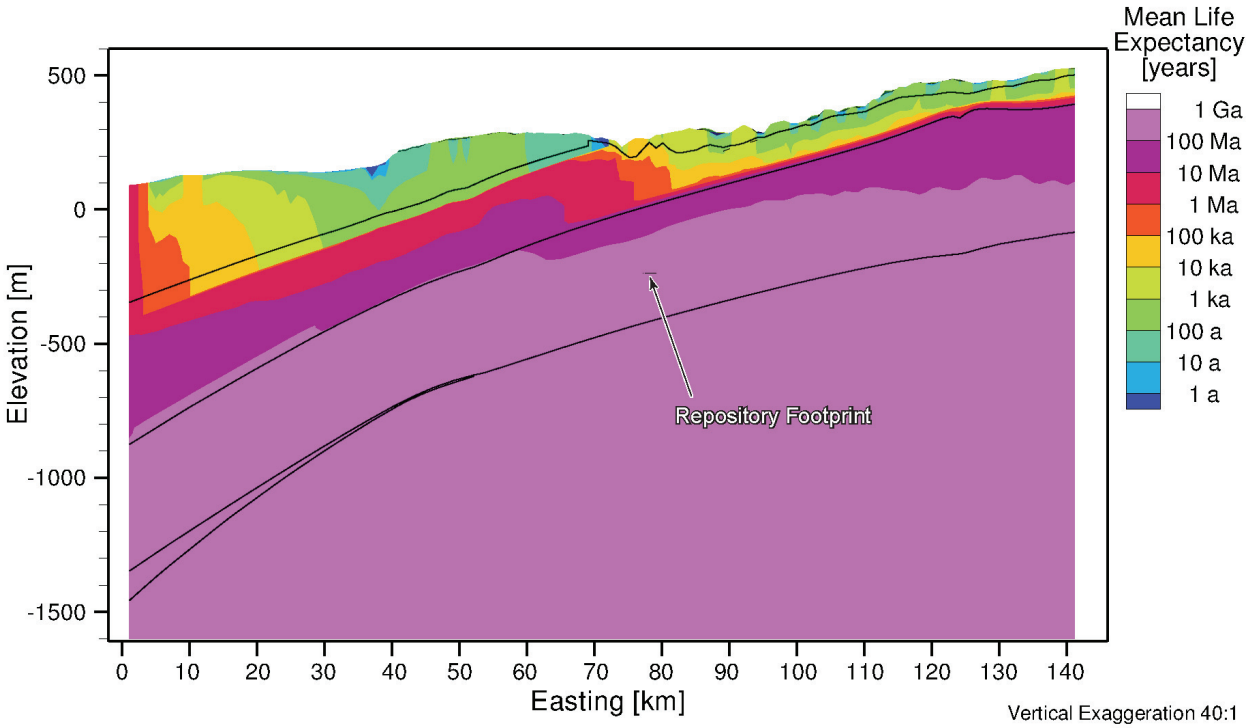

Figure 2-16: Reference Case Mean Life Expectancy at Pseudo Equilibrium Time of One Million Years at East-West Cross-Section through the Hypothetical Repository Footprint

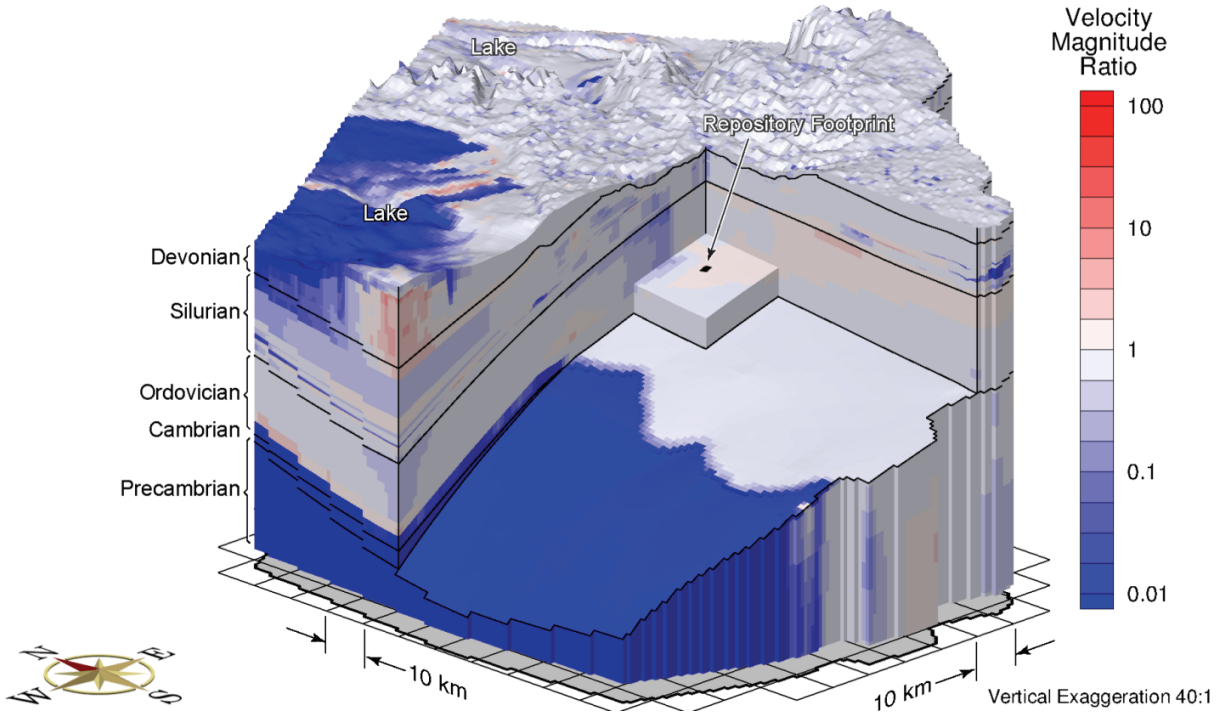

Figure 2-17: Ratio of Velocity Magnitudes of Steady-State Groundwater Flow to Density-Dependent Flow Reference Case

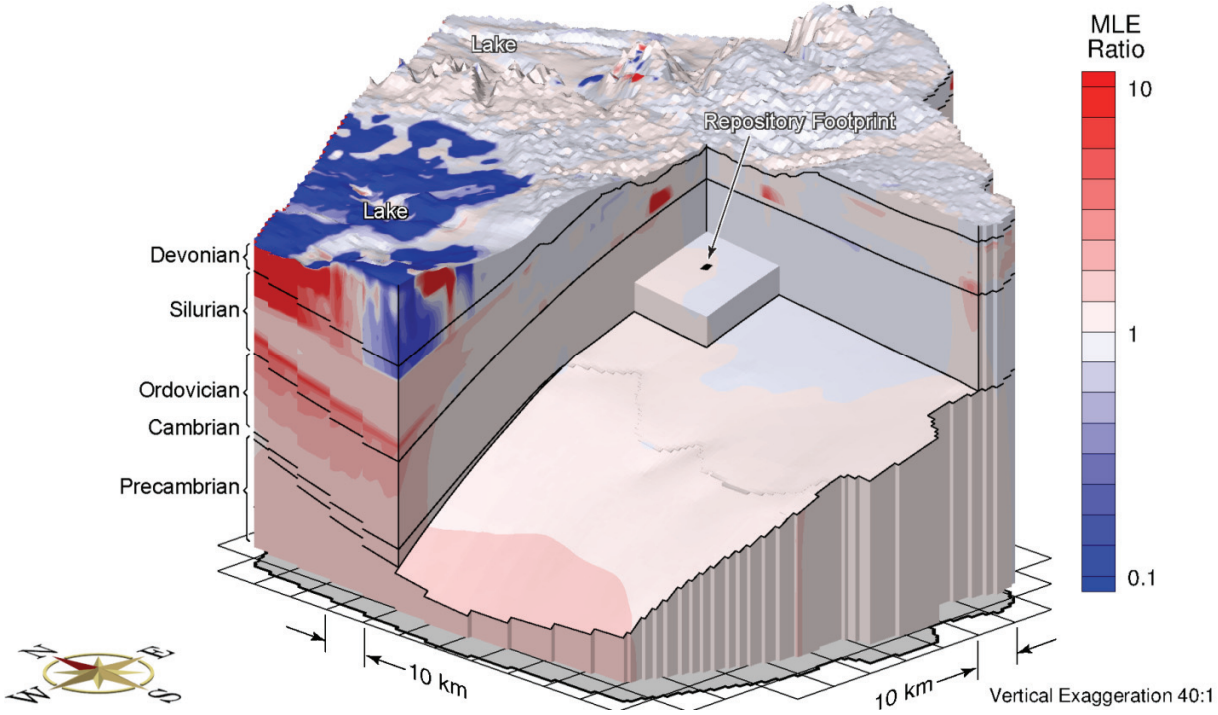

Figure 2-18: Ratio of MLEs of Steady-State Groundwater Flow to Density-Dependent Flow Reference Case

In contrast, the density-dependent solution is also affected by the evolving TDS distribution even at one million years of simulation time. In this case study, the groundwater flow induced by non-equilibrated TDS gradients is more significant than the inhibition of the groundwater flow system by density effect, which leads to a lower MLE. The relative difference in the MLE for the two cases is considered to be trivial. For a system dominated by low permeability units, the MLE is not sensitive to fluid density effects.

To investigate the impact of enhanced hydraulic conductivities on the groundwater flow system, the permeability profiles for all geologic units were increased by one order-of-magnitude, except for the upper 50 m of bedrock scenario (fr-sens). Higher hydraulic conductivities allow the groundwater system to transport TDS from the Salina group to the shallow groundwater system and then to flush the TDS from the system in a shorter period of time. Figure 2-19 shows the total dissolved solids at one million years for the sensitivity case. A comparison of the results to those of the reference case (fr-base), shown in Figure 2-11, reveals that the TDS concentrations in the Salina group are much lower than those from the reference case. The difference in freshwater heads between the sensitivity case and the reference case are shown in Figure 2-20. In the Silurian and below, freshwater heads are generally decreased as a result of lower TDS when compared to TDS values in the reference case.

The ratio of porewater velocities between the sensitivity case and the reference case is shown in Figure 2-21. Due to the enhancement of hydraulic conductivities, the porewater velocities are consistently greater throughout the modelling domain, excluding portions of upper layers beneath the lake. Higher hydraulic conductivities allow the groundwater system to equilibrate to a more stable state quicker than for the reference case at one million years. Therefore, an increase in hydraulic conductivity by a given factor under similar hydraulic gradients will result in an increase in porewater velocities and a decrease in travel times by a similar factor. The MLE ratios shown in Figure 2-22 generally indicate a decrease in the MLE values for the sensitivity case, resulting in an MLE for the hypothetical repository of 114 Ma. At the location of the hypothetical repository footprint, the corresponding mean life expectancy for the sensitivity case decreases by a factor of 1.6, significantly less than the one order-of-magnitude increase in the hydraulic conductivities. This highly nonlinear relationship between MLE and hydraulic conductivities indicates the dominance of molecular diffusion in the transport mechanism.

2.3.4.3 Paleohydrogeologic Sensitivity Cases

A total of eleven paleohydrogeologic simulations were performed to investigate the role of varying paleoclimate boundary conditions and the characterization of hydro-mechanical coupling. These simulations are summarized in Table 2-8. The reference case model (fr-base) is used as the basis for all simulations and the initial conditions for both freshwater heads and brine distribution come from the transient brine simulation at one million years, as described in Section 2.3.3.4. A conservative tracer of unit concentration is applied as a Cauchy boundary condition at the top surface of the model domain. This tracer represents the migration of recharge water, including glacial meltwater, which occurs during a paleohydrogeologic simulation. The tracer migration at 120,000 years for the paleohydrogeologic reference case simulation (fr-base-paleo) is shown in Figure 2-23. The 5% isochlor is considered conservative because it represents a pore fluid containing 5% recharge water and provides an indication of recharge water migration into the subsurface. For the reference case, the 5% isochlor migrates to the top of the Ordovician in the vicinity of the hypothetical repository footprint. The model units in the Salina and the Ordovician are of comparatively low hydraulic conductivity and tend

to retard the downward advective migration of the tracer, which indicates that diffusion is the dominant transport mechanism. Furthermore, Figure 2-24 shows the tracer concentration with depth at the location of the hypothetical repository footprint. Tracer penetration depth can be determined by the intersection of tracer concentration with a vertical line representing the 5% isochlor concentration. All paleohydrogeologic simulations are plotted on the same figure for comparison. The tracer concentrations do not reach formations below the Queenston in any of the paleoclimate scenarios.

To apply the same logic as the temperate transient sensitivity cases, the analysis of a no density scenario (fr-base-paleo-nobrine) in Table 2-8 investigates the impact of assuming that groundwater flow is independent of density. Additionally, the impact of enhanced hydraulic conductivities on the paleohydrogeologic groundwater flow system (fr-base-paleo-sens) is investigated by increasing the permeability profiles for all the geologic units by one order-of-magnitude, except for the upper 50 m of bedrock. The initial conditions for these two paleohydrogeolgic simulations are from the density-independent steady-state and enhanced hydraulic conductivities sensitivity case simulations, respectively. The importance of fluid density and enhanced hydraulic conductivities in impacting the paleogeologic groundwater flow system is revealed in a comparison of the results obtained from these scenarios with the reference case (see Figure 2-24). The increase in density of the deeper fluids will act as an inhibiter of active flow at depth (Park et al. 2009); higher hydraulic conductivity leads to deeper tracer migration, as confirmed by Figure 2-24 which shows slightly higher tracer concentration profiles and deeper penetration depth than does the reference case.

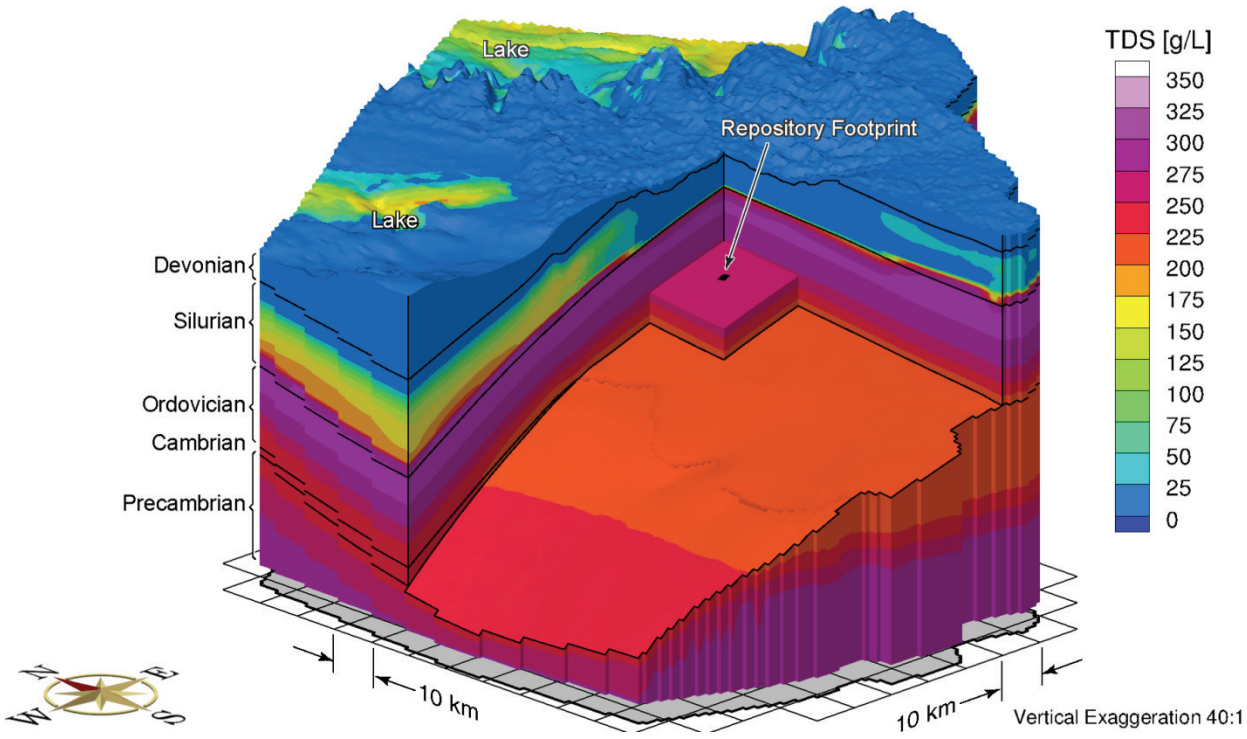

Figure 2-19: The Total Dissolved Solids Concentrations at Pseudo Equilibrium Time of One Million Years for an Increased Rock Mass Hydraulic Conductivity

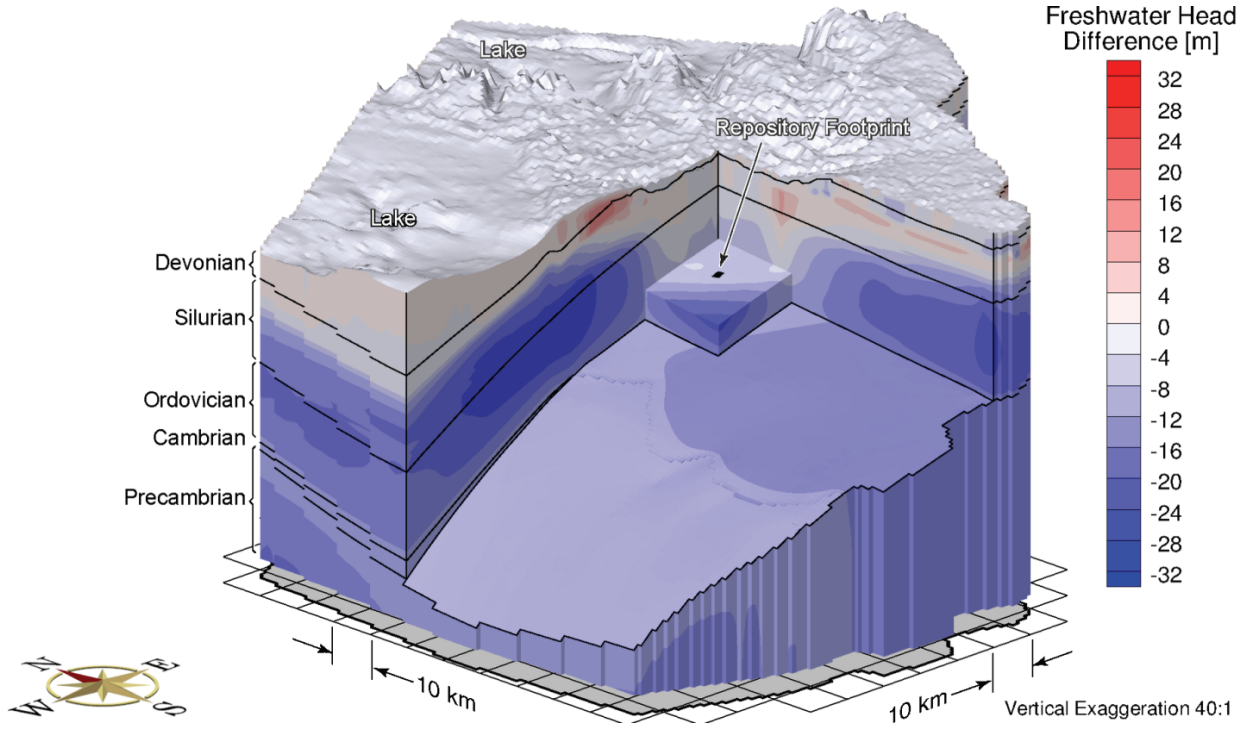

Figure 2-20: Difference in Freshwater Heads between a Simulation Using an Increased Rock Mass Hydraulic Conductivity and Reference Case

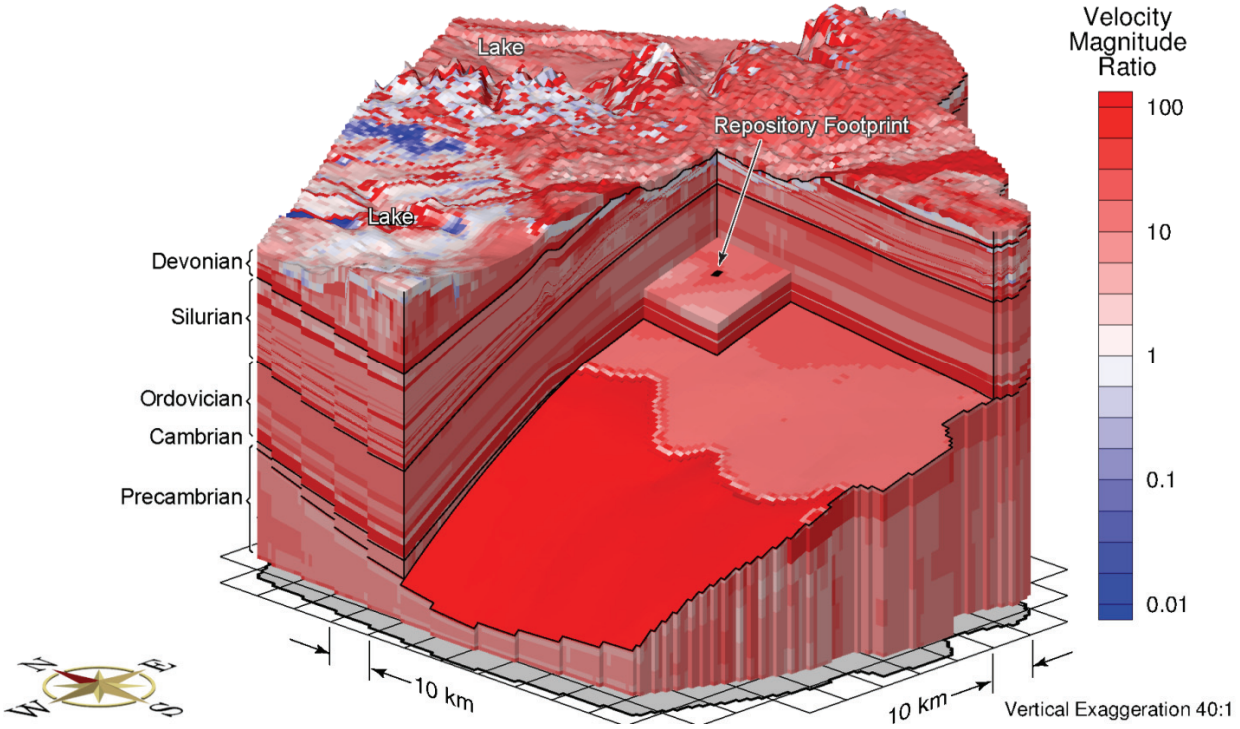

Figure 2-21: Ratio of Pore Velocity Magnitudes of Sensitivity Case using an Increased Rock Mass Hydraulic Conductivity to Reference Case

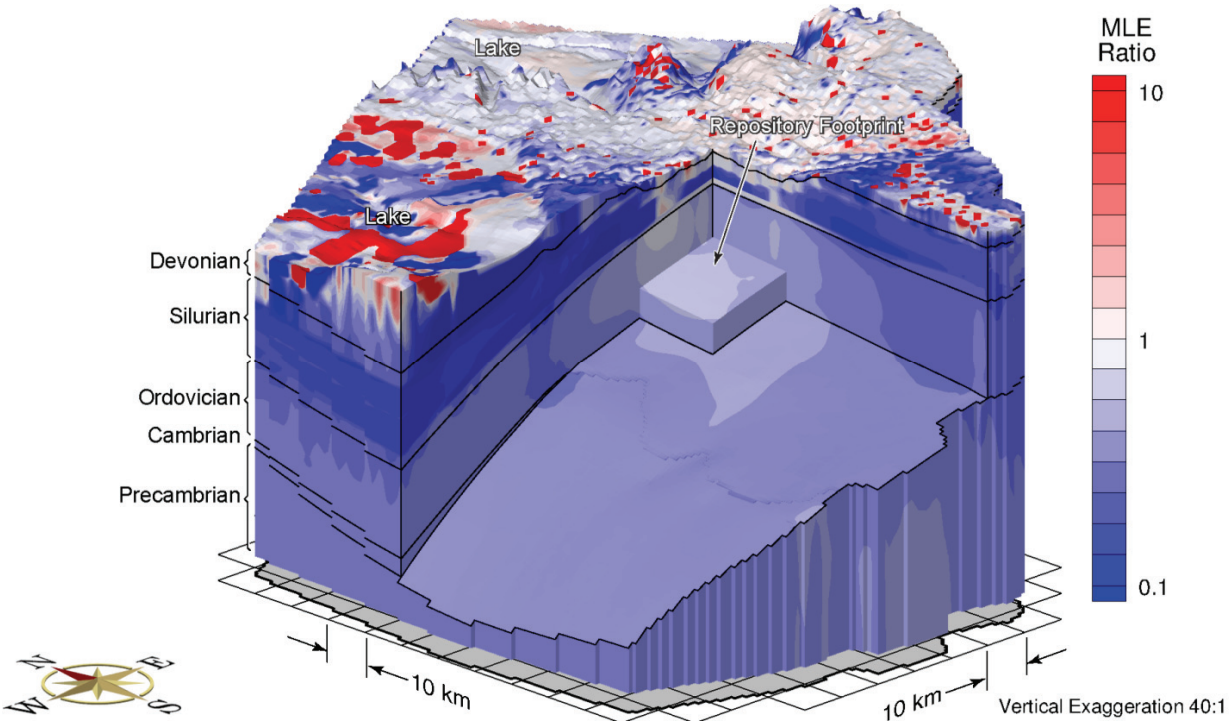

Figure 2-22: MLE Ratio of Increased Rock Mass Hydraulic Conductivities Simulation to Reference Case Simulation

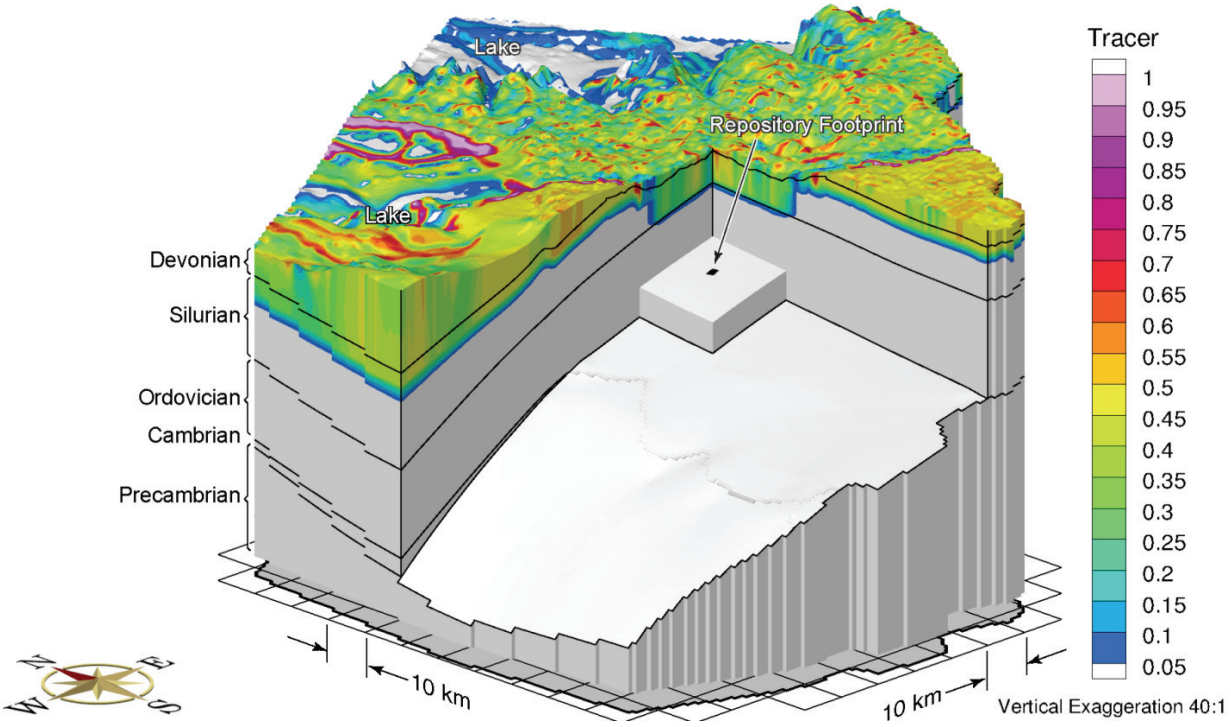

Figure 2-23: Block View Showing the Depth of Penetration of a Tracer after 120,000 Years for a Reference Case Paleohydrogeologic Scenario

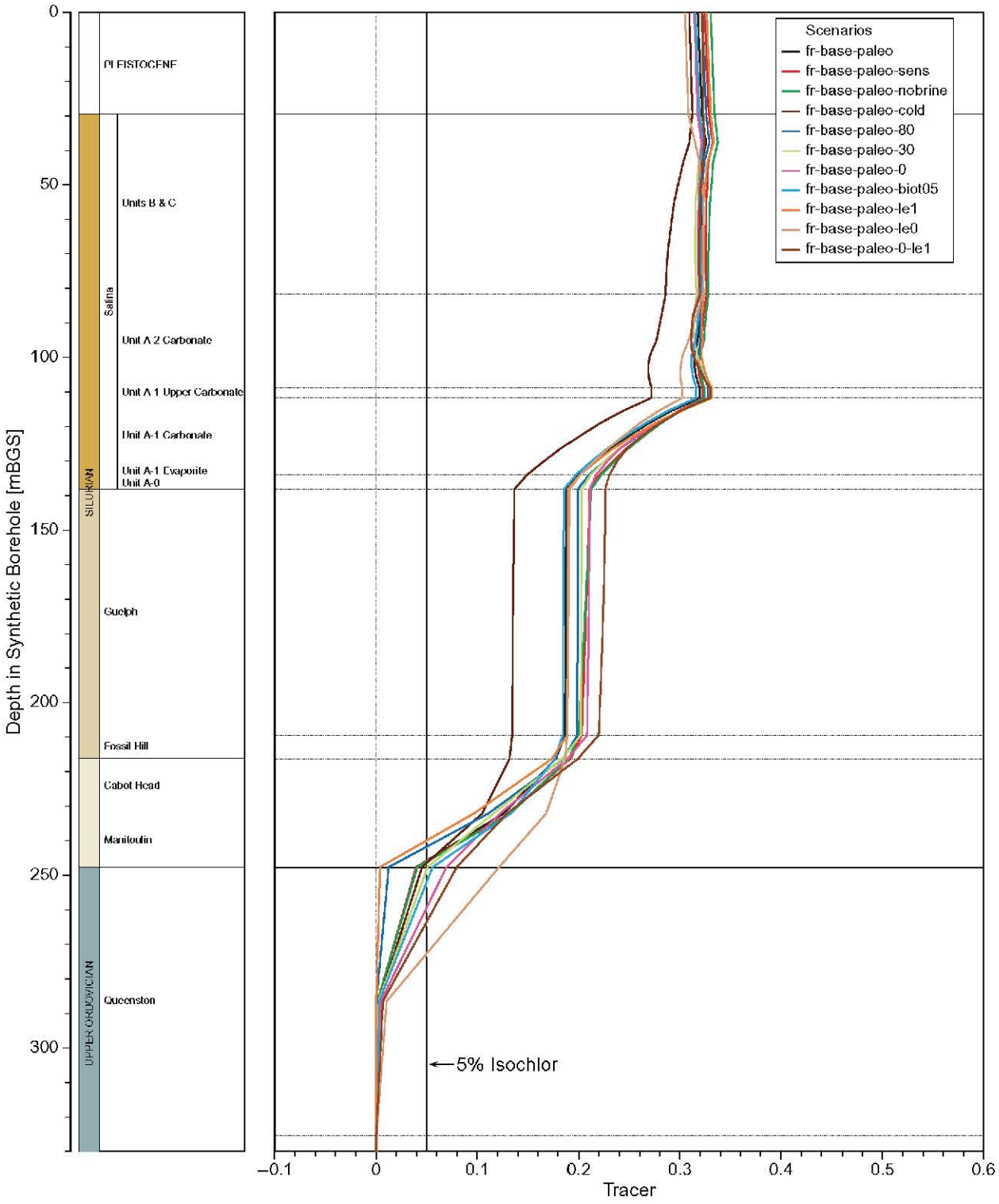

Figure 2-24: Vertical Profile Plots of Tracer Concentrations for the Paleohydrogeologic Simulations at the Location of the Hypothetical Repository Footprint at 120,000 Years

Peltier (2011) reconstructs eight paleoclimate glacial systems models (GSM). The reference case paleohydrogeologic simulation (fr-base-paleo) uses paleoclimate simulation nn9930, representing a warm-based ice-sheet condition. An alternate paleoclimate simulation, nn9921 (fr-base-paleo-cold), represents much more extensive permafrost over the 120,000 year paleoclimate time span and more ice-sheet advance/retreat cycles than nn9930. Both of the GSM models provide ice thickness, lake depth and permafrost depth over the 120,000 year simulation period, as shown in Figure 2-2 and Figure 2-3, respectively. These outputs are applied to the paleohydrogeologic groundwater flow simulations.

Figure 2-25 shows the tracer migration at 120,000 years for the nn9921 paleoclimate boundary conditions. In comparison to the reference case simulation, there is a significant decrease of tracer concentrations in the Silurian formations, as shown in Figure 2-24. Decreased tracer migration is a result of the longer duration of permafrost conditions.

The top surface hydraulic boundary condition can be varied using different percentages of ice-sheet thickness. The reference case uses 100% of ice-sheet thickness in calculating the equivalent freshwater head. Paleohydrogeologic scenarios with equivalent freshwater heads of 0%, 30%, and 80% (named fr-base-paleo-0, fr-base-paleo-30, and fr-base-paleo-80, respectively) of ice-sheet thickness were performed to allow for some reduction in heads beneath the ice-sheet. The 30% and 80% cases result in a tracer concentration profiles that are very similar to the reference case. For the 0% case, representing zero fluid pressure at the top surface, upward flow occurs during glacial loading, and downward flow occurs during glacial unloading due to in situ pore fluid pressure changes resulting from hydromechanical coupling. Higher tracer concentrations occur for the fr-base-paleo-0 case than for the reference case.

In addition to the surface hydraulic boundary condition, an equally important parameter is the one-dimensional loading efficiency. The loading efficiency is calculated based on the pore fluid and rock matrix compressibilities. In the reference case simulation, the one-dimensional loading efficiencies use this computed value for each geologic unit in Table 2-5. In two paleohydrogeologic sensitivity scenarios, the one-dimensional loading efficiencies are set to zero (fr-base-paleo-le0) to investigate the role of neglecting hydro-mechanical coupling, and unity (fr-base-paleo-le1) to evaluate the impact of full hydro-mechanical coupling on the groundwater flow system at depth. Both the loading efficiency and specific storage values are affected by the choice of Biot[1] coefficient. An additional sensitivity case investigates the role of the Biot coefficient on hydro-mechanical coupling. For a Biot coefficient of 0.5 (fr-base-paleo-biot05), alternate one-dimensional loading efficiencies and specific storages for each unit are listed in Table 2-6. The final simulation (fr-base-paleo-0-le1) uses a loading efficiency of unity and a 0% of ice-sheet thickness equivalent freshwater head for the surface hydraulic boundary condition. Of the paleohydrogeologic simulations with nn9930 paleoclimate boundary conditions, two extreme scenarios are represented by fr-base-paleo-le0 (having the most downward flow) and fr-base-paleo-0-le1 (having the most upward flow) during the loading portion of ice-sheet advance.

[1] According to Wang (2000), "The Biot-Willis parameter α is the ratio of increment of fluid content to change in bulk volume when the pore fluid remains at constant pressure [...]. It would be exactly one if all of the bulk strain were due to pore volume change (i.e., the solid phase is incompressible). It is less than one for a compressible solid phase because the change in bulk volume is greater than the change in pore volume by the amount of the change in the solid volume."

For the nn9930 paleoclimate boundary conditions, fr-base-paleo-le1 (Figure 2-26) represents the shallowest predicted tracer depth, while fr-base-paleo-le0 (Figure 2-27) represents the deepest penetration depth of tracer. As the one-dimensional loading efficiency is decreased, vertical gradients increase because in situ pore pressures are reduced during ice-sheet loading for the same 100% of ice-sheet thickness equivalent freshwater head surface hydraulic boundary condition. Similar to the comparison between fr-base-paleo-0 and fr-base-paleo, higher tracer concentrations occur in the fr-base-paleo-0-le1 (Figure 2-28) simulation as compared to fr-base-paleo-le1, as shown in Figure 2-24. Deeper tracer migration is attributed to larger downward vertical gradients resulting from the combination of a zero pressure hydraulic surface boundary condition with full hydromechanical coupling and a loading efficiency of unity.

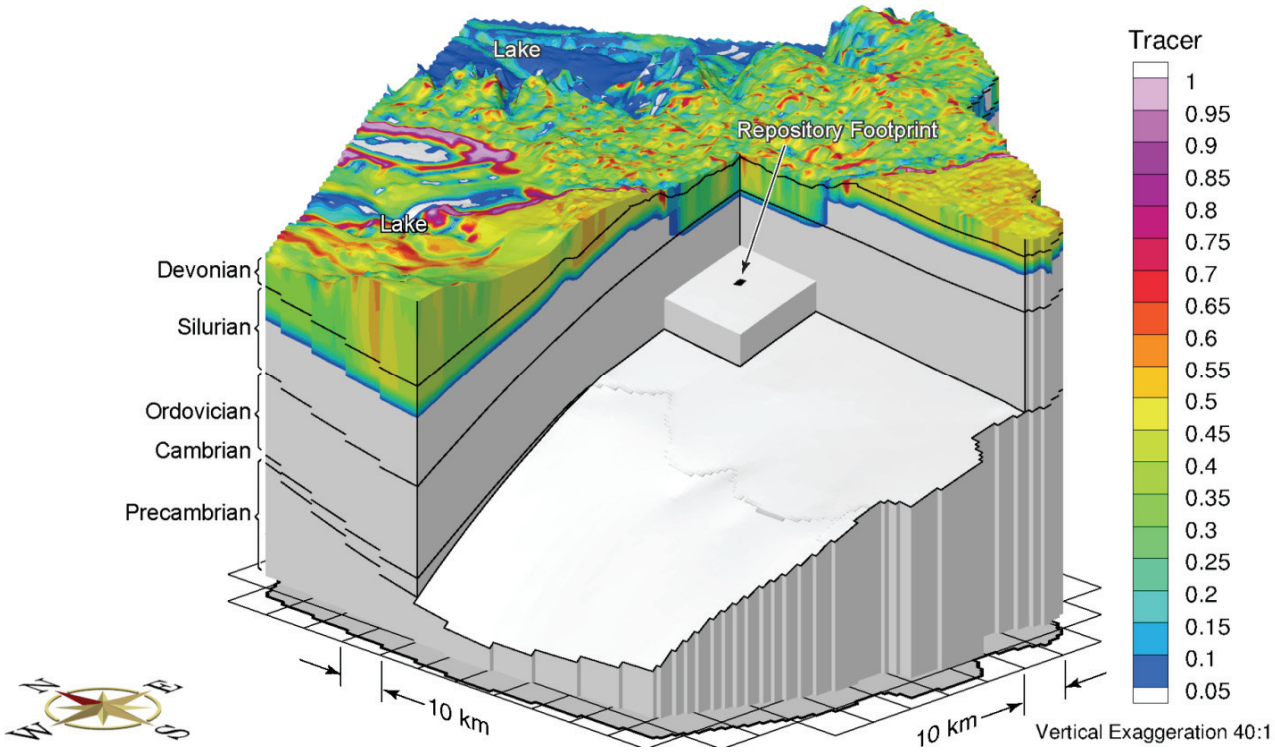

Figure 2-25: Block View Showing the Depth of Penetration of a Tracer after 120,000 Years for the nn9921 Paleoclimate Boundary Conditions (fr-base-paleo-cold)

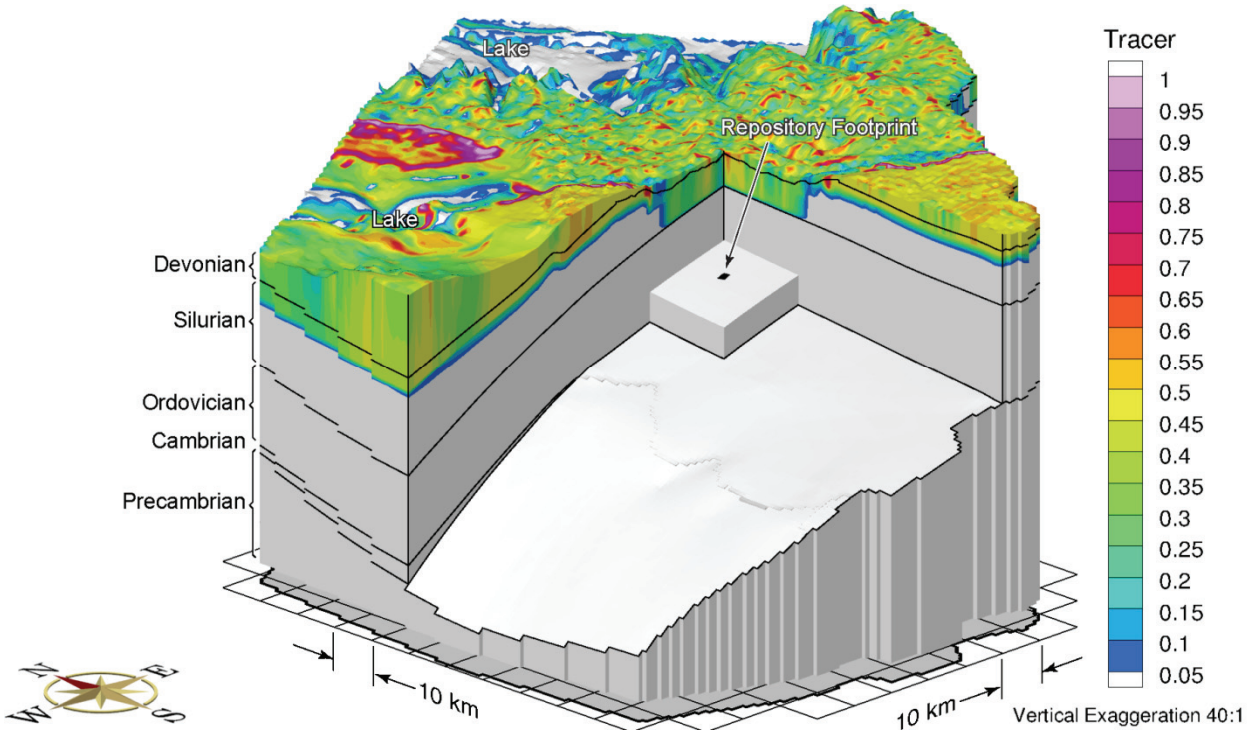

Figure 2-26: Block View Showing the Depth of Penetration of a Tracer after 120,000 Years for the nn9930 Paleoclimate Boundary Conditions and a Loading Efficiency of 1 (fr-base-paleo-le1)

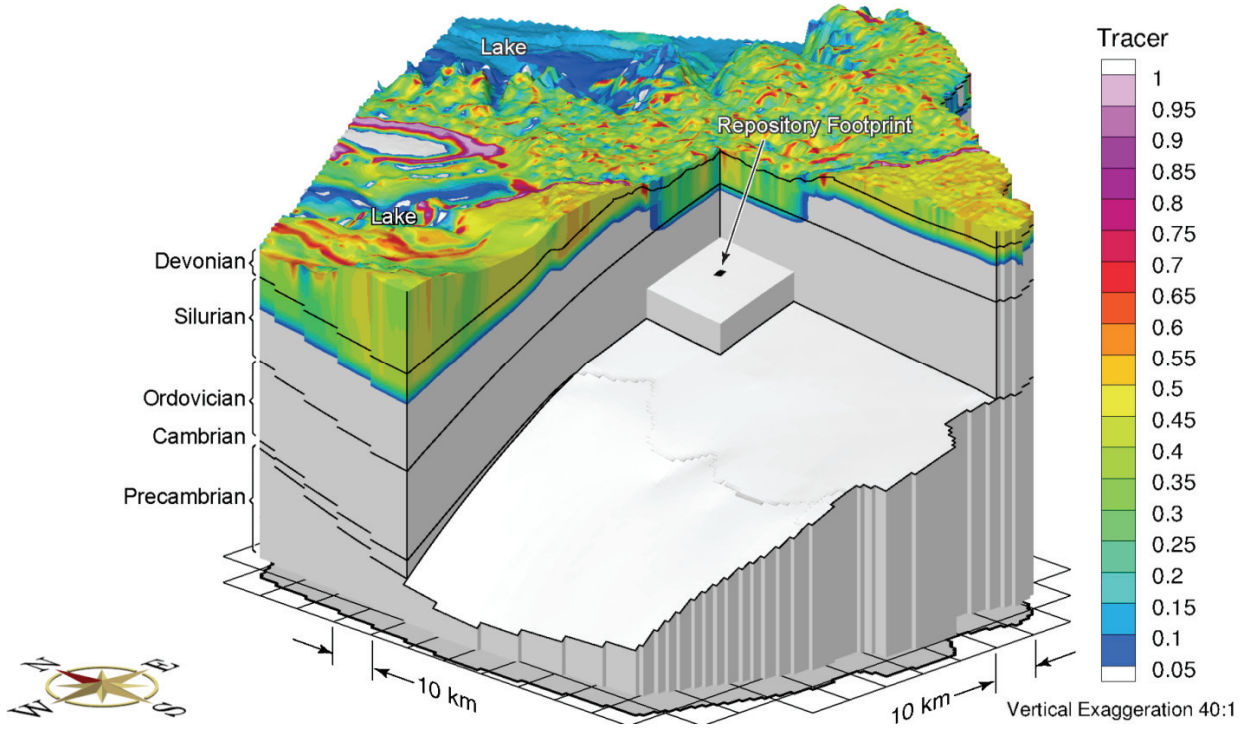

Figure 2-27: Block View Showing the Depth of Penetration of a Tracer after 120,000 Years for the nn9930 Paleoclimate Boundary Conditions and a Loading Efficiency of 0 (fr-base-paleo-le0)

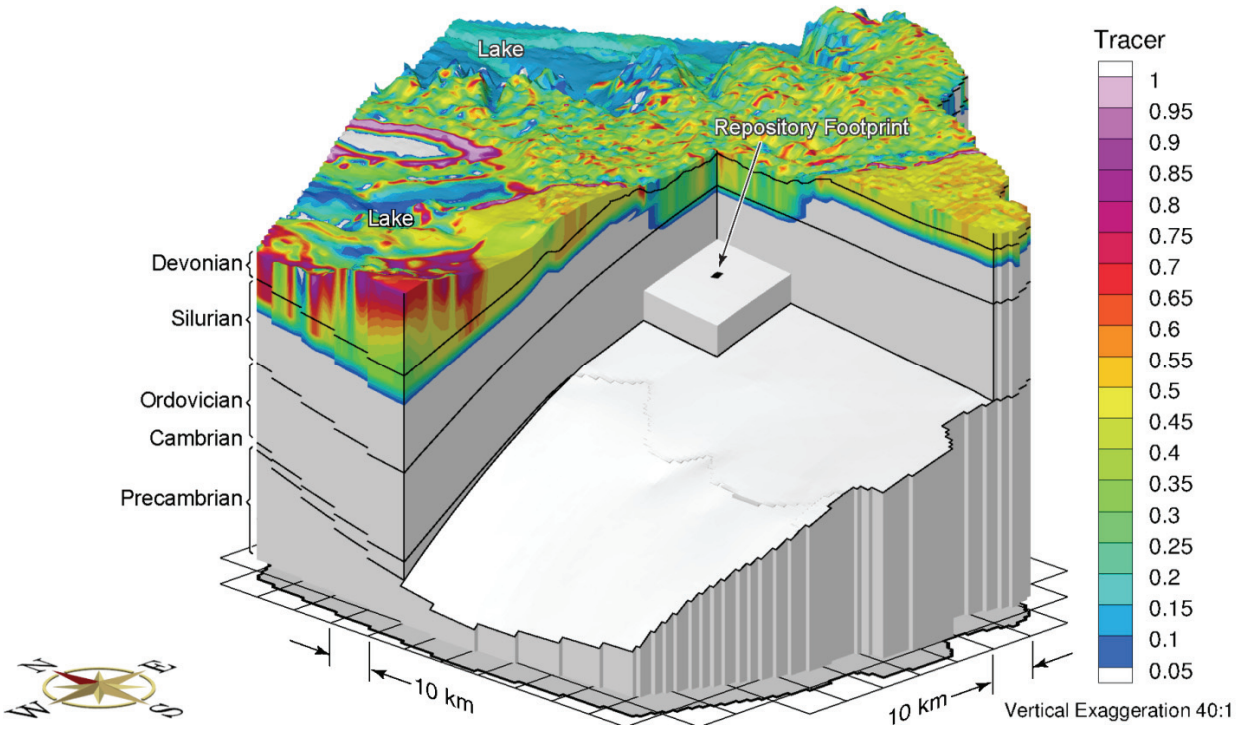

Figure 2-28: Block View Showing the Depth of Penetration of a Tracer after 120,000 Years for the nn9930 Paleoclimate Boundary Conditions, a Loading Efficiency of 1, and a 0% of Ice-Sheet Thickness Equivalent Freshwater Head for the Surface Hydraulic Boundary Condition (fr-base-paleo-0-le1)

The Péclet number, calculated as a ratio of the product of the porewater velocity and a characteristic length to the effective diffusion coefficient (Bear 1988), serves as an indicator for the dominance of advection or diffusion in mass transport processes. A plot of the Péclet number of molecular diffusion versus time for the reference case paleohydrogeologic scenario (fr-base-paleo), with a characteristic length of unity, is shown in Figure 2-29, and illustrates the stability of the geosphere during glacial advances and retreats. Five time series curves of the Péclet number are extracted at the center, west corner, north corner, east corner, and south corner of the hypothetical repository footprint, respectively. The grey regions in the figure represent upward groundwater movement, while the white regions represent downward groundwater movement. Through the duration of the glacial cycle, the Péclet number is well below the transition region, which indicates diffusion as the dominant transport mechanism for the reference case.

Select sensitivity cases illustrating the Péclet numbers versus time for scenarios fr-base-paleo-sens, fr-base-paleo-le0, and fr-base-paleo-0-le1, are shown in Figure 2-30, Figure 2-31, and Figure 2-32, respectively. These scenarios were chosen based upon porewater velocities, which are governed by hydraulic conductivities and head gradients. The Péclet numbers for the scenario with enhanced rock mass hydraulic conductivities (fr-base-paleo-sens), as illustrated in Figure 2-30, are slighter greater than for the reference case, but are still far below the transition zone. Thus, diffusion remains the dominant transport mechanism for the duration of the glacial cycles.

Scenarios fr-base-paleo-le0 and fr-base-paleo-0-le1 have the greatest downward and upward hydraulic gradients during glacial loading, however, their Péclet numbers versus time curves show less variation than the reference case, which can be explained by two main reasons. Firstly, the uniform loading efficiencies for these two cases means that inter-formational vertical gradients will not be generated during the glacial cycles. Secondly, the hydraulic conductivities of the Salina and Ordovician sediments are so low that the hydraulic boundary conditions at the top surface will not propagate into the deep groundwater flow system at the hypothetical repository footprint level. Both of the scenarios have Péclet numbers consistently far less than 0.4, which indicates that solute transport is dominated by molecular diffusion (Bear 1988).

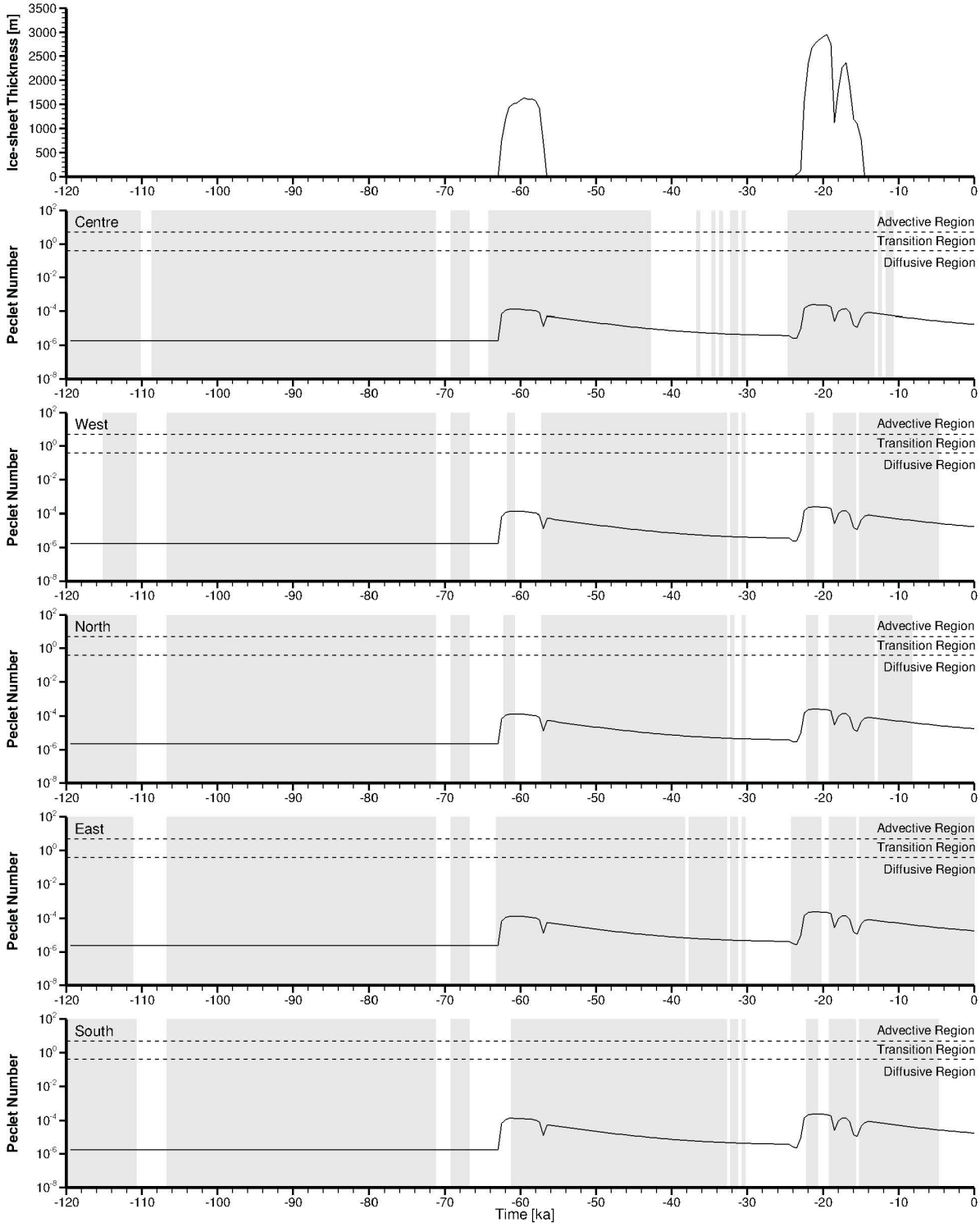

Note: Grey regions represent upward flow and white regions represent downward flow.

Figure 2-29: Péclet Number of Molecular Diffusion versus Time at the Hypothetical Repository Footprint for the Reference Paleohydrogeological Scenario (fr-base-paleo)

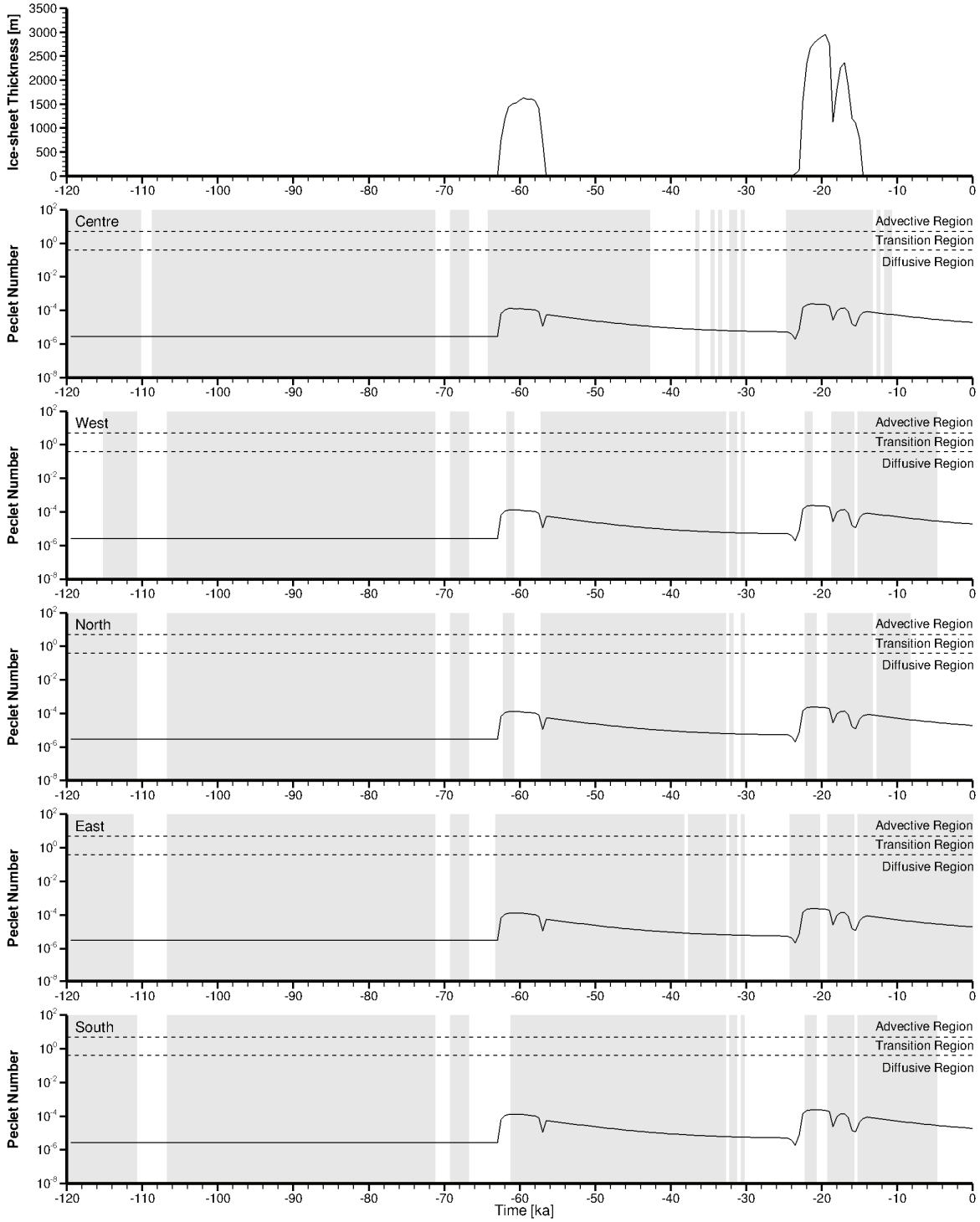

Figure 2-30: Péclet Number of Molecular Diffusion versus Time at the Hypothetical Repository Footprint for the Paleohydrogeological Scenario with Increased Rock Mass Hydraulic Conductivity (fr-base-paleo-sens)

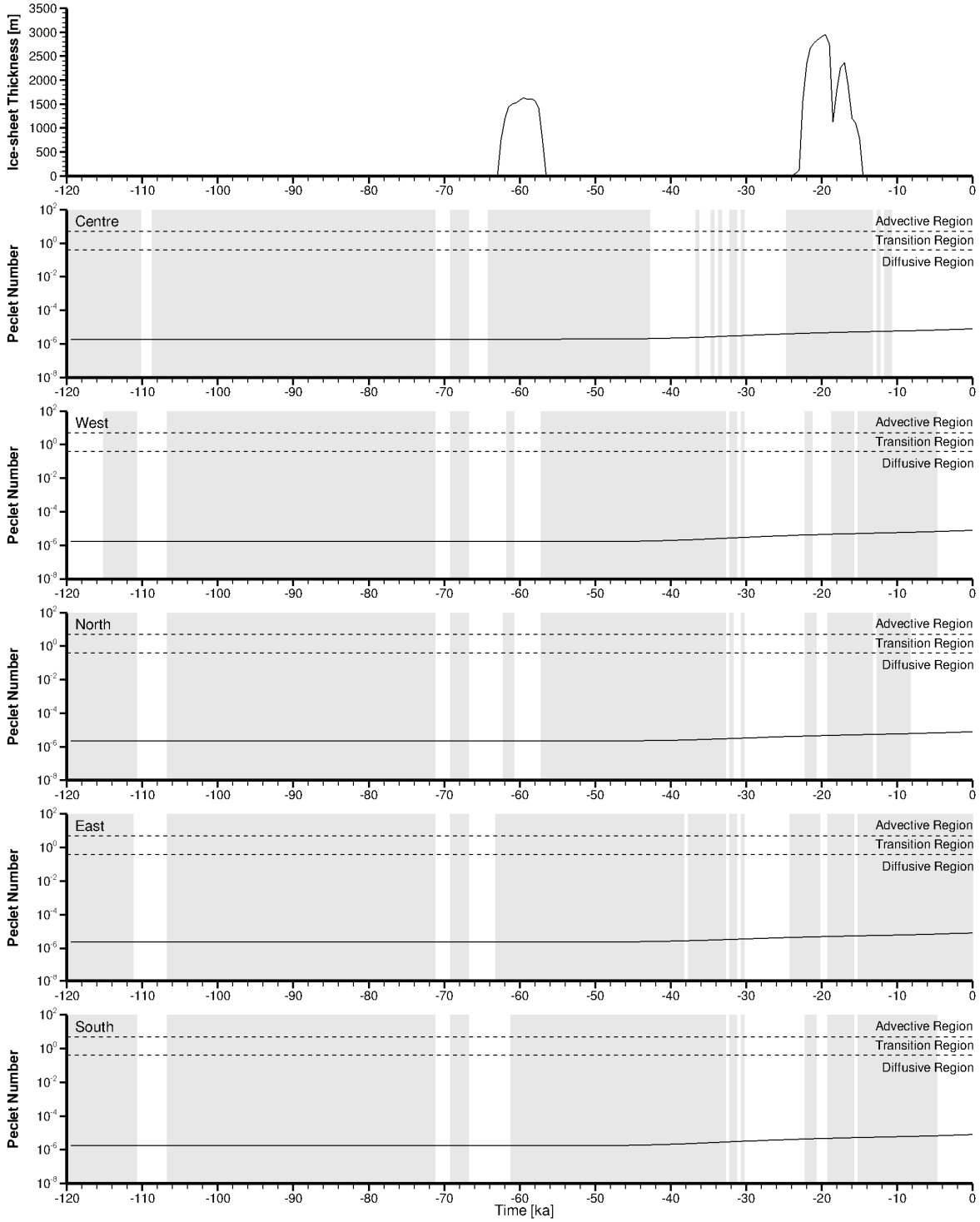

Figure 2-31: Péclet Number of Molecular Diffusion versus Time at the Hypothetical Repository Footprint for nn9930 Paleoclimate Boundary Conditions and a Loading Efficiency of 0 (fr-base-paleo-le0)

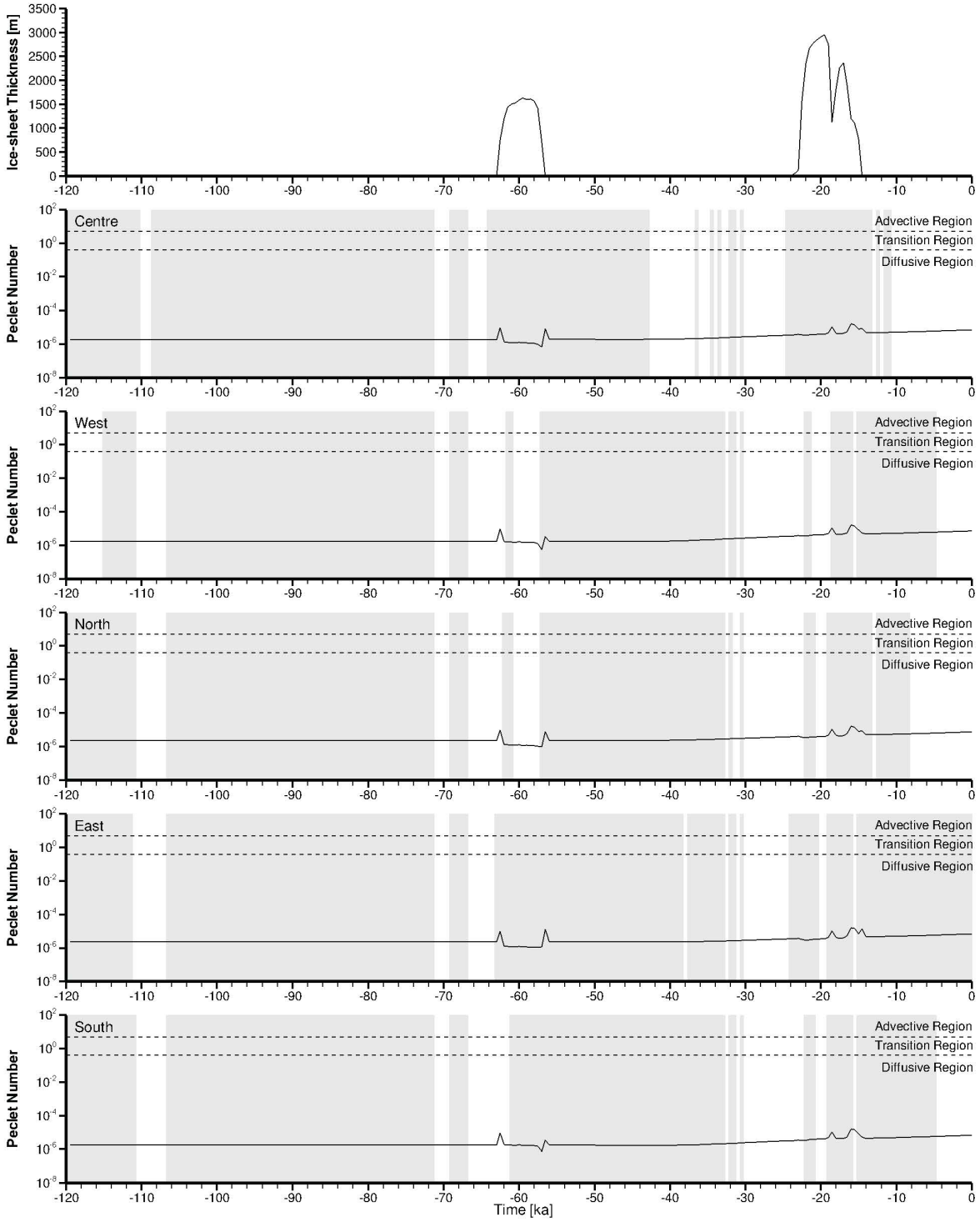

Figure 2-32: Péclet Number of Molecular Diffusion versus Time at the Hypothetical Repository Footprint for nn9930 Paleoclimate Boundary Conditions, a Loading Efficiency of 1, and a 0% of Ice-Sheet Thickness Equivalent Freshwater Head for the Surface Hydraulic Boundary Condition (fr-base-paleo-0-le1)

In a density-dependent groundwater flow system, freshwater head can only be used to determine hydraulic gradients along a horizontal plane; and environmental heads define hydraulic gradients along a vertical line (Lusczynski 1961). For the reference case paleohydrogeologic scenario (fr-base-paleo), a plot of environmental head versus time for various formations (Figure 2-33) indicates vertical gradients due to head differences across formations at the hypothetical repository footprint during the nn9930 glacial cycle. A large portion of the hydraulically conductive Guelph Formation is exposed to the Quaternary drift layer, which creates a hydraulic connection between the Guelph Formation and the top surface of the model. Therefore, Figure 2-33 shows that minimal vertical hydraulic gradients exist between the top surface and Guelph Formation throughout the 120,000 years paleohydrogeologic simulation. The very low hydraulic conductivities in the Salina units and Ordovician sediments ensure the deep groundwater flow system is not hydraulically connected to the surface boundary conditions, even during ice-sheet advance and retreat. The variations of heads over time are caused by one-dimensional hydro-mechanical coupling. The vertical hydraulic gradients at depth are mainly determined by the relative magnitude of loading efficiency for each formation. The Queenston Formation has the smallest loading efficiency and the value for the Precambrian is the largest. The resulting vertical hydraulic gradients from the Queenston to the Precambrian are mostly upward during the loading and unloading intervals. Figure 2-34 and Figure 2-35 show the time series plots of environmental heads for fr-base-paleo-le0 and fr-base-paleo-0-le1, respectively. The same conclusion can be drawn (as for the preceding section) that uniform loading efficiencies result in zero vertical hydraulic gradients in this case. Additionally, it is worth noting that the environmental heads in the Queenston Formation behave differently. At the location of hypothetical repository footprint, most of the Salina units pinch out west of the site such that the heads above the Ordovician sediments will be affected by the surface boundary conditions during the glacial cycles to some degree.

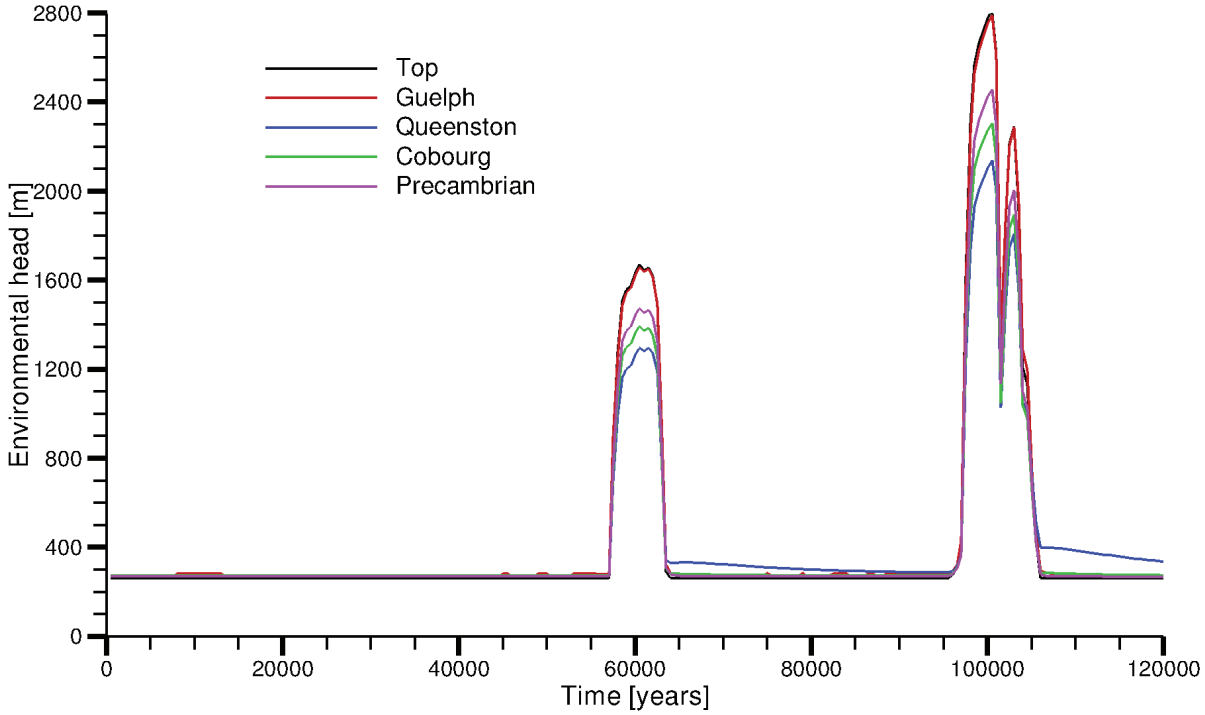

Figure 2-33: **Environmental Head versus Time for the Reference Paleohydrogeological Scenario (fr-base-paleo)**

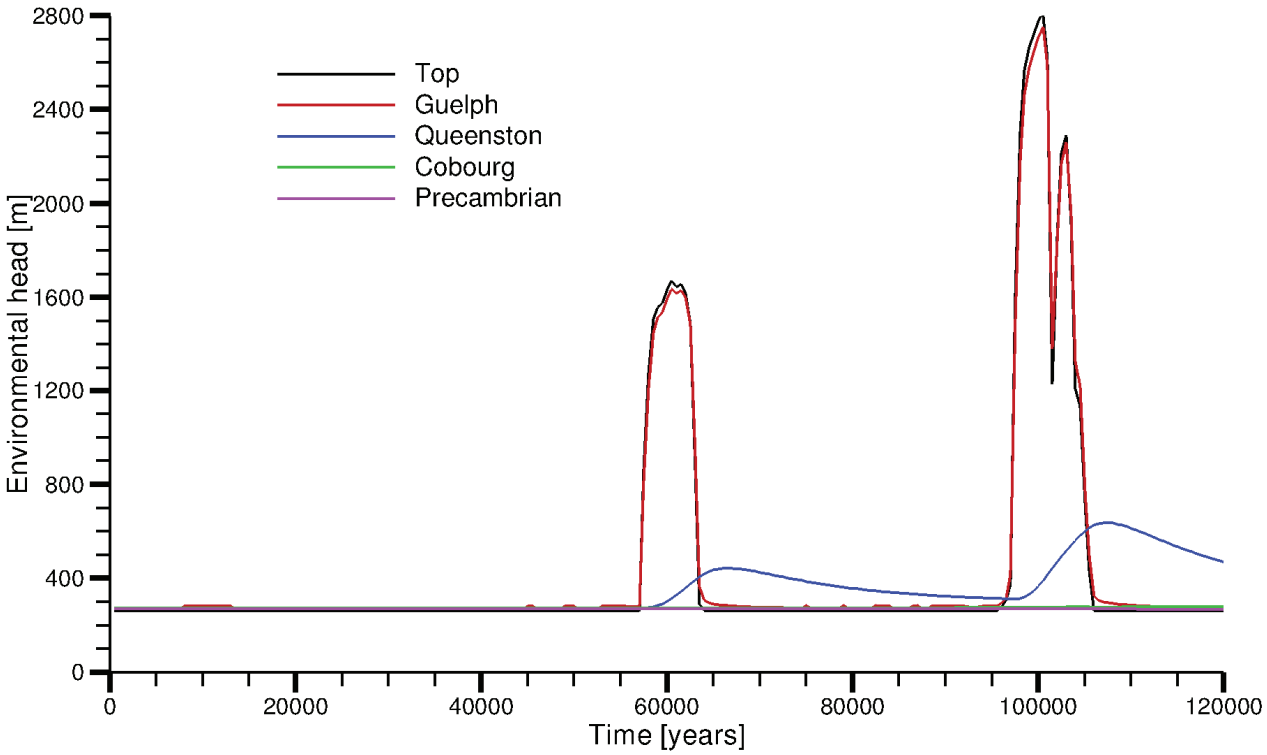

Figure 2-34: Environmental Head versus Time for nn9930 Paleoclimate Boundary Conditions and a Loading Efficiency of 0 (fr-base-paleo-le0)

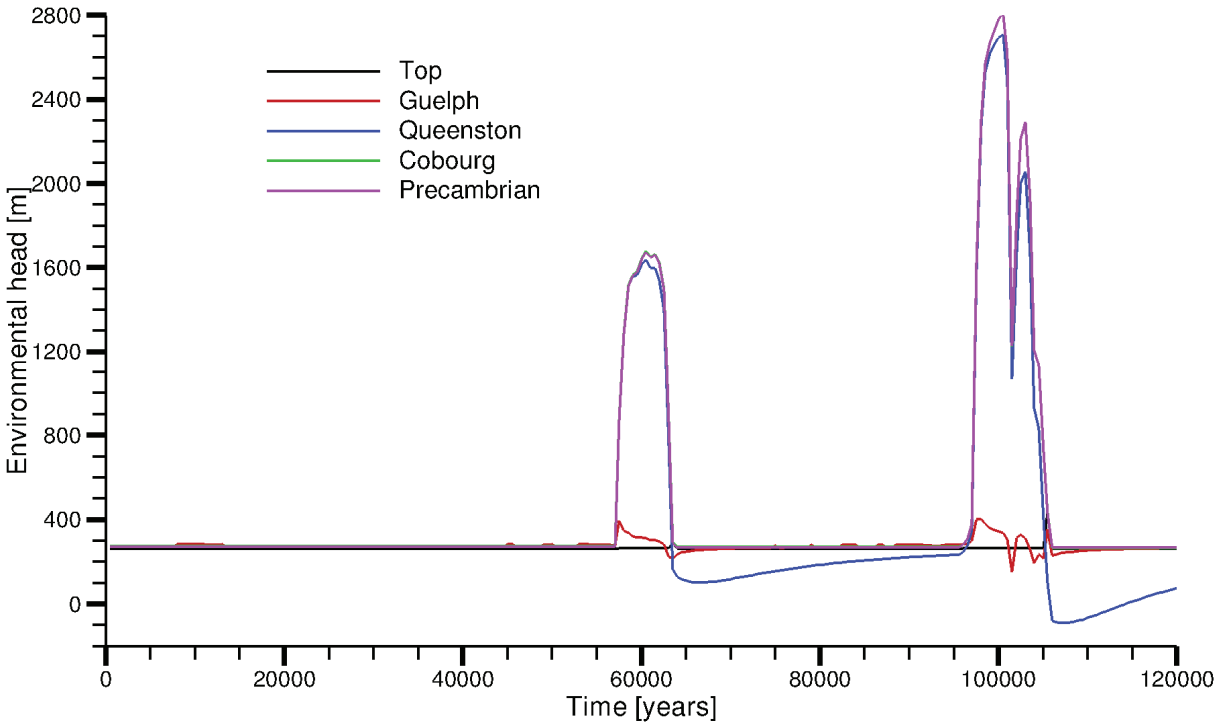

Figure 2-35: **Environmental Head versus Time for nn9930 Paleoclimate Boundary Conditions, a Loading Efficiency of 1, and a 0% of Ice-Sheet Thickness Equivalent Freshwater Head for the Surface Hydraulic Boundary Condition (fr-base-paleo-0-le1)**

2.3.4.4 Groundwater System Behaviour

2.3.4.4.1 Glaciation

The role of using a different paleoclimate model was investigated by scenario fr-base-paleo-cold using the nn9921 paleoclimate simulation. Through a comparison of Figure 2-25 to Figure 2-26, nn9921 includes more glaciation episodes, and longer glacial duration and permafrost presence at the hypothetical repository footprint within a 120,000 years period than paleoclimate model nn9930. Glacial presence tends to induce downward tracer migration and groundwater dilution by recharge water. Permafrost presence, on the contrary, tends to retard these processes by reducing the effective hydraulic conductivity of the layer. Figure 2-24 shows that the tracer migration for model nn9921 is still largely contained within the Silurian, and tracer concentrations are largely less than the tracer profile of the reference case. Figure 2-36 indicates that TDS concentrations in the Silurian are consistently greater for model nn9921 (fr-base-paleo-cold) than TDS concentrations in the reference scenario. Therefore, the impact of permafrost presence on the tracer migration outweighs the role of glaciation.

The reference case uses 100% of ice-sheet thickness in calculating the equivalent freshwater head. Alternate hydraulic boundary conditions applied to the surface of the modelling domain are analyzed in this study. These hydraulic boundary conditions are set to 80%, 30%, and 0% of the ice thickness equivalent freshwater head. For the reference scenario, glaciation generally results in downward flow during the loading phase and upward groundwater flow during the unloading phase. In the shallow units, the tracer migrates from surface and is then flushed out within one glacial episode. For the 0% case, representing zero fluid pressure at the top surface, upward flow occurs during glacial loading, and downward flow occurs during glacial unloading, primarily due to increased pore fluid pressures resulting from hydromechanical coupling. Thus, slightly deeper tracer migration occurs when compared to the reference case (as shown in Figure 2-24). The 30% case results in the tracer profiles situated between the reference case (100%) and the 0% case. The 80% case demonstrates a lower tracer concentration than the reference case, primarily due to loading efficiencies in the upper formations close to a value of 0.8 (see Table 2-2); a loading efficiency of 0.8 would result in no vertical gradients from glacial loading or unloading. The different TDS distributions in Figure 2-36 for these four scenarios are attributed to the relative magnitude of ice-sheet loading and unloading rates, in addition to the relative proportion of the surface hydraulic boundary condition to the one-dimensional loading efficiency for various formations.

2.3.4.4.2 Permafrost

Permafrost develops in advance of the ice-sheet because the ground surface is directly exposed to climate variations, whereas ice-sheets thermally insulate the underlying geosphere from climate influences (Peltier 2002). Permafrost with very low permeability often acts as the inhibitor of surface water migration downward and groundwater discharge. By a comparison of tracer migration in Figure 2-24 and TDS distribution at 120,000 years in Figure 2-36 (between the reference case with the nn9930 paleoclimate condition and fr-base-paleo-cold with the nn9921 paleoclimate condition), it is found that the cold-based paleohydrogeologic simulation has higher TDS concentrations in the shallow regime and less penetration depth of recharge water. In fact, Figure 2-26 demonstrates that the more frequent glacial cycles and longer permafrost presence in the nn9921 model, as compared to the nn9930 model, will inhibit both surface recharge water migration downward and the dilution of brines with fresh water.

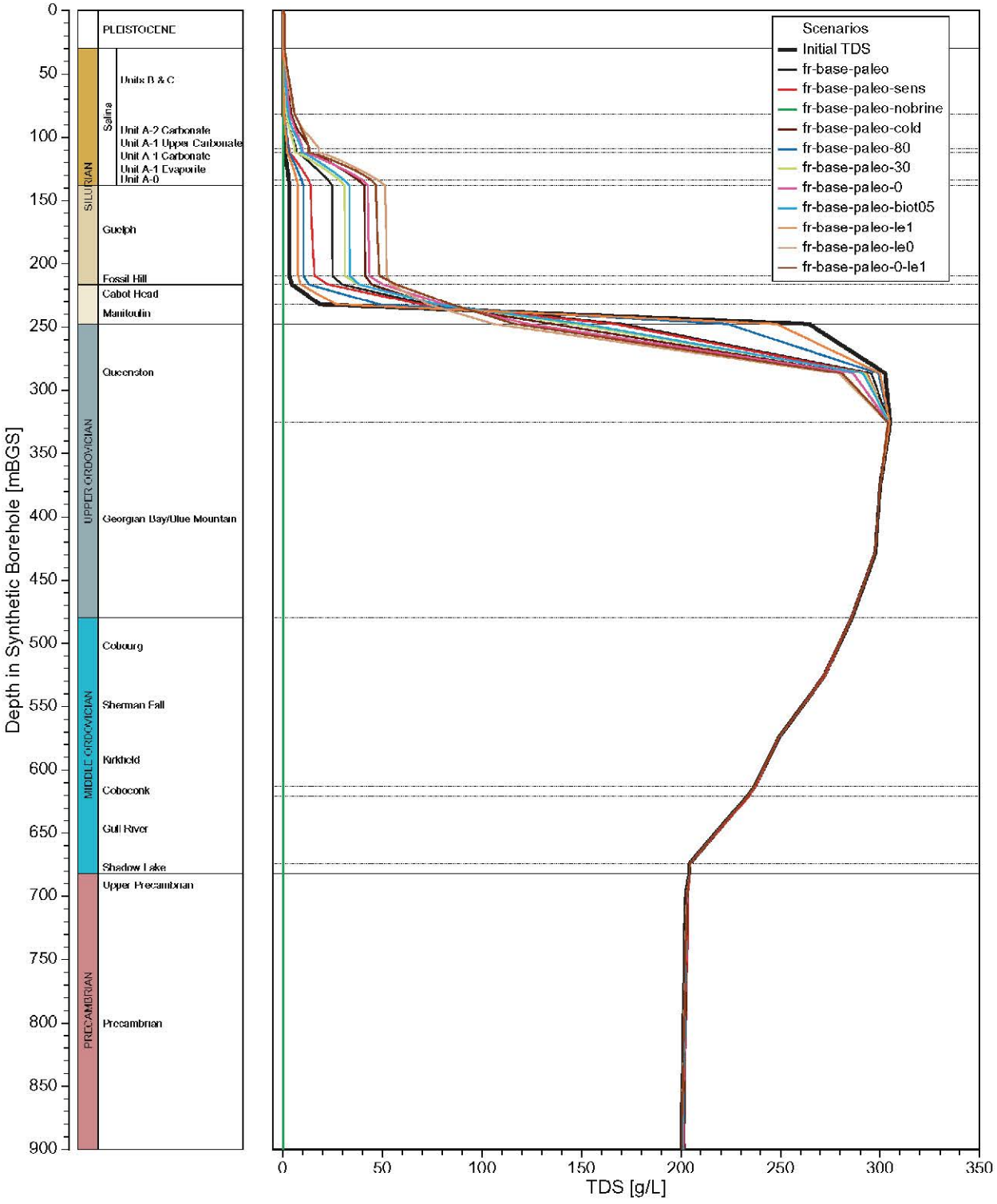

Figure 2-36: Vertical Profile Plots of TDS Concentrations for the Paleohydrogeologic Simulations at 120,000 Years at the Location of Hypothetical Repository Footprint

2.3.4.4.3 Depth of Surficial Recharge and Pathways

A tracer summary plot at 120,000 years for all paleohydrogeologic simulations is shown in Figure 2-24. The penetration depths of surficial recharge are represented by the intercepts between a straight line at a concentration of 0.05 and tracer concentration profiles at the hypothetical repository footprint at 120,000 years. The tracer for all the simulations only migrates into the bottom of the Silurian or the top of the Queenston Formation at 120,000 years. Thus, the downward migration of tracer is largely retarded by the low permeable Ordovician formations, which indicates the dominance of diffusion as a transport mechanism in the Ordovician. The greatest downward tracer migration occurs for the scenario fr-base-paleo-le0 with zero loading efficiency and 100% of ice-sheet thickness equivalent freshwater head for the surface hydraulic boundary condition. This tends to induce the greatest downward hydraulic gradient during the glacial loading phase. Scenario fr-base-paleo-le1 has the shallowest penetration depth, as the additional in-situ head induced by the mechanical coupling always equilibrates to the hydraulic surface boundary conditions with 100% of ice-sheet thickness equivalent freshwater head. Thus, for this scenario, negligible vertical hydraulic gradients exist throughout the paleohydrogeologic simulation period, including during glaciation cycles. The tracer in this case migrates downward mostly by diffusion.

2.3.4.4.4 The Role of Density

The increase in density of fluids at depth tends to slow down active flow in the deep groundwater system because resistance to driving forces increases with denser groundwater at depth (Park et al. 2009). However, the comparison of porewater velocities between steady-state and density-dependent simulation results in Figure 2-17 show that the velocity magnitude at depth in the steady-state model without brine (fr-base-nobrine) is slightly less than that in the reference model (fr-base). This can also be verified by the MLE comparison plot in Figure 2-18. Except for the portion beneath the lake, the mean life expectancies are generally higher in the freshwater simulation, which indicates a more stagnant groundwater system. The apparent contradiction can be explained by factors that influence fluid movement. A steady-state solution can be derived from the freshwater model, where the groundwater flow is purely driven by topography. The groundwater flow system of the reference case (with salinity) is still experiencing slow evolution at one million years of simulation time. Groundwater movement is not only driven by topography, but also is affected by the evolving TDS distribution.

For the paleohydrogeologic simulations, Figure 2-24 shows that no major difference in tracer profiles is observed between the reference case and the sensitivity case without salinity (fr-base-paleo-nobrine). Tracer only migrates into the shallow groundwater regime, which has low TDS concentrations in Figure 2-36. The groundwater system with high salinity at depth is diffusion dominant. The impact of density on the tracer migration cannot be evaluated based on these two paleohydrogeologic simulations. A plot of environmental head versus time for the paleohydrogeologic scenario without brine (in Figure 2-37) shows the vertical gradients at the hypothetical repository footprint. The direction and magnitude of the vertical gradients at depth are almost identical throughout the simulation period, as in the reference case shown in Figure 2-33.

2.3.4.4.5 Anomalous Heads

A summary plot of freshwater heads versus depth at 120,000 years for all paleohydrogeologic simulations is shown in Figure 2-38. At the Upper Ordovician, including the Queenston and Georgian Bay/Blue Mountain formations, no under or over-pressures are simulated for the scenario (fr-base-paleo-le1) with a loading efficiency of unity and a 100% ice-sheet thickness as equivalent freshwater head for the surface hydraulic boundary condition. The increase or decrease of hydraulic heads, due to hydro-mechanical coupling, always equilibrates to the surface hydraulic boundary condition; no vertical gradients are imposed by glacial loading and unloading.

Three scenarios (fr-base-paleo-0, fr-base-paleo-30, and fr-base-paleo-0-le1) result in under-pressured head distributions, owing to the reduced surface boundary heads. Among them, fr-base-paleo-0-le1 has the greatest under-pressures in the Upper Ordovician, as the loading efficiency of unity, combined with a free surface boundary condition, causes the largest upward hydraulic gradient during glacial loading. Discharge of groundwater during glacial loading leads to a deficit of water and the formation of under-pressures during glacial unloading. As compared to the reference case with a slight over-pressure, a reduction of surface boundary heads can shift the head distribution in the Upper Ordovician from over-pressured to under-pressured. Simulations with 80%, 30%, and 0% of ice-sheet thickness as equivalent freshwater heads result in less over-pressure than the reference case, slight under-pressure and more under-pressure in the Upper Ordovician, respectively.

Scenario fr-base-paleo-le0 has the greatest over-pressures due to the lack of hydro-mechanical coupling, which does not allow for an increase in in-situ pore pressures throughout the domain as a result of glacially induced hydro-mechanical coupling. The increase in pore pressure tends to diminish the vertical hydraulic gradient from the surface boundary condition for a non-zero loading efficiency. The increased downward gradients lead to the greatest residual heads of all the paleohydrogeologic simulations.

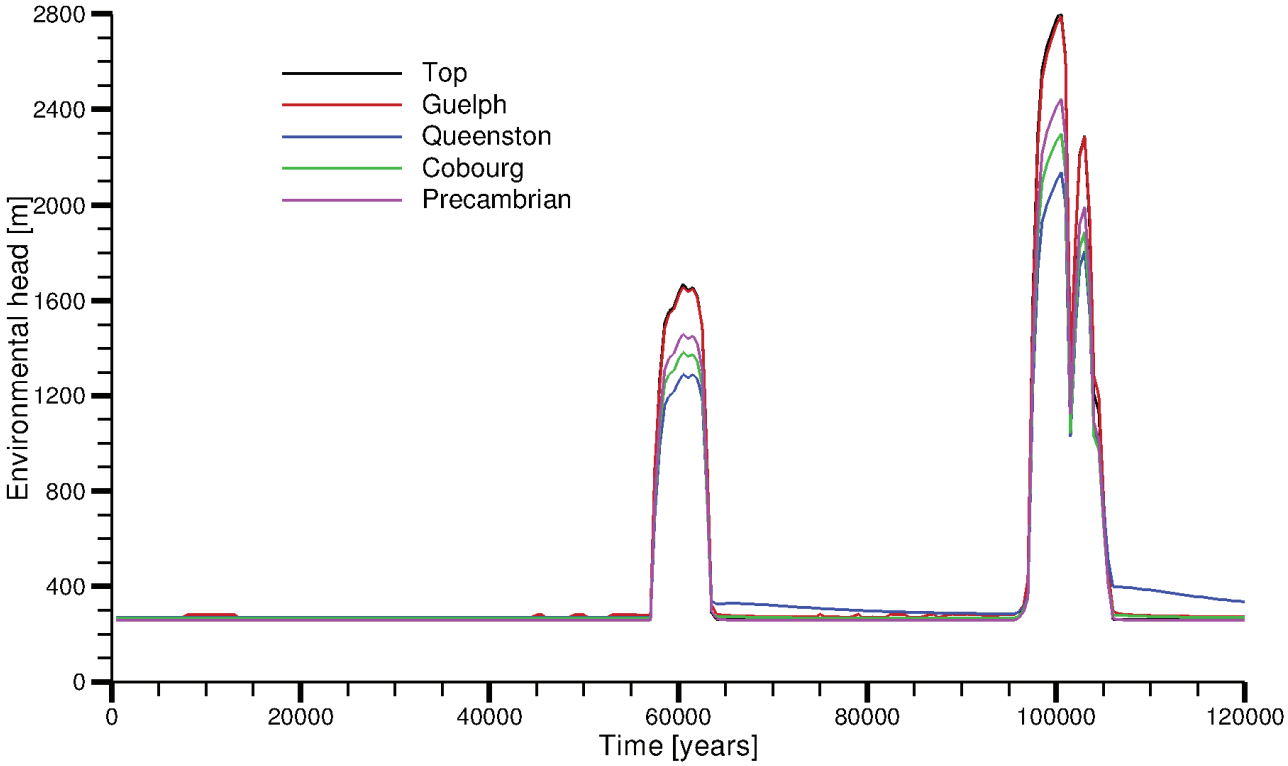

Figure 2-37: Environmental Head versus Time for the Paleohydrogeological Scenario without Salinity (fr-base-paleo-nobrine)

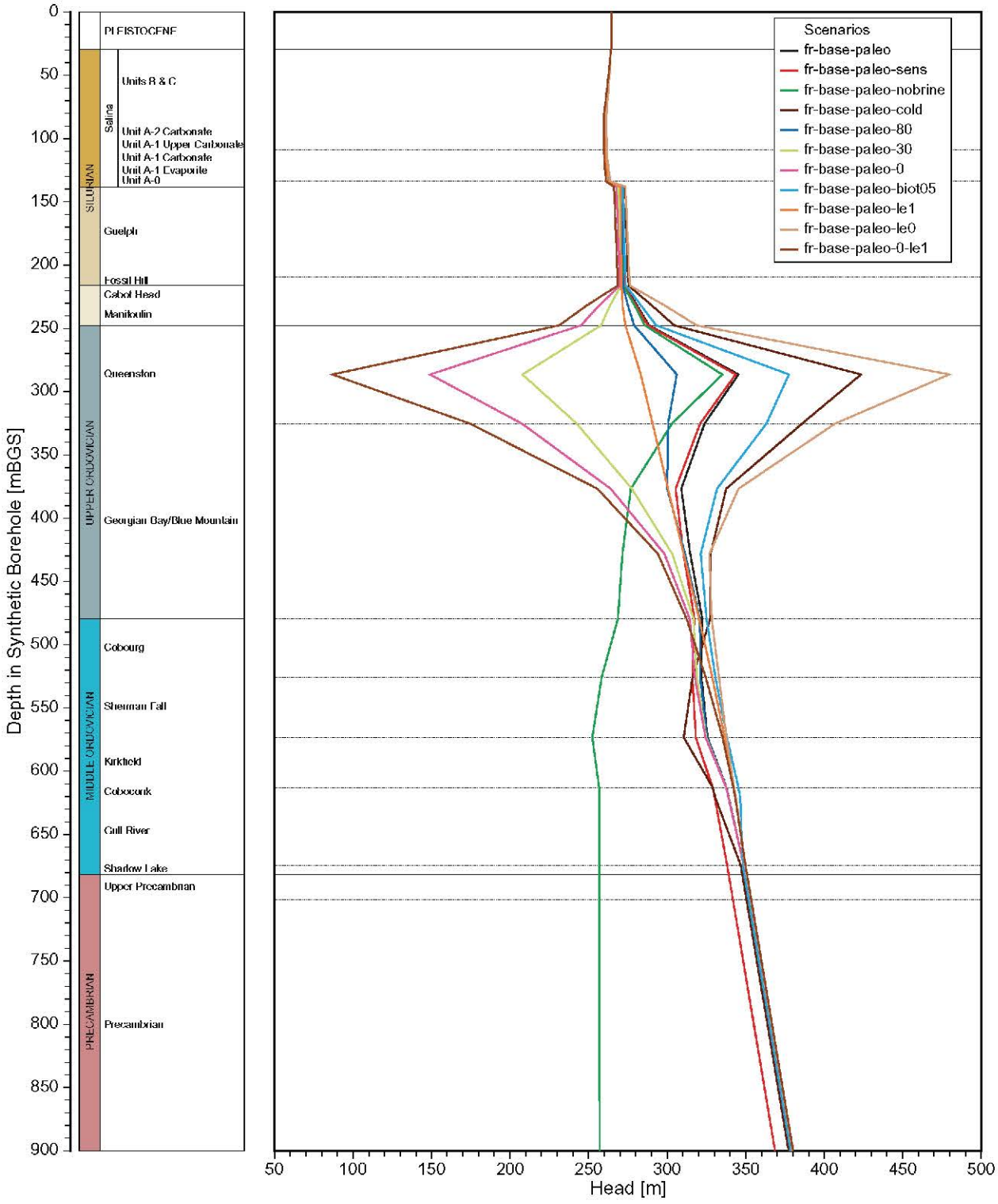

Figure 2-38: Vertical Profile Plots of Freshwater Heads for the Paleohydrogeologic Simulations at 120,000 Years at the Location of Hypothetical Repository Footprint

2.3.5 Additional Temperate Transient Sensitivity Analyses

Additional temperate scenarios were developed to determine the sensitivity of system performance to parameters including diffusion coefficients, dispersivities and hydraulic conductivities. Generally, an increase in diffusion or dispersion leads to mean life expectancy (MLE) spreading and overall reductions in MLE values. Similarly, total dissolved solids (TDS) are more uniformly distributed. At pseudo-equilibrium times of one million years, the groundwater system state is closer to equilibrium and can result in higher MLE values. The sensitivity of MLE to parameter changes is represented using dimensionless or normalized local sensitivities.

The base case (fr-base) MLE value at the repository footprint is 177 Ma. Table 2-9 lists MLE values at the center of the repository footprint for the reference case and for the additional temperate scenarios. Free solution diffusion coefficients for both brine and mean life expectancy were increased by one order of magnitude, resulting in an MLE value of 19.1 Ma at the repository footprint, nearly one-tenth the MLE of the base case. The local sensitivity was determined by perturbing the diffusion coefficients by 1%; the normalized local sensitivity (the percentage change in computed MLE divided by the percentage change in diffusion coefficients) is -0.74 at the repository footprint. In this case, MLEs are considered sensitive and negatively correlated to diffusion coefficients; increasing diffusion coefficients will yield lower MLEs.

Increasing the free solution diffusion coefficients affects both brine and MLE transport. In coupled density-dependent groundwater systems, a change to TDS distributions throughout the domain also affects the flow system and porewater velocities; changes to the flow system affect MLE transport. To separate the combined effects of changes to both MLE and to the flow system, resulting from modified transport parameters, further simulations were performed using the base case velocity fields to compute MLE, and are listed in Table 2-9. MLE values at the repository footprint for scenarios with diffusion coefficients increased by 1% and increased by one order of magnitude are 175 Ma and 19.0 Ma, respectively. These values are slightly lower than their counterpart MLE values because the base case velocity fields are further from equilibrium, due to the lower diffusion coefficients for brine transport. By comparing the differences in MLE values, it can be concluded that the direct impact of MLE diffusion coefficients on MLE values is more important than the brine diffusion coefficients, which have an indirect influence on MLEs through a more evenly distributed TDS field and a more equilibrated velocity field.

Figure 2-39 and Figure 2-40 show the vertical MLE and TDS profiles, respectively, at the repository footprint for the reference case and the additional scenarios. TDS and MLE profiles for scenarios with a 1% increase in diffusion coefficients (fr-de1p) are almost indistinguishable from the reference case. A one order of magnitude increase (fr-de10) in diffusion coefficients significantly increases solute transport by diffusion, forcing high initial TDS in the upper Ordovician to dissipate upward to the Silurian and downward to the lower Ordovician much faster than in the reference case. The resulting MLE profiles are well below the reference case. Additionally, because the correlation coefficient of -0.74 is near to -1, this indicates that MLE transport is dominated by molecular diffusion.

The second set of analyses increased dispersivity values by 1%, 10%, and 100% and are identified as scenarios fr-disp1p, fr-disp10p, and fr-disp2. The local sensitivity analysis of dispersivities, determined by perturbing dispersivities by 1%, indicates that MLEs are positively correlated to dispersivities with a coefficient of 0.62 and an increase in MLE values relative to the base case. Further increases in dispersivity tend to yield similar MLE values within 5% of the base case (see Table 2-9); MLEs at the repository footprint are, therefore, not deemed to be sensitive to changes in dispersivity, and are largely attributed to the diffusion dominant transport regime below the Guelph Formation. Figure 2-39 and Figure 2-40 demonstrate that TDS and MLE profiles for scenarios with alternate dispersivities are either very close to or almost indistinguishable from the reference case. In doubling dispersivities (100% increase) for both brine and MLE, the MLE value at the repository footprint decreases to 171 Ma with a normalized sensitivity of -0.036.

Scenarios using the reference case porewater velocity field (fr-base prefix) and enhanced dispersivities for MLE were performed for two purposes: to evaluate the direct impact of MLE dispersivities on performance measures; and separately, to evaluate the indirect influence of brine dispersivities. Increasing MLE dispersivities always contributes to lower MLEs at the repository footprint, as shown in Table 2-9. Brine dispersivity enhancement leads to greater equilibration in TDS distribution and the groundwater flow field, leading to greater MLEs. For the 1% and 10% alternate dispersivity scenarios, brine dispersivities contribute to increased MLE, while the 100% cases result in decreased MLE at the repository footprint. For the third sensitivity analysis, hydraulic conductivities were enhanced by three orders-of-magnitude for the low permeability units between the Guelph and the Cambrian formations. The substantial increase in hydraulic conductivities results in more brine and TDS being flushed from the groundwater system, as shown in Figure 2-41. Compared to the reference case (Figure 2-13), Figure 2-42 shows that the velocity magnitude in those units with enhanced hydraulic conductivities is approximately increased by three orders-of-magnitude. The solute transport at the repository footprint is still dominated by diffusion; the Peclet number of molecular diffusion of 0.05 for a characteristic length of unity is well below 0.4 (Bear 1988). The mean life expectancy at the repository footprint is 6.3 Ma. Solute transport, by both advection and diffusion, from the upper Ordovician, with high initial TDS upward to the Silurian and downward to the lower Ordovician, is greatly enhanced during the one million year pseudo-equilibrium simulation. This results in lower TDS in the upper Ordovician shales and higher TDS in the Silurian formations and in the Ordovician carbonate formations, due to advective transport, than are observed in the reference case (Figure 2-40). Figure 2-39 and Figure 2-40 demonstrate that higher TDS concentrations in the shallow groundwater flow regime within the Silurian formations contributes to lower groundwater flow velocity magnitude and larger MLEs than in the reference case. As noted by Park et al. (2009), the increase in pore fluid density often acts to retard active flow. The MLEs in the Ordovician are significantly less than in the reference case due to higher velocity magnitudes caused by the increase of hydraulic conductivities in these units. In the Precambrian, the same profiles of MLE versus depth are observed, as the properties of this portion of the model domain remain unchanged.

Table 2-9: Computed MLE Values at the Repository Footprint for Alternate Temperate Scenarios

Scenario	Transport Parameter Application	
	Brine and MLE*	MLE**
Base case (fr-base)	177 Ma	177 Ma
Increase diffusion coefficient by 1% (prefix-de1p)	176 Ma	175 Ma
Increase diffusion coefficient by 1 order of magnitude (prefix-de10)	19.1 Ma	19.0 Ma
Increase dispersivities by 1% (prefix-disp1p)	178 Ma	177 Ma
Increase dispersivities by 10% (prefix-disp10p)	177 Ma	176 Ma
Increase dispersivities by 100% (prefix-disp2)	171 Ma	169 Ma
Increase hydraulic conductivity by 3 orders of magnitude (fr-hc1000)	6.34 Ma	N/A

Note: * prefix = ‘fr‘ in Column 1, ** prefix = ‘fr-base‘ in Column 1

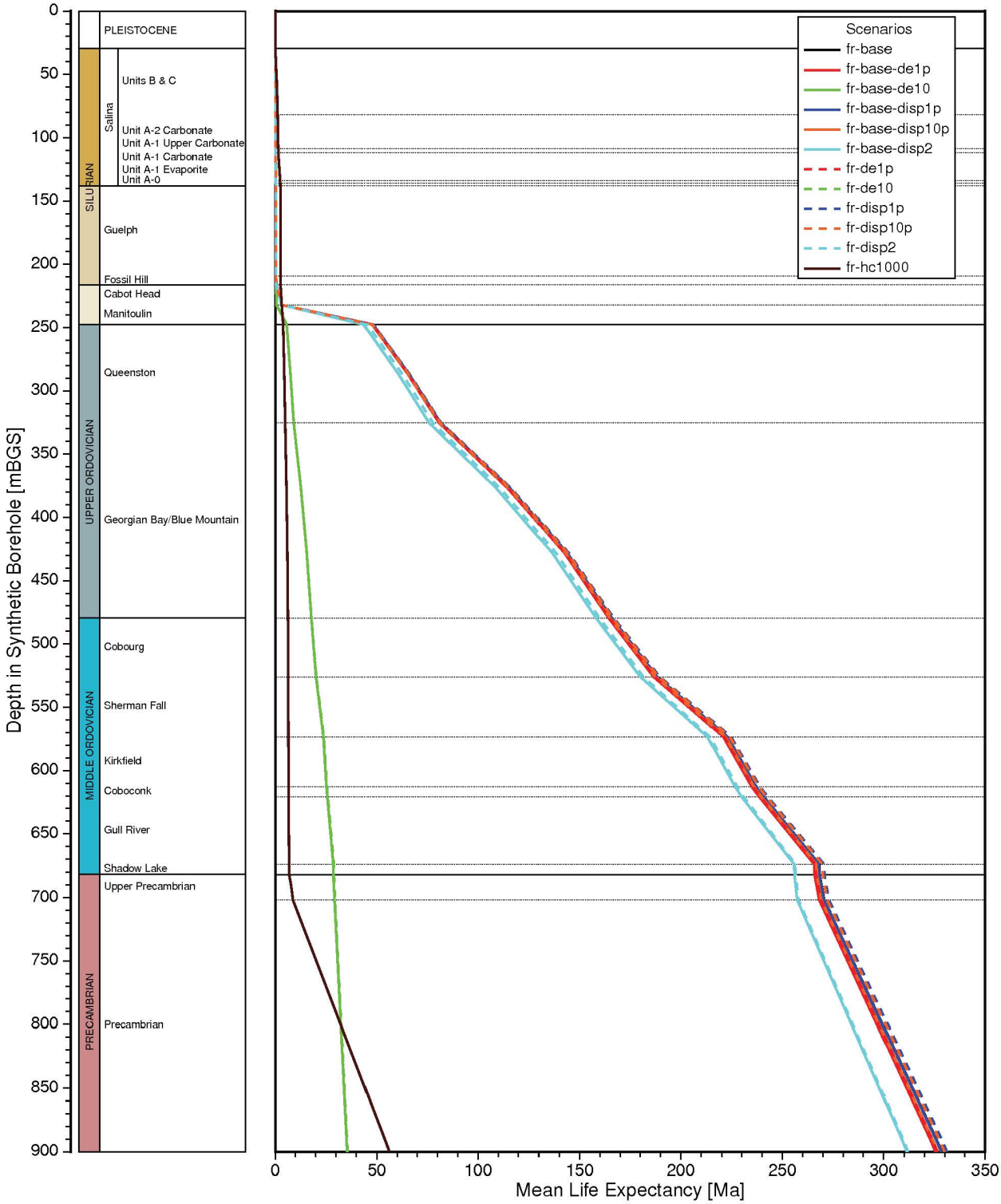

Notes: Solid lines represent scenarios which use the base case porewater velocity field.
Scenarios fr-base-de10 and fr-de-10 overlap.

Figure 2-39: Vertical Profile Plots of Mean Life Expectancies at One Million Years for the Reference Case and Additional Sensitivity Scenarios

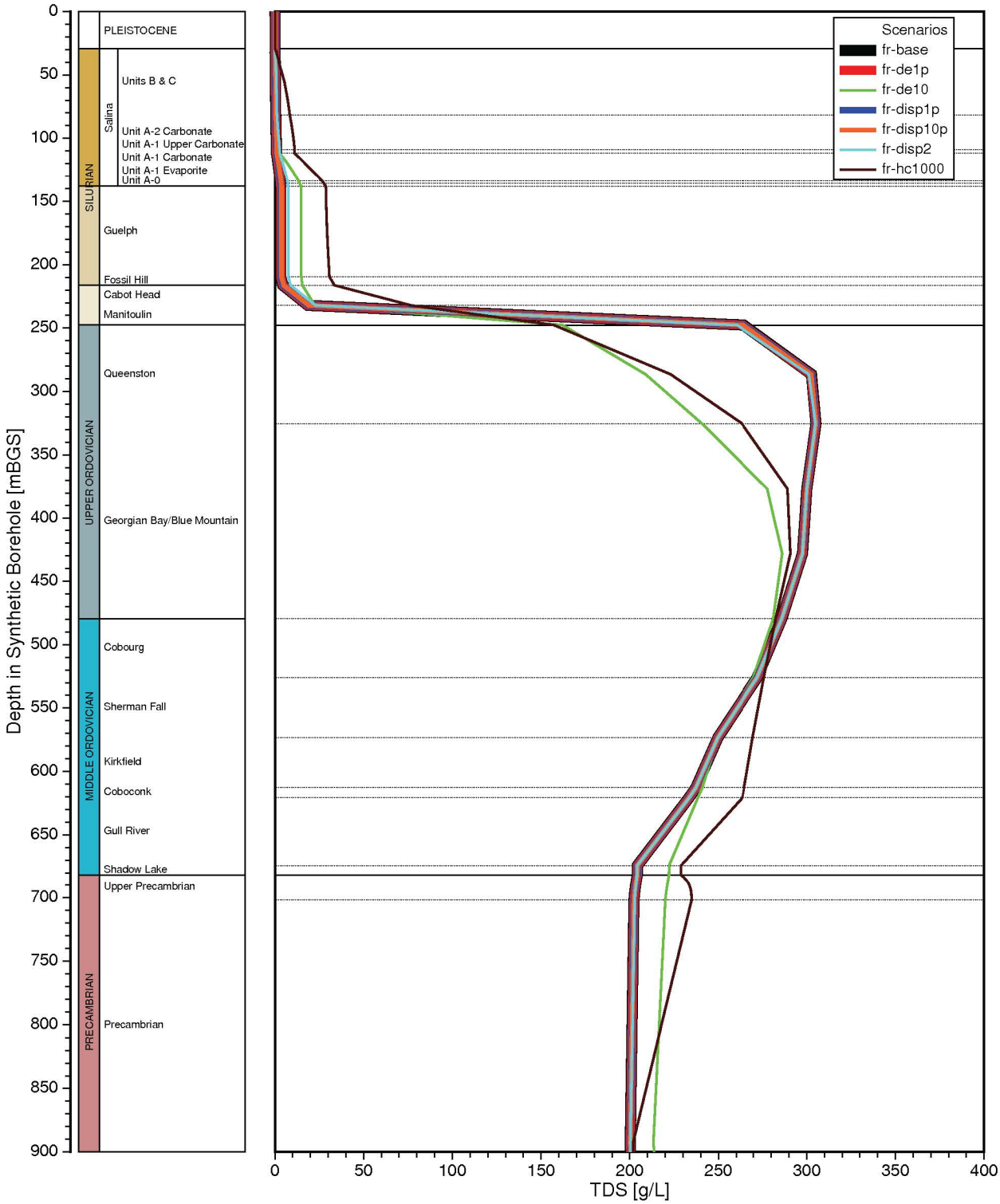

Figure 2-40: **Vertical Profile Plots of Total Dissolved Solids Concentrations at One Million Years for the Reference Case and Additional Sensitivity Scenarios**

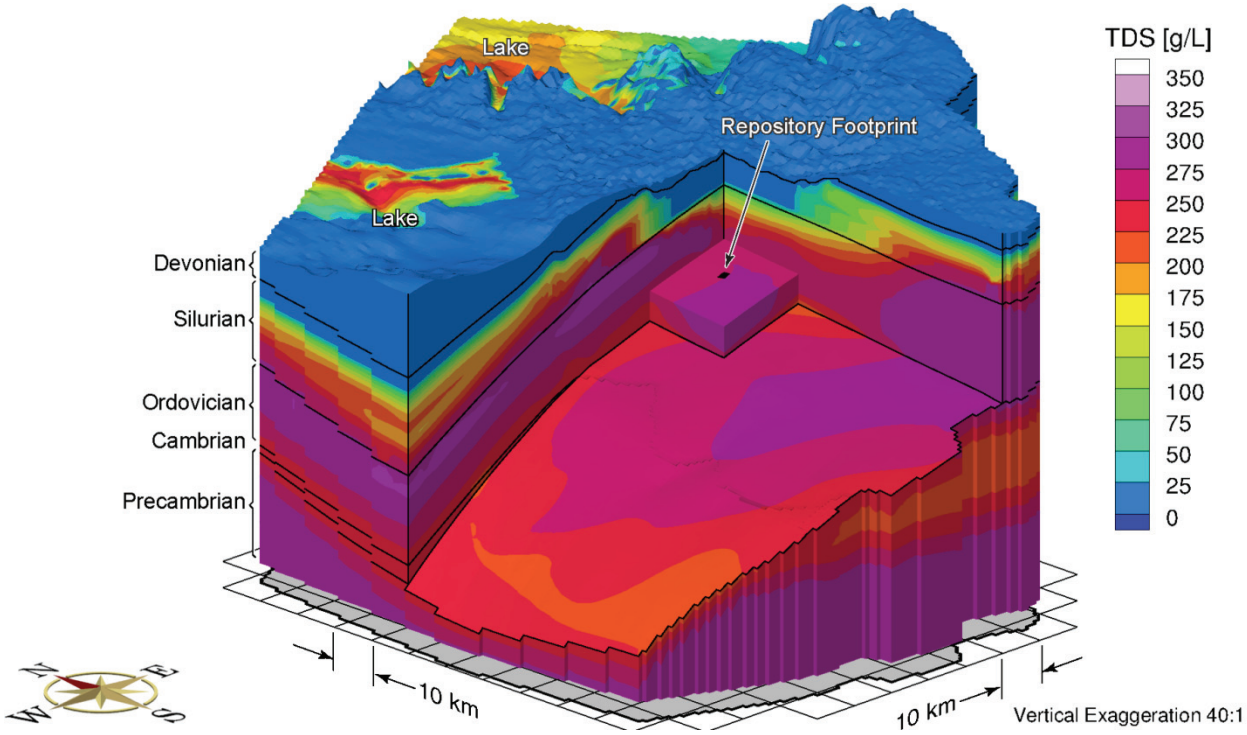

Figure 2-41: **Total Dissolved Solids Concentrations at One Million Years for a Three Order of Magnitude Enhancement in Hydraulic Conductivities**

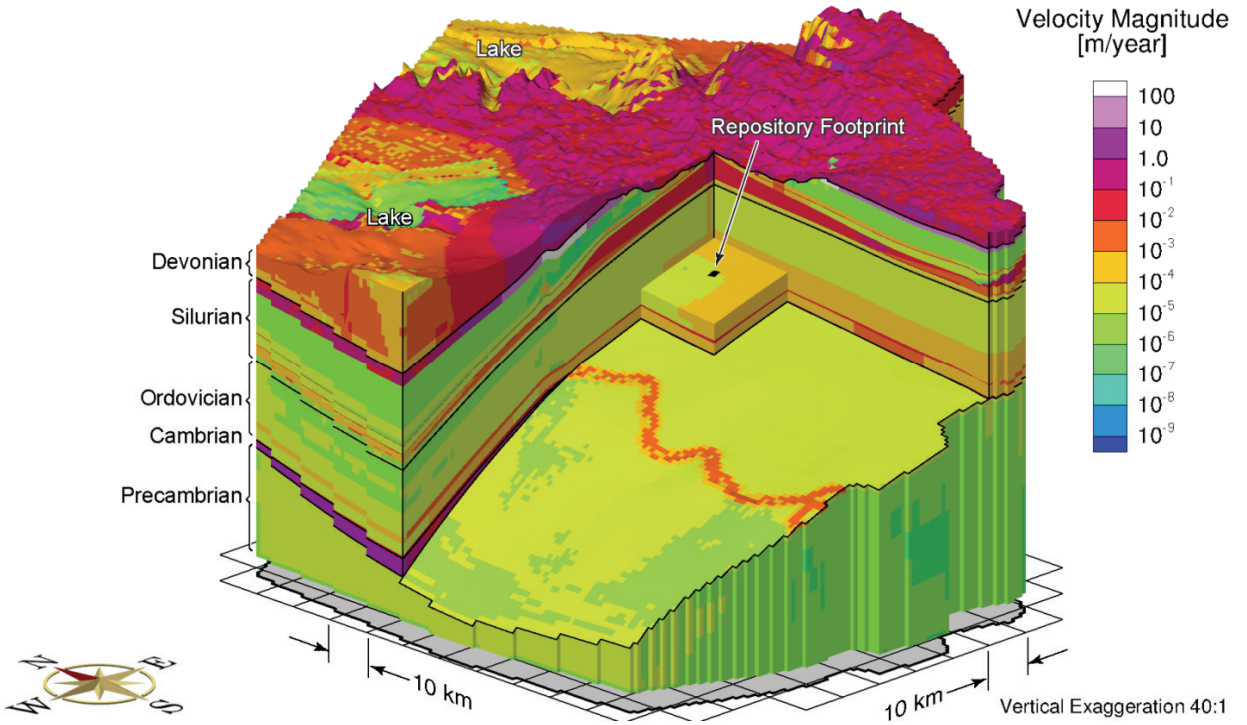

Figure 2-42: **Porewater Velocity Magnitude for a Three Order of Magnitude Enhancement in Hydraulic Conductivities**

2.4 Summary and Conclusions

This chapter describes a geosphere dataset for a hypothetical sedimentary rock site. The geosphere data set described in this chapter was provided for the purpose of performing an illustrative postclosure safety assessment. Three groundwater systems are considered: shallow, intermediate and deep. The behaviour of the groundwater systems during temperate and glacial conditions was explored through a suite of sensitivity cases.

The sedimentary rock overlying the hypothetical repository contains a thick sequence of low permeability limestones and shales. Temperate hydrogeologic modelling illustrates the role played by the low permeability limestones and shales as natural barriers to groundwater movement and contaminant transport.

The hydrogeological domain for the geosphere described in this chapter is divided into three groundwater systems: shallow (0- 215 mBGS), intermediate (215-250 mBGS) and deep (>250 mBGS). These systems are identified, in part, by rock mass hydraulic conductivities, as well as groundwater total dissolved solids (TDS) concentrations and redox conditions. The shallow groundwater zone occurs in the upper 215 m and comprises glacial sediment overlying a relatively permeable sequence of limestone and dolostone. In the shallow system, groundwater is considered to be fresh, oxygen-rich and isolated from the deeper groundwater systems. The intermediate groundwater system is a transition zone in which the groundwater becomes progressively more mineralized and reducing with depth. Within the deep groundwater system, groundwater conditions are saline and reducing. With increasing depth, the general increase in salinity and decreased rock mass hydraulic conductivities leads to improved groundwater system stability at time frames relevant to repository safety.

Péclet numbers and MLEs were used as illustrative performance measures to gain insight into the processes most influencing mass transport. For an assumed reference case, the shallow groundwater system is advective, whereas at greater depths, the low permeability rock mass results in low rates for mass transport. Further groundwater system stability occurs as a result of salinity gradients within the intermediate and deep groundwater systems.

Paleohydrogeological simulations were used to illustrate the long-term evolution and stability of the geosphere and groundwater systems to external perturbations. The distribution and duration of permafrost at the repository location play a role in governing the depth to which meltwater penetrates. Paleohydrogeologic simulations suggest that glacial meltwaters will not reach the repository horizon, due to the low hydraulic conductivity of the overlying shales dolostones and evaporites of the Salina Group. Glacial recharge penetrating below the shallow groundwater system is not expected to be oxygenated or to influence redox conditions at the repository horizon. For the paleohydrogeologic sensitivity cases performed, the glacial perturbations did not materially change mass transport rates at repository depth and mass transport remained diffusion dominated throughout the glacial cycle.

2.5 References for Chapter 2

Armstrong, D.K. and T.R. Carter. 2010. The Subsurface Paleozoic Stratigraphy of Southern Ontario. Ontario Geological Survey, Special Volume 7.

Armstrong, D.K. and J.E.P. Dodge. 2007. Paleozoic geology of southern Ontario. Ontario Geological Survey, Miscellaneous Release-Data 219.

Armstrong, D.K. and T.R. Carter. 2006. An Updated Guide to the Subsurface Paleozoic Stratigraphy of Southern Ontario. Ontario Geological Survey, Open File Report 6191.

Armstrong, D.K. and W.R. Goodman. 1990. Stratigraphy and depositional environments of Niagaran carbonates, Bruce Peninsula, Ontario. Field Trip No. 4 Guidebook. American Association of Petroleum Geologists, 1990 Eastern Section Meeting, hosted by the Ontario Petroleum Institute. London, Ontario.

Barker, J.F. and S.J. Pollock. 1984. The Geochemistry and Origin of Natural Gases in Southern Ontario. Bulletin of Canadian Petroleum Geology 32, 313-326.

Bear, J. 1988. Dynamics of Fluids in Porous Media. Dover Publications Inc., New York, USA.

Berry, F.A.F. 1969. Relative factors influencing membrane filtration effects in geologic environments. Chemical Geology 4, 293-301.

Bredehoeft, J.D., C.R. Blyth, W.A. White and G.G. Maxey. 1963. Possible mechanism for concentration of brines in subsurface formations. American Association of Petroleum Geologists Bulletin 47, 257-269.

Carpenter, A.B. 1978. Origin and chemical evolution of brines in sedimentary basins. Oklahoma Geological Survey Circular 79, 60-77.

Cornaton, F. and P. Perrochet. 2006a. Groundwater age, life expectancy and transit time distributions in advective–dispersive systems: 1. Generalized reservoir theory. Advances in Water Resources 29(9), 1267–1291.

Cornaton, F. and P. Perrochet. 2006b. Groundwater age, life expectancy and transit time distributions in advective–dispersive systems: 2. Reservoir theory for sub-drainage basins. Advances in Water Resources 29(9), 1292–1305.

Frape, S.K. and P. Fritz. 1987. Geochemical trends for groundwaters from the Canadian Shield. In Saline Water and Gases in Crystalline Rocks (P. Fritz and S.K. Frape, eds.). Number 33 in Geological Association of Canada Special Paper, 19–38.

Graf, D.L. 1982. Chemical osmosis and the origin of subsurface brines. Geochimica et Cosmochimica Acta 46, 1431-1448.

Hanor, J.S. 2001. Reactive transport involving rock-buffered fluids of varying salinity. Geochimica et Cosmochimica Acta 65(21), 3721-3732.

Hobbs, M.Y., S.K. Frape, O. Shouakar-Stash and L.R. Kennell. 2011. Regional Hydrogeochemistry – Southern Ontario. Nuclear Waste Management Organization Report NWMO DGR-TR-2011-12 R000. Toronto, Canada.

Huysmans, M. and A. Dassargues. 2005. Review of the use of Péclet numbers to determine the relative importance of advection and diffusion in low permeability environments. Hydrogeology Journal 13, 895–904.

INTERA. 2011. Descriptive Geosphere Site Model. Nuclear Waste Management Organization Report NWMO DGR-TR-2011-24 R000. Toronto, Canada.

ITASCA. 2011. Long Term Geomechanical Stability Analysis. Nuclear Waste Management Organization Report NWMO DGR-TR-2011-17 R000. Toronto, Canada.

ITASCA CANADA and AECOM. 2011. Three-Dimensional Geological Framework Model. Nuclear Waste Management Organization Report NWMO DGR-TR-2011-42 R000. Toronto, Canada.

Kharaka, Y.K. and J.S. Hanor. 2005. Deep fluids in the Continents: 1. Sedimentary Basins. In: J.I. Drever (Ed.). Treatise on Geochemistry, Surface and Groundwater, Weathering, and Soils 5, 499-540.

Kharaka, Y.K., A.S. Maest, W.W. Carothers, L.M. Law, P.J. Lamothe and T.L. Fries. 1987. Geochemistry of metal-rich brines from central Mississippi Salt Dome Basin, U.S.A. Applied Geochemistry 2, 543-561.

Kharaka Y.K. and F.A.F. Berry. 1973. Simultaneous flow of water and solutes through geological membranes I: Experimental investigation. Geochimica et Cosmochimica Acta 37, 2577-2603.

Land, L.S. 1997. Mass transfer during burial diagenesis in the Gulf of Mexico sedimentary basin: an overview. Society for Sedimentary Geology 57, 29-39.

Land, L.S. and D.R. Prezbindowski. 1981. The origin and evolution of saline formation water, Lower Cretaceous carbonates, south-central Texas, U.S.A. Journal of Hydrology 54, 51-74.

Lusczynski, N.J. 1961. Head and flow of ground water of variable density. Journal of Geophysical Research 66(12), 4247–4256.

McCauley, C.A., D.M. White, M.R. Lilly and D.M. Nyman. 2002. A comparison of hydraulic conductivities, permeabilities and infiltration rates in frozen and unfrozen soils. Cold Regions Science and Technology 34(2), 117–125.

McIntosh, J.C. and L.M. Walter. 2006. Paleowaters in Silurian-Devonian carbonate aquifers: Geochemical evolution of groundwater in the Great Lakes region since the late Pleistocene. Geochimica et Cosmochimica Acta 70, 2454-2479.

NWMO. 2011. Geosynthesis. Nuclear Waste Management Organization Report NWMO DGR-TR-2011-11 R000. Toronto, Canada.

Normani, S.D. 2009. Paleoevolution of Pore Fluids in Glaciated Geologic Settings. Ph.D. thesis, University of Waterloo. Ontario, Canada.

Normani, S.D., Y.J. Park, J.F. Sykes, and E.A. Sudicky. 2007. Sub-regional Modelling Case Study 2005-2006 Status Report. Nuclear Waste Management Organization Report NWMO TR-2007-07. Toronto, Canada.

Park, Y-J., E.A. Sudicky and J.F. Sykes. 2009. Effects of shield brine on the safe disposal of waste in deep geologic environments. Advances in Water Resources 32, 1352–1358.

Park. Y.-J., E.A. Sudicky, S. Panday, J.F. Sykes, and V. Guvanasen. 2008. Application of implicit sub-time stepping to simulate flow and transport in fractured porous media. Advances in Water Resources, 31(7), 995-1003.

Peltier, W.R. 2011. Long-Term Climate Change. Nuclear Waste Management Organization Report NWMO DGR-TR-2011-14 R000. Toronto, Canada.

Peltier, W.R. 2002. A design basis glacier scenario. Ontario Power Generation Report 06819-REP-01200-10069-R00. Toronto, Canada.

Rittenhouse, G. 1967. Bromine in oil-field waters and its use in determining possibilities of origin of these waters. American Association of Petroleum Geology Bulletin 51(12), 2430-2440.

Sherwood Lollar, B. 2011. Far-field Microbiology Considerations Relevant to a Deep Geological Repository – State of Science Review. Nuclear Waste Management Organization Report NWMO TR-2011-09.

Sherwood Lollar B., S.M. Weise, S.K. Frape and J.F. Barker. 1994. Isotopic constraints on the migration of hydrocarbon and helium gases of southwestern Ontario. Bulletin of Canadian Petroleum Geology 42, 283-295.

Singh, B.P. and B. Kumar. 2005. Isotopes in Hydrology, Hydrogeology, and Water Resources. Narosa Publishing House Pvt. Ltd., New Delhi, India.

Stroes-Gascoyne, S., C. Sergeant, A. Schippers, C.J. Hamon, S. Nèble, M.-H. Vesvres, V. Barsotti, S. Poulain and C. Le Marre. 2011. Biogeochemical processes in a clay formation *in situ* experiment: Part D - Microbial analyses - Synthesis of results. Applied Geochemistry 26, 980-989.

Stroes-Gascoyne, S. and C.J. Hamon. 2008. Preliminary Microbial Analysis of Limestone and Shale Rock Samples. Nuclear Waste Management Organization Report NWMO TR-2008-09. Toronto, Canada

Sykes, J.F., S.D. Normani and Y. Yin. 2011. Hydrogeologic Modelling. Nuclear Waste Management Organization Report NWMO DGR-TR-2011-16 R000. Toronto, Canada.

Sykes, E.A. 2007. Hydrogeologic modelling to assess conditions related to OPG's proposed Deep Geologic Repository in Tiverton, Ontario. Master's thesis, University of Waterloo. Ontario, Canada.

Therrien, R., R.G. McLaren, E.A. Sudicky, S.M. Panday, and V. Guvanasen. 2010. FRAC3DVS_OPG: a three-dimensional numerical model describing subsurface flow and solute transport. User's Guide. Groundwater Simulations Group, University of Waterloo, Ontario, Canada.

Vilks. P., N.H. Miller and K. Felushko. 2011. Sorption Experiments in Brine Solution with Sedimentary Rock and Bentonite. Nuclear Waste Management Organization Report NWMO TR-2011-11. Toronto, Canada.

Vilks, P. 2009. Sorption in Highly Saline Solutions – State of the Science Review. Nuclear Waste Management Organization Report NWMO TR-2009-18. Toronto, Canada.

Weast, R.C. (Ed.). 1983. CRC Handbook of Chemistry and Physics. 64th edition. CRC Press, Inc., Boca Raton, Florida, USA.

Wersin, P., S. Stroes-Gascoyne, F.J. Pearson, C. Tournassat, O.X. Leupin and B. Schwyn. 2011. Biogeochemical processes in a clay formation *in situ* experiment: Part G - key interpretations and conclusions. Implications for repository safety. Applied Geochemistry 26, 1023-1034.

THIS PAGE HAS BEEN LEFT BLANK INTENTIONALLY